

Rational Generation of Lasso Peptides Based on Biosynthetic Gene Mutations and Site-Selective Chemical Modifications

Tan Liu,^{†,‡} Xiaojie Ma,^{†,‡} Jiahui Yu,[†] Wensheng Yang,[§] Guiyang Wang,[†] Zhengdong Wang,[†] Yuanjie Ge,[†] Juan Song,[†] Hua Han,[§] Wen Zhang,[§] Donghui Yang,[†] Xuehui Liu,^{¶*} and Ming Ma^{†,*}

[†]State Key Laboratory of Natural and Biomimetic Drugs, School of Pharmaceutical Sciences, Peking University, 38 Xueyuan Road, Haidian District, Beijing 100191, China

[§]School of Medicine, Tongji University, 1239 Siping Road, Shanghai 200092, China

[¶]CAS Research Platform for Protein Sciences, Institute of Biophysics, Chinese Academy of Sciences, 15 Datun Road, Chao-yang District, Beijing 100101, China.

[‡]These authors contributed equally

*To whom correspondence should be addressed: Xuehui Liu, Email: xhliu@ibp.ac.cn;
Ming Ma, Email: mma@bjmu.edu.cn

Supplementary Information

General materials and experimental procedures	S5
Bacterial strains, plasmids and DNA sequences	S5
Fermentation of <i>Streptomyces</i> sp. PKU-MA01240	S5
Construction of the <i>stla</i> expression plasmid	S6
Gene activation by the insertion of promoter <i>KasOp*</i> at the upstream of <i>stlaA</i>	S6
Site-directed mutagenesis of <i>stlaA</i> gene	S6
Heterologous expression, fermentation and HPLC analysis	S7
Large-scale fermentation and isolation of stlassins	S8
Solution NMR structures determination	S9
Thermal stability assays and carboxypeptidase Y-treatment experiments	S9
Site-selective glycosylation of stlassin F15Y (16) and stlassin I4C (21)	S10
Site-selective S-arylation of stlassin I4C (21)	S10
Bis-alkylation-elimination reaction of stlassin I4C (21)	S10
Conjugate addition of 2-mercaptoethanol and conjugate addition of <i>N</i> -acetylcysteamine	S10
Biological activity assays of stlassins	S11
Table S1. The deduced functions of genes in the <i>stla</i> gene cluster	S13
Table S2. Primers used in this study	S14
Table S3. Plasmids and strains used in this study	S17
Table S4. The HRESIMS data of compounds 1-25	S22
Table S5. Assignment of ¹ H, ¹³ C and ¹⁵ N signals (ppm) of stlassin (1)	S23
Table S6. Assignment of ¹ H, ¹³ C and ¹⁵ N signals (ppm) of stlassin V3A (3)	S24
Table S7. Assignment of ¹ H, ¹³ C and ¹⁵ N signals (ppm) of stlassin I4A (4)	S25
Table S8. Assignment of ¹ H signals (ppm) of stlassin W14F (14)	S26
Table S9. Assignment of ¹ H signals (ppm) of stlassin F15Y (16)	S27
Table S10. Assignment of ¹ H and ¹³ C signals (ppm) of stlassin V2C/A11C (18)	S28
Table S11. The Optical density (OD) values and inhibition ratios (% in parentheses) from parallel ELISA experiments for each stlassins against the binding of LPS to TLR4	S29
Table S12. Inhibition ratios from parallel ELISA experiments for each concentration in dose-response determination	S30
Figure S1. The phylogenetic analysis of strain PKU-MA01240	S31
Figure S2. The construction of plasmid pMM2002 for the heterologous expression	S32
Figure S3. The HPLC analysis of fermentations of heterologous expression strains.....	S33
Figure S4. The construction of plasmid pMM2003 and pMM2004	S34
Figure S5. HPLC analysis of stlassin (1 , labeled with asterisk) in cells and supernatant of the heterologous expression strain MM20003 (<i>S. coelicolor</i> A3(2) with pMM2004 integrated) after fermentation using three different media.	S35
Figure S6. The HPLC analysis of thermal stability and peptidase-treatment reactions	S36
Figure S7. The diagram for site-directed mutagenesis of <i>stlaA</i> gene	S37
Figure S8. The HPLC analysis of stlassin (1) and its derivatives produced in the crude extracts of different strains	S38
Figure S9. The design of double mutations for introducing two cysteine residues	S39

Figure S10. The lasso presentation of the structures of compounds 1-27	S40
Figure S11. The superimposition of the 20 solution structures with the lowest total energy	S41
Figure S12. The superimposition of solution NMR structures	S42
Figure S13. Amplified region of NOESY spectra of 1, 3, 4, 14 and 16 showing the correlations between Val3 (or Ala3) and Pro12	S43
Figure S14. The OD values of four control ELISA experiments (N1–N4)	S44
Figure S15. The antagonistic activities of stlassins at different concentrations	S45
Figure S16. The HRESIMS spectrum of stlassin (1)	S46
Figure S17. The HRESIMS spectrum of stlassin V2A (2)	S46
Figure S18. The HRESIMS spectrum of stlassin V3A (3)	S47
Figure S19. The HRESIMS spectrum of stlassin I4A (4)	S47
Figure S20. The HRESIMS spectrum of stlassin V5A (5)	S48
Figure S21. The HRESIMS spectrum of stlassin Q6A (6)	S48
Figure S22. The HRESIMS spectrum of stlassin N10A (7)	S49
Figure S23. The HRESIMS spectrum of stlassin A11G (8)	S49
Figure S24. The HRESIMS spectrum of stlassin P12A (9)	S50
Figure S25. The HRESIMS spectrum of stlassin L1A (10)	S50
Figure S26. The HRESIMS spectrum of stlassin A7G (11)	S51
Figure S27. The HRESIMS spectrum of stlassin D8E	S51
Figure S28. The HRESIMS spectrum of stlassin W9F (12)	S52
Figure S29. The HRESIMS spectrum of stlassin W9Y (13)	S52
Figure S30. The HRESIMS spectrum of stlassin W14F (14)	S53
Figure S31. The HRESIMS spectrum of stlassin W14Y (15)	S53
Figure S32. The HRESIMS spectrum of stlassin F15Y (16)	S54
Figure S33. The HRESIMS spectra of stlassin F15W (17)	S54
Figure S34. The HRESIMS spectra of stlassin V2C/A11C (18)	S55
Figure S35. The HRESIMS spectra of stlassin V3C/P12C (19)	S55
Figure S36. The HRESIMS spectra of stlassin F15Y-I (20)	S56
Figure S37. The HRESIMS spectrum of stlassin I4C (21)	S56
Figure S38. The HRESIMS spectrum of stlassin I4C-I (22)	S57
Figure S39. The HRESIMS spectra of stlassin I4C-II (23)	S57
Figure S40. The HRESIMS spectrum of stlassin I4C-III (24)	S58
Figure S41. The HRESIMS spectrum of stlassin I4C-IV (25)	S58
Figure S42. The HRESIMS spectrum of stlassin I4C-V (26a)	S59
Figure S43. The HRESIMS spectrum of stlassin I4C-VI (26b)	S59
Figure S44. The ESIMS spectrum of stlassin I4C-VII (27a)	S60
Figure S45. The ESIMS spectrum of stlassin I4C-VIII (27b)	S60
Figure S46. The TOCSY spectrum and NOESY spectrum of stlassin (1)	S61
Figure S47. The ¹ H- ¹³ C HSQC spectrum of stlassin (1)	S62
Figure S48. The ¹ H- ¹⁵ N HSQC spectrum of stlassin (1)	S63
Figure S49. The TOCSY spectrum and NOESY spectrum of stlassin V3A (3)	S64
Figure S50. The ¹ H- ¹³ C HSQC spectrum of stlassin V3A (3)	S65
Figure S51. The ¹ H- ¹⁵ N HSQC spectrum of stlassin V3A (3)	S66
Figure S52. The TOCSY spectrum and NOESY spectrum of stlassin I4A (4)	S67

Figure S53. The ^1H - ^{13}C HSQC spectrum of stlassin I4A (4)	S68
Figure S54. The ^1H - ^{15}N HSQC spectrum of stlassin I4A (4)	S69
Figure S55. The TOCSY spectrum and NOESY spectrum of stlassin W14F (14)	S70
Figure S56. The ^1H - ^{13}C HSQC spectrum of stlassin W14F (14)	S71
Figure S57. The TOCSY spectrum and NOESY spectrum of stlassin F15Y (16)	S72
Figure S58. The ^1H - ^{13}C HSQC spectrum of stlassin F15Y (16)	S73
Figure S59. The TOCSY spectrum and NOESY spectrum of stlassin V2C/A11C (18)	S74
Figure S60. The ^1H - ^{13}C HSQC spectrum of stlassin V2C/A11C (18)	S75
References	S76

General materials and experimental procedures

NMR data were collected on a Bruker Avance 600 MHz spectrometer (Bruker Corporation, Billerica, MA, USA) equipped with an inverse triple resonance ^1H - ^{13}C - ^{15}N probe with z-gradient. High-resolution mass spectra were obtained on a Shimadzu IT-TOF spectrometer (Shimadzu, Kyoto, Japan) and a Waters Alliance e2695-SQD spectrometer (Waters, Milford, MA, USA). HPLC analysis was performed on an Agilent 1260 series (Agilent Technologies, Santa Clara, CA, USA) with a C_{18} RP-column (Extend- C_{18} , 250×4.6 mm, $5 \mu\text{m}$, Agilent Technologies, Santa Clara, CA, USA). Semi-preparative HPLC was performed on a SSI 23201 system (Scientific Systems Inc., State College, PA, USA) with a YMC-Pack ODS-A column (250×10 mm, $5 \mu\text{m}$, YMC CO., LTD. Shimogyo-ku, Kyoto, Japan). Medium pressure liquid chromatography (MPLC) was performed on a LC3000 series (Beijing Tong Heng Innovation Technology, Beijing, China) with a ClaricepTM Flash i-series C_{18} cartridge ($20\text{-}35 \mu\text{m}$, 40 g, Bonna-Agela, Wilmington, DE, USA). All fermentations were carried out in MQD-B1R shakers (Minquan Instrument Co., Ltd., Shanghai, China).

Antibiotics were purchased from Sangon Biotech Co., Ltd. (Shanghai, China) and Fisher-Scientific (Waltham, MA, USA), respectively. The α -D-fluoroglucose tetraacetate was purchased from Beijing Chemsynlab Co., Ltd. (Beijing, China). The 2-nitrophenylboronic acid was purchased from Energy Chemical (Shanghai, China).

Bacterial strains, plasmids and DNA sequences

Strain *Streptomyces* sp. PKU-MA01240 was isolated from a sponge sample collected from Xieyang island, Guangxi Province, China.¹ Genomic DNA of *Streptomyces* sp. PKU-MA01240 was extracted following standard protocols² and sequenced by Majorbio Co. (Shanghai, China). The 16S rRNA gene (GeneBank accession number MT826211.1) was amplified by PCR using the forward primer (5'-AGAGTTTGATCMTGGCTCAG-3') and reverse primer (5'-TACGGYTACCTTGTTACGACTT-3').³ Common DNA sequencing and synthesis of all oligonucleotide primers used in this study (Table S2) were performed by RuiBiotech Co., Ltd. (Beijing, China). Bacterial strains and plasmids used and generated in this study are listed in Table S3. The secondary metabolite gene clusters were analyzed with antiSMASH (<http://antismash.secondarymetabolites.org/>).⁴ The gene functional annotations were performed with BLAST on the NCBI website. Multiple alignments were performed with Clustal Omega (<https://www.ebi.ac.uk/Tools/msa/clustalo/>)⁵ and the phylogenetic tree was generated with Mega 6.0 using the Neighbor-Joining algorithm.

Small-scale fermentation of wild-type *Streptomyces* sp. PKU-MA01240

The *S.* sp. PKU-MA01240 strain was preserved as a spore solution at $-80 \text{ }^\circ\text{C}$. Each of 250 mL Erlenmeyer flasks, containing 50 mL of the M1 medium (yeast extract 1 g, peptone 5 g, beef extract 1 g, FePO_4 0.01 g, and sea salt 33 g in 1.0 L distilled H_2O , pH 7.4) with 3% sea salt, was inoculated with 50 μL of the PKU-MA01240 spore solution and incubated in shaker at $28.0 \text{ }^\circ\text{C}$, 200 rpm for three days, to afford the seed culture. The seed culture was inoculated into 50 mL of three different production media including M2 medium (yeast extract 4 g, malt extract 10 g, glucose 4 g, in 1.0 L distilled H_2O , pH 7.2) with 3% sea salt, medium M3 (sucrose 100 g, glucose 10 g, casamino acids 0.1 g, yeast extract 5 g, MOPS 21 g, trace elements (FeSO_4 1 g, MnCl_2 1 g, ZnSO_4 1 g, in 1 L distilled H_2O) 1 mL, K_2SO_4 0.25 g, $\text{MgCl}_2 \cdot 6\text{H}_2\text{O}$ 10 g, in 1.0 L distilled H_2O , pH 7.0) with 3% sea salt, and medium M4 (glycerol 20 g, malt extract 4 g, yeast extract 4 g, NZ Amine A 2 g, trace elements 1 mL, in 1.0 L distilled H_2O , pH 7.0) with 3% sea salt. The fermentation continued at $28 \text{ }^\circ\text{C}$, 200 rpm for seven days.

The Amberlite XAD-16 (2 g/50 mL) resins were added into each of the fermentation flasks 12 h before the fermentation finished. The resins and cells were harvested by centrifugation, washed with distilled H₂O and extracted with 50 mL of MeOH at 28 °C, 200 rpm for 3 h. Then, the extract was concentrated and dissolved in 2 mL of MeOH/H₂O (1/1, v/v). Ten µL of each concentrated extract was used for HPLC analysis, using an elution program of 5% CH₃CN in H₂O (0.1% formic acid) from 0 to 5 min; 5% CH₃CN in H₂O (0.1% formic acid) to 100% CH₃CN from 5 to 23 min; 100% CH₃CN from 23 to 28 min, with a flow rate of 1 mL/min under the UV detection at 280 nm. No stlassin (**1**) was detected in these fermentation.

Construction of the *stla* expression plasmid

All procedures were performed according to those reported previously.^{6,7} Ten micrograms of genomic DNA digested with *Bgl*III was used for the RecET-mediated direct cloning. The p15A vector used to clone the 20.3-kb fragment released with *Bgl*III digestion was amplified with pMM2001-F and pMM2001-R as the primers (Table S2) using p15A-*cm-tetR-tetO-hyg-ccdB* as the template. Then the direct cloning procedure was conducted following previous publication,⁷ and the subsequent recombinant p15A plasmid (pMM2001) containing the *stla* gene cluster was extracted from colonies selected on LB plates containing chloramphenicol and verified with *Apa*LI restriction analysis (Figure S2). To construct the *E. coli-Streptomyces* shuttle vector pMM2002 for integration into heterologous hosts, 200 ng of *apra-oriT-attP-phiC31* cassette was electroporated into GB05RedTrfA-containing pMM2001, which had been treated with L-rhamnose to induce the expression of Redαβ.⁷ The pMM2002 plasmid was extracted from colonies selected on LB plates containing apramycin and verified with *Apa*LI restriction analysis (Figure S2).

Gene activation by the insertion of promoter *KasOp** at the upstream of *stlaA*

The *KasOp** promoter and 40-bp homology arms for Redαβ recombineering was attached to ampicillin resistance gene by overlap extension PCR using primers listed in Table S2. In the first round PCR, the ampicillin-resistance gene *Amp* was amplified with pET32a(+) as the template using the primers pMM2003-1-F and pMM2003-1-R (Table S2), both of which had been introduced with a *Ac*II-recognition sequence. The PCR products was purified with the FastPure Gel DNA Extraction Mini Kit (Vazyme Biotech Co., Ltd.) after agarose gel electrophoresis and used as the template for the second round PCR. The second round PCR products were amplified with primers pMM2003-2-F and pMM2003-2-R, and then electroporated into the GB05RedTrfA-containing pMM2002, which had been treated with L-rhamnose to induce expression of Redαβ. The correct recombinant plasmid pMM2003 was extracted from colonies selected based on ampicillin resistance and verified with *Apa*LI restriction analysis. The plasmid pMM2003 was further digested by *Ac*II and self-ligated by T4 DNA ligase to generate the *KasOp** insertion plasmid pMM2004 (Figure S4).

Site-directed mutagenesis of *stlaA* gene

The heterologous expression plasmids with site-directed mutagenesis of *stlaA* were constructed as the following steps:

(i) Construction of the plasmid pMM2007 with the *KasOp**-*stlaA* cassette deletion. To delete the *KasOp**-*stlaA* cassette within pMM2004, the *Amp* gene flanked by *Ac*II sites and 40-bp homologous arms for Redαβ recombineering was amplified by PCR with primers pMM2006-F and pMM2006-R (Table S2). Then, the PCR product was purified and used to replace the *KasOp**-*stlaA* region in pMM2004 by Redαβ

recombineering following standard protocols mentioned above, to generate the plasmid pMM2006 (Figure S7). The plasmid pMM2006 was identified with *Apa*LI restriction digestion analysis and further digested by *Ac*II and self-ligated by T4 DNA ligase to generate the plasmid pMM2007.

(ii) Preparation of *Amp-KasOp**-*stlaA* cassette bearing mutations for *Reda* β recombineering. To perform the site-directed mutagenesis of *stlaA* gene via PCR, plasmid pMM2005 carrying *Amp-KasOp**-*stlaA* cassette was constructed. The p15A-*cm* and *Amp-KasOp**-*stlaA* cassettes were amplified by PCR from plasmids p15A-*cm-tetR-tetO-hyg-ccdB* and pMM2003, respectively, using primers listed in Table S2. The two fragments were ligated with the Gibson assembly method and then transformed into *E. coli* DH5 α to yield the plasmid pMM2005. Then, site-directed mutagenesis was performed by PCR amplification using two overlapping primers (Table S2) containing the mutation sites with pMM2005 as the template. The resulting mixtures containing the mutated plasmids were digested with *Dpn*I for 1 h at 37 °C to remove residual template DNA. After transforming into *E. coli* DH5 α , the mutated plasmids were individually prepared from transformants and confirmed by DNA sequencing. Using these mutated plasmids as the templates, the *Amp-KasOp**-*stlaA* cassette bearing different mutations for recombineering were individually amplified by PCR, using the same primers *stla*-2-F and *stla*-2-R.

(iii) Construction of the heterologous expression plasmids pMM2008-pMM2037 with mutated *stlaA*. The *Amp-KasOp**-*stlaA* cassettes prepared from step ii were inserted into pMM2007 constructed in step i following standard protocols for *Reda* β recombineering. Afterwards, to construct the heterologous expression plasmids pMM2008-pMM2037 with mutated *stlaA*, *Amp* gene was removed by *Ac*II digestion and self-ligation by T4 DNA ligase. All the plasmids pMM2008-pMM2037 were identified with *Apa*LI restriction digestion and DNA sequencing.

Heterologous expression, fermentation and HPLC analysis

According to the standard procedure, all of the heterologous expression plasmids were first transformed into *E. coli* ET12567/pUZ8002 and then conjugated into heterologous hosts *S. coelicolor* A3(2) or *S. lividans* K4-114. Colonies of exconjugants (MM20001-MM20034) were selected for apramycin resistance and verified by PCR with *stla*-1-F and *stla*-1-R as the primers.

For detection of stlassin (**1**) and its variants, a two-stage culture procedure was used in the small-scale fermentations. The seed cultures of heterologous expression strains generated above were prepared by inoculating spores into 250 mL flasks containing 50 mL of medium M1, and incubated at 28.0 °C, 200 rpm for three days. The seed cultures were then inoculated (2% v/v) into 50 mL of medium M2, and the fermentation continued at 28 °C, 200 rpm for seven days. Another two production media, medium M3 and medium M4 were also used. The Amberlite XAD-16 (2 g/50 mL) resins were added into each of the fermentation flasks 12 h before the fermentation finished. The resins and cells were harvested by centrifugation, washed with distilled H₂O and extracted with 50 mL of methanol at 28 °C, 200 rpm for 3 h. Then, the extract was concentrated and dissolved in 2 mL of MeOH/H₂O (1/1, v/v). Ten μ L of each concentrated extract was used for HPLC analysis, using an elution program of 5% CH₃CN in H₂O (0.1% formic acid) from 0 to 5 min; 5% CH₃CN in H₂O (0.1% formic acid) to 100% CH₃CN from 5 to 23 min; 100% CH₃CN from 23 to 28 min, with a flow rate of 1 mL/min under the UV detection at 280 nm. For detection of stlassin I4C (**21**), dithiothreitol (DTT, final concentration: 100 mM) was added to the concentrated extract samples and stirred at 25 °C overnight before HPLC analysis.

Production yields of stlassin (**1**) were calculated from the HPLC peak areas in the analytical HPLC based on a linear equation of peak area of purified **1** versus quantity. The relative production yields of derivatives from mutations were calculated based on the comparison of their peak areas to that of **1**. Triplicate

experiments were carried out for each production yields calculation.

Large-scale fermentation and isolation of stlassins

To obtain enough stlassin (**1**) for solution NMR structure determination, large-scale fermentation (5 L) of the strain MM20003 was carried out with similar procedures used in the small-scale fermentation. After the fermentation, the resins and cells were separated from supernatants by centrifugation, and extracted with 2 L of MeOH for three times at 28 °C, 200 rpm for 3 h. The MeOH extract was concentrated under reduced pressure to give a crude extract. The crude extract was resuspended in H₂O and extracted with EtOAc for three times. Since the EtOAc soluble fraction contains little amount of **1**, only the water soluble fraction that contains most of **1** was subjected to MPLC eluted with a gradient of MeOH in H₂O (0% to 100% over 30 min) followed by 100% MeOH for 10 min at a flow rate of 8 mL/min under the UV detection at 210 nm, to give 22 fractions (a1-a22). The fractions a17-a20 were combined based on HPLC analysis and further purified by semi-preparative HPLC eluted with a gradient of CH₃CN in H₂O (0.1% formic acid) from 40% to 60% over 30 min with a flow rate of 2 mL/min under the UV detection at 210 nm, to afford compound **1** (51 mg).

Compounds **3**, **4** and **21** were isolated using the similar procedures as that for **1**, except that the purification of compound **4** by semi-preparative HPLC was carried out with an increasing gradient of CH₃CN in H₂O (0.1% formic acid) from 40% to 55% over 30 min; and for the isolation of compound **21**, dithiothreitol (DTT, final concentration: 100 mM) was added to the combined MPLC fractions and stirred at 25 °C overnight. Totally 26 mg of **3**, 20 mg of **4** and 30 mg of **21** were isolated from 5 L fermentation of MM20007, 4 L fermentation of MM20008 and 12 L fermentation of MM20034, respectively.

The isolation of compounds **14**, **16**, **18** and **19** was carried out using similar procedures as that for **1** with changes listed below. Firstly, after the crude extracts were resuspended in H₂O and extracted with EtOAc, the EtOAc extracts, instead of the water soluble fractions, were used for further purification. Secondly, the elution programs used for compound **16** purification by semi-preparative HPLC was the same as that for **4**; the purification of compound **14** by semi-preparative HPLC was carried out with an increasing gradient of CH₃CN in H₂O (0.1% formic acid) from 44% to 62% over 30 min; and the purification of compounds **18** and **19** by semi-preparative HPLC was carried out with 43% CH₃CN in H₂O (0.1% formic acid) over 30 min. Finally, 18 mg of **14**, 27 mg of **16**, 33 mg of **18** and 15 mg of **19** were isolated from 6 L fermentation of MM20024, 16 L fermentation of MM20028, 6 L fermentation of MM20031 and 30 L fermentation of MM20032, respectively.

For biological activity assays, more derivatives were isolated from large-scale fermentations of mutants, which were carried out with similar procedures used in that of MM20003. After the fermentation, the treatments with MeOH and EtOAc were similar as those in the isolation of **1**. L1A (**10**), V2A (**2**), V5A (**5**), Q6A (**6**) and A7G (**11**) were isolated using the similar MPLC procedures as that for **1**, while N10A (**7**), A11G (**8**), P12A (**9**), W9F (**12**) and W14Y (**15**) were isolated using the similar MPLC procedures as that for **14**. The purification of compounds **2**, **5** and **10** by semi-preparative HPLC were carried out with an increasing gradient of CH₃CN in H₂O (0.1% formic acid) from 40% to 55% over 30 min. Totally 25 mg of **2**, 18 mg of **5** and 1.8 mg of **10** were isolated from 5.2 L fermentation of MM20006, 5.2 L fermentation of MM20009 and 6 L fermentation of MM20005, respectively. The purification of compounds **6**, **7**, **9** and **11** by semi-preparative HPLC were carried out with an increasing gradient of CH₃CN in H₂O (0.1% formic acid) from 45% to 65% over 30 min. Totally 20 mg of **6**, 10 mg of **7**, 8.6 mg of **9** and 2.4 mg of **11** were isolated from 4.8 L fermentation of MM20010, 4.4 L fermentation of MM20017, 5.6 L fermentation of MM20019 and 5.2 L fermentation of MM20011, respectively. The purification of compounds **8**, **12** and **15**

by semi-preparative HPLC were carried out with an increasing gradient of CH₃CN in H₂O (0.1% formic acid) from 40% to 60% over 30 min. Totally 21 mg of **8**, 10 mg of **12** and 16 mg of **15** were isolated from 4 L fermentation of MM20018, 6 L fermentation of MM20015 and 4 L fermentation of MM20025 respectively.

F15Y-I (**20**) was generated by site-selective glycosylation reaction of **16**. The purification of compounds **20** by semi-preparative HPLC was carried out with an increasing gradient of CH₃CN in H₂O (0.1% formic acid) from 36% to 55% over 30 min. I4C-III (**24**) was generated by site-selective *S*-arylation reaction of **21**. The purification of compounds **24** by semi-preparative HPLC was carried out with an increasing gradient of CH₃CN in H₂O (0.1% formic acid) from 52% to 67% over 30 min. Finally, 5.3 mg of **20** and 6.5 mg of **24** were isolated respectively.

Solution NMR structures determination

Compounds **1**, **3**, **4**, **14** and **16** (5 mg for each compound) were dissolved in 500 μ L of 20% DMSO-*d*₆, 80% H₂O, 100 mM NaCl, and compound **18** (8 mg) was dissolved in 500 μ L of 100% DMSO-*d*₆ for the NMR experiments. All NMR spectra were acquired at 298 K on an Agilent DD2 or a Bruker Avance-600 spectrometer equipped with cold probes. The DMSO-*d*₆ in the samples served as the deuterium lock solvent. For **1**, **3** and **4**, TOCSY, NOESY, ¹H-¹³C HSQC and ¹H-¹⁵N HSQC spectra were collected. For **14**, **16** and **18**, TOCSY, NOESY, ¹H-¹³C HSQC spectra were collected. All the TOCSY experiments were carried out using a 70 ms DIPSI-2 spin-lock pulse with a field strength of 6000 Hz. The mixing time for the NOESY experiments were 300 ms. The spectra widths were 8445.9*8445.9 Hz for the ¹H-¹H, 8445.9*21124.9 Hz for the ¹H-¹³C and 8445.9*1450 Hz for the ¹H-¹⁵N correlation spectra, and 200, 128 and 32 complex points were collected for the indirect proton, carbon and nitrogen dimension respectively, while 512 complex points were collected for the directly observing proton dimension. The chemical shifts for the samples in 20% DMSO-*d*₆ were referenced to the external DSS at 0.00 ppm for the proton and indirectly for the carbon and nitrogen dimension,⁸ and those for the sample in 100% DMSO-*d*₆ were referenced to the internal TMS at 0.00 ppm. All NMR data were processed using the NMRPipe⁹ and analyzed with CcpNmr program suite.¹⁰ Signal assignment was obtained by following the method developed by Wuthrich¹¹ and inter-proton distance restraints were derived from the NOESY spectra. Initial structure calculation, NOE peak refinement and assignment were performed simultaneously by using the program CNS¹² and ARIA2.¹³ Then the structure calculation was carried out using Xplor-NIH¹⁴ with distance constraints derived from ARIA2. Patched topology and parameter files were used for creating the isopeptide bond between the amino group of Leu1 and the carbonyl group of the Asp8 side chain. A total of 100 structures were calculated and the 20 structures with the lowest total energy were selected to perform a refinement procedure in water. The structures of **1**, **3**, **4**, **14**, **16** and **18** have been deposited in Protein Data Bank with the PDB IDs of 7BZA, 7BZ8, 7BZ9, 6M19, 7BZ7, and 7CU6, respectively. The chemical shift assignments of **1**, **3**, **4**, **14**, **16** and **18** have been deposited in the Biological Magnetic Resonance Data Bank with the accession numbers of 36351, 36349, 36350, 36317, 36348, and 36372 (<http://www.bmrb.wisc.edu>), respectively. The structures were displayed and analyzed with PyMOL (<http://www.pymol.org/>).

Thermal stability assays and carboxypeptidase Y-treatment experiments

The thermal stability of **1**, **3**, **4**, **14**, **16** and **18** was tested by heating the compound in a sealed tube containing 50 μ L of 50% CH₃CN in H₂O for 3 h at 55 °C, 75 °C and 95 °C. Each compound was separately tested at the three temperatures followed by immediate cooling to room temperature. After the heating experiments, the samples were subjected to HPLC analysis with the program of 5% CH₃CN in H₂O (0.1%

formic acid) from 0 to 5 min; 5% CH₃CN in H₂O (0.1% formic acid) to 100% CH₃CN from 5 to 23 min; 100% CH₃CN from 23 to 28 min, with a flow rate of 1 mL/min under the UV detection at 280 nm. The incubation of stlassin V3A (**3**) at 95 °C for 3 h generated compounds A and B with the same molecular weight as that of **3** based on HPLC and HRESIMS analysis (Figure S6B and S6C). Compounds A and B were purified by semi-preparative HPLC from repeated heating experiments at 95 °C, and treated with carboxypeptidase Y individually.¹⁵⁻¹⁷ Compound B cannot be hydrolyzed by carboxypeptidase Y, suggesting it is the threaded **3**. Compound A was hydrolyzed to compound C, which was identified as stlassin V3A-ΔC6 that lost the C-terminal six residues Asn10-Phe15 based on HRESIMS analysis. Thus, compound A was identified as the unthreaded **3**.

For carboxypeptidase Y-treatment experiments, the tested compound was dissolved in 50 μL of 50 mM sodium acetate buffer (pH 6.0), and 0.05 U carboxypeptidase Y (0.05 U/μL) was added to the solution. The reaction was carried out at 28 °C for 12 h and analyzed by HPLC with the same program as that for the thermal stability assays.

Site-selective glycosylation of stlassin F15Y (16) and stlassin I4C (21).

To prepare the glycosyl donor α-D-fluoroglucose, deacetylation of α-D-Fluoroglucose tetraacetate was performed with NaOMe as previously described.¹⁸ For the glycosylation of lasso peptides **16** and **21**, a 300 μL of reaction system containing **16** or **21** (final concentration: 1 mM, 1.0 equiv.), α-D-Fluoroglucose (final concentration: 1 M, 1000.0 equiv.) and Ca(OH)₂ (final concentration: 1 M, 1000.0 equiv.) in H₂O was prepared. The mixture was stirred vigorously at 25 °C for 1 h, and the reaction was quenched with 900 μL of EDTA solution (0.5 M, pH 8.0), and centrifuged at 13,000 rpm for 10 min. The supernatant was analyzed by HPLC with the program of 5% CH₃CN in H₂O (0.1% formic acid) from 0 to 5 min; 5% CH₃CN in H₂O (0.1% formic acid) to 100% CH₃CN from 5 to 23 min; 100% CH₃CN from 23 to 28 min, with a flow rate of 1 mL/min under the UV detection at 280 nm.

Site-selective S-arylation of 21

The site-selective S-arylation of **21** was carried out according to the published procedures.¹⁹ A 1 mL of reaction system containing **21** (0.3 mM, 1.0 equiv.), 2-nitrophenylboronic acid (3 mM, 10.0 equiv.), and Ni(OAc)₂ (1.5 mM, 5.0 equiv.) in 10 mM *N*-methylmorpholine (NMM) buffer (pH 7.5) was prepared. The mixture was stirred vigorously at 25 °C for 30 min, quenched with 120 μL of EDTA solution (0.5 M, pH 8.0), and centrifuged at 13,000 rpm for 10 min. The supernatant was analyzed by HPLC with the same program as that for glycosylation products.

Bis-alkylation-elimination reaction of 21

The bis-alkylation-elimination reaction of **21** was performed with α,α'-dibromo-adipyl(bis)amide as previously described.²⁰ A 100 μL of reaction system containing **21** (2.0 mM, 1.0 equiv.), K₂CO₃ (10.0 mM, 5.0 equiv.) and α,α'-dibromo-adipyl(bis)amide (10.0 mM, 5.0 equiv.) in DMF was prepared. The mixture was stirred vigorously at room temperature for 30 min and then stirred for 4 h at 37 °C. After the reaction, the mixture was concentrated and dissolved in 1 mL of MeOH/H₂O (1/1, v/v). After centrifuged at 13,000 rpm for 10 min, the supernatant was analyzed by HPLC with the same program as that for glycosylation products.

Conjugate addition of 2-mercaptoethanol and N-acetylcysteamine

For conjugate addition of 2-mercaptoethanol, a 100 μL system containing **25** (0.12 μM, 1.0 equiv.),

sodium methoxide (12 μ M, 100 equiv.) and 2-mercaptoethanol (0.6 mM, 5000 equiv.) in MeOH was prepared. The mixture were stirred at 37 $^{\circ}$ C for 2 h, and **21** was used instead of **25** for a negative control. Conjugate addition of *N*-acetylcysteamine was performed with the same method as that for 2-mercaptoethanol. The HPLC analysis was performed with the same program as that for glycosylation products.

Biological activity assays of stlassins

To evaluate the biological activity of **1**, we first carried out the antibacterial and cytotoxicity assays. However, compound **1** showed no antibacterial activities (MIC > 32 μ g/mL) against Gram-positive *Staphylococcus aureus* ATCC 29213, *Bacillus subtilis* ATCC 6051, vancomycin resistant *Enterococcus faecalis* 1010798, Gram-negative *Escherichia coli* ATCC 25922, *Pseudomonas aeruginosa* 14, and *Klebsiella pneumoniae* WNX-1. This compound also showed no cytotoxicity (10 μ M) against human breast adenocarcinoma MCF-7, human ileocecal colorectal adenocarcinoma HCT-8, non-small cell lung carcinoma A549 and human hepatocellular carcinoma SMMC-7721 cell lines.

Then, the antagonistic activities of stlassins against the binding of LPS to TLR4 were assayed by ELISA. NCM460 (human colonic epithelial cell line) were grown in RPMI 1640 medium (Gibco, Grand Island, NY, USA) supplemented with 10% FBS (fetal bovine serum, Gibco, Grand Island, NY, USA) and penicillin-streptomycin (final concentration: 100 U/mL) (Gibco, Grand Island, NY, USA,) at 37 $^{\circ}$ C in a 5% CO₂ incubator, and were allowed to reach approximately 90% confluence. The cells were washed with PBS (phosphate buffered saline) and lysed with RIPA (radio immunoprecipitation assay, Sangon Biotech Co., Ltd, Shanghai, China) kit for 30 min at 4 $^{\circ}$ C. After that, the lysates were centrifuged to obtain the supernatant, which contains the NCM460 proteins including TLR4.

Mouse anti-TLR4 antibody (Sangon Biotech Co., Ltd, Shanghai, China) (2.5 μ g/well) was coated onto PVC (polyvinyl chloride) plates at 4 $^{\circ}$ C overnight and washed with TBST (Tris buffered saline containing 0.05% Tween-20, Solarbio Science & Technology Co., Ltd., Beijing, China). After blocking with TBST containing 5% powdered milk (200 μ L/well) for 1 h at room temperature, the plates were washed with TBST. Then NCM460 proteins (final concentration: 100 μ g/well) were added to the plates and allowed to incubate for 2 h at 37 $^{\circ}$ C. The plates were washed with TBST for three times. Another round of blocking with TBST containing 5% powdered milk was carried out. To test how much amounts of TLR4 proteins have been absorbed to the PVC plates, the HRP (horseradish peroxidase)-labeled rabbit anti-mouse TLR4 antibody (Sangon Biotech Co., Ltd, Shanghai, China) solution was added (200 μ L/well) and incubated for 1 h at 37 $^{\circ}$ C. Then the plates were washed with TBST for three times, and reacted with TMB (3,3',5,5'-tetramethylbenzidine, Solarbio Science & Technology Co., Ltd., Beijing, China) at room temperature in the dark for 30 min. The reaction was quenched with the addition of 10% sulfuric acid. Optical density (OD) values were measured at 450 nm using a microplate reader (SpectraMax M5, Molecular Devices, CA, USA). Determining the amount of TLR4 by such ELISA method has been commonly used in literature,²¹ and similar ELISA kit and manual are commercial available (such as Elabscience online manual at https://sceti.co.jp/images/psearch/pdf/WEB_E-EL-H1539_p.pdf). The amount of TLR4 proteins that have been absorbed to the PVC plates was calculated as 0.266 ± 0.013 ng/well, based on the linear equation ($Y = 0.2496X + 0.0882$) of OD values versus standard TLR4 concentrations (Shanghai FANKEWEI biotechnology) (Note: the linear equation was generated by adding standard TLR4 proteins with different concentrations including 0.16, 0.32, 0.63, 1.25, 2.5, 5.0, and 10 ng/mL to the mouse anti-human TLR4 antibody-coated PVC plates).

To test the antagonistic activities of stlassins against the binding of LPS to TLR4, the NCM460 proteins

(final concentration: 100 µg/well) were added to the PVC plates as described above. Then biotin-labeled LPS (InvivoGen, CA, USA) with DMSO (negative control), TAK-242 (positive control, final concentration: 1 µg/mL, MedChemexpress, NJ, USA) or stlassins (final concentration: 1 µg/mL) were added to the plates. The plates were incubated for 2 h at 37 °C, washed with TBST and incubated with HRP-labeled streptavidin for another 1 h at 37 °C. The plates were washed with TBST for three times and reacted with TMB at room temperature in the dark for 30 min. The reaction was quenched with the addition of 10% sulfuric acid. Optical density (OD) values were measured at 450 nm with four parallel experiments (Table S11) for each sample. The statistical significances (versus DMSO treatments) were generated by SPSS Statistics 25.0 (IBM, NY, USA) and GraphPad Prism 7.0 (GraphPad Software, CA, USA) using one-way ANOVA with Dunnett's test.

In above tests, we also set several control experiments N1–N4: compared to the complete ELISA procedures described above, N1 only omits the mouse anti-human TLR4 antibody in the coating step; N2 only omits the addition of the NCM460 proteins; N3 uses biotin instead of biotin-labeled LPS; and N4 uses LPS instead of biotin-labeled LPS. All N1–N4 gave only background OD values compared to the large OD values in the DMSO control experiments (Figure S14), supporting the reasonable procedures for determining TLR4-LPS binding in our ELISA experiments.

To test the antagonistic activities of stlassin and variants I4A, I4C, I4C-III, F15Y, and F15Y-I at different concentrations, we carried out more ELISA experiments by adding these compounds in different final concentrations (0.01, 0.05, 0.5, 2, 10, and 100 µM). The OD values, inhibition ratio values (inhibition ratio = $(OD_{DMSO} - OD_{compound})/OD_{DMSO} \times 100\%$) and error bars were calculated as mean \pm standard deviation from three parallel experiments, showing increased antagonistic activities along with increased concentrations (Figure S15). The IC₅₀ values were determined based on the dose-response curves using GraphPad Prism 7.0.

Table S1. The deduced functions of genes in the *stla* gene cluster.

Genes	Annotation based on BLAST			
	Numbers of amino acids	Proposed functions	Accession numbers of closest homologues	Identities with homologues
<i>Orf-13</i>	278	hypothetical protein	ACU71420.1	28.89%
<i>Orf-12</i>	172	hypothetical protein	KPL33761.1	97.06%
<i>Orf-11</i>	252	SDR family oxidoreductase	WP_098891688.1	99.60%
<i>Orf-10</i>	357	ABC transporter ATP-binding protein	WP_073746171.1	98.88%
<i>Orf-9</i>	280	ABC transporter permease	KPL33696.1	99.64%
<i>Orf-8</i>	330	ABC transporter permease	WP_073960779.1	97.06%
<i>Orf-7</i>	382	extracellular solute-binding protein	WP_057663678.1	99.48%
<i>Orf-6</i>	246	GntR family transcriptional regulator	WP_073746179.1	99.19%
<i>Orf-5</i>	215	HAD family phosphatase	WP_073746181.1	99.07%
<i>Orf-4</i>	203	dihydrofolate reductase family protein	WP_073805183.1	98.52%
<i>Orf-3</i>	397	RtcB family protein	WP_073746185.1	99.24%
<i>Orf-2</i>	290	hypothetical protein	WP_073960781.1	96.92%
<i>Orf-1</i>	286	hypothetical protein	WP_050358740.1	98.26%
<i>stlaA</i>	37	lasso RiPP family leader peptide-containing protein	WP_157420307.1	73.68%
<i>stlaC</i>	602	asparagine synthetase	EHM23871.1	98.84%
<i>stlaB1</i>	85	lasso peptide biosynthesis PqqD family chaperone	WP_069813828.1	67.06%
<i>stlaB2</i>	191	lasso peptide biosynthesis B2 protein	WP_007460371.1	93.19%
<i>Orf1</i>	228	hypothetical protein	WP_097967018.1	98.25%
<i>Orf2</i>	495	membrane protein	KND34369.1	97.05%
<i>Orf3</i>	603	lysine-tRNA ligase	WP_179890838.1	98.98%
<i>Orf4</i>	590	arginine--tRNA ligase	WP_098893103.1	98.31%

Table S2. Primers used in this study.

Primer	Sequence (5'-3')
For direct cloning (sequences underlined indicate the upstream and downstream homologous sequences of the <i>stla</i> gene cluster)	
pMM2001-F	<u>GGGACCGGGTGGTGGCCCTCCAGGCCGGGACCCCGAGACGCTGGAG</u> <u>CTGTGGCACCGCTTCGTGACGAGTCGAAGATCAGATCCGAAAACCCC</u> AAGTTACGGATCTTAAG
pMM2001-R	<u>GGGCCGGAGCGAAGCGGCCGAGGACGTCGCGGAGCTGCTCCTTGGGG</u> <u>CGTTCGCTGTAGATGTACGCCCCGCCAGATCAGATCCTTTCTCCTCTT</u> TAGATCTTTTGAATTC
For PCR confirmation of conjugation	
stla-1-F	GAACGCTCCCGGCTGGTTCTAGTAACTC
stla-1-R	GTTGAGCTGCCAGTACTCTCCGCTCTTG
For promoter <i>KasOp</i>* insertion (sequences underlined indicate the upstream and downstream homologous sequences for <i>Redaβ</i> recombineering, and the bold sequences indicate the <i>AcII</i> recognition sites)	
pMM2003-1-F	<u>CCCCAAGTCGACGACGAAGCCGAAGGCCAAGTCGAGCTGAAACGTTTC</u> GCGGAACCCCTATTTGTTTATTTTTC
pMM2003-1-R	CACGACTTTACAACACCGCACAGCATGTTGTCAAAGCAGAGACGGTTC GAATGTGAACAA ACGTTT TACCAATGCTTAATCAGTGAGGCACC
pMM2003-2-F	CCCCAAGTCGACGACGAAGCCGAAG
pMM2003-2-R	<u>CAGCGGTGAACTCAGGGGTCTCGTAGAAAGCCTTCTTCATATGGACT</u> CCTTACTTAGACTGTCGTATTCTCCTGGCCACGACTTTACAACACCGCAC AG
For PCR confirmation of <i>KasOp</i>* insertion and <i>Amp-KasOP</i>*-<i>stlaA</i> cassette preparation for <i>Redaβ</i> recombineering	
stla-2-F	GTCGACGACGAAGCCGAAGG
stla-2-R	GAAGGATGGTCGATCGACTTCAGAC
For construction of plasmid pMM2005 (sequences underlined indicate the homologous sequences for Gibson assembly)	
pMM2005-1-F	<u>GATATCGACGTCGTCGACGACGAAGCCGAAGGCC</u>
pMM2005-1-R	<u>CGGATCTGAAGGATGGTCGATCGACTTCAGACCGG</u>
pMM2005-2-F	<u>GACCATCCTTCAGATCCGAAAACCCCAAGTTACGG</u>
pMM2005-2-R	<u>CGTCGACGACGTCGATATCTGGCGAAAATGAG</u>
For <i>KasOP</i>*-<i>stlaA</i> cassette deletion (sequences underlined indicate the upstream and downstream homologous sequences of the <i>KasOP</i>*-<i>stlaA</i> cassette, and the bold sequences indicate the <i>AcII</i> recognition sites)	
pMM2006-F	<u>GTCGACGACGAAGCCGAAGGCCAAGTCGAGCTGAAACGTTTCGCGGAA</u> CCCCTATTTGTTTATTTTTC
pMM2006-R	<u>GAAGGATGGTCGATCGACTTCAGACCGGGATGCGTCGAACAACGTTT</u> ACCAATGCTTAATCAGTGAGGCACC
For site mutation (the bold codes indicate the mutation sites)	
L1A-F	AAGACCGGCGCGGTCGTCATCGTC

L1A-R ATGACGAC**CG**CGCCGGTCTTGCTG
L1C-F AAGACCGGCT**GC**GTTCATCGTC
L1C-R ATGACGAC**GC**AGCCGGTCTTGCTG
V2A-F AAGACCGGCT**GG**CGTCATCGTC
V2A-R ATGAC**GGC**CAGGCCGGTCTTGCTG
V2C-F AAGACCGGCT**GT**GCATCGTC
V2C-R ATGAC**GC**ACAGGCCGGTCTTGCTG
V3A-F GCCTGGT**CGC**CATCGTCCAGGCC
V3A-R TGGACGAT**GG**CGACCAGGCCGGTC
V3C-F GCCTGGTCT**GC**ATCGTCCAGGCC
V3C-R TGGACGAT**GC**AGACCAGGCCGGTC
I4A-F TGGTCGT**CGC**CGTCCAGGCCGAC
I4A-R CTGGAC**GGC**GACGACCAGGCCGG
I4C-F TGGTCGTCT**GC**GTCCAGGCCGAC
I4C-R CTGGAC**GC**AGACGACCAGGCCGG
V5A-F TCGTCAT**CGC**CCAGGCCGACTGG
V5A-R TCGGCCT**GGG**CGATGACGACCAGG
Q6A-F TCGTCATCGT**CG**CGCCGACTGGAAC
Q6A-R TCGGCC**CG**GACGATGACGACCAG
A7G-F TCGTCCAG**GGC**GACTGGAACGCTC
A7G-R TTCCAGT**CGC**CTGGACGATGACGACC
A7C-F TCGTCCAGT**GC**GACTGGAACGCTC
A7C-R TTCCAGT**CGC**ACTGGACGATGACGACC
D8E-F CAGGCC**GAG**TGGAACGCTCCCGG
D8E-R AGCGTT**CCA**CTCGGCCTGGACGATG
W9A-F AGGCCGAC**CGA**ACGCTCCCGGC
W9A-R AGCGTT**CGC**TCGGCCTGGACGATG
W9F-F AGGCCGACT**TCA**ACGCTCCCGGC
W9F-R AGCGTT**GA**AGTCGGCCTGGACGATG
W9Y-F AGGCCGACT**TCA**ACGCTCCCGGC
W9Y-R AGCGTT**GTA**GTTCGGCCTGGACGATG
W9R-F AGGCCGAC**CGT**AACGCTCCCGGC
W9R-R AGCGTT**AC**GGTCGGCCTGGACGATG
N10A-F AGGCCGACTGG**GC**CGCTCCCGGC
N10A-R GAGC**GGC**CCAGTTCGGCCTGGACG
A11G-F ACTGGAAC**GGC**CCCGGCTGGTTCTAG
A11G-R AGCCGGG**GC**CGTTCCAGTCGGCC
A11C-F ACTGGAAC**TG**CCCGGCTGGTTCTAG
A11C-R AGCCGGG**GC**AGTTCCAGTCGGCC
P12A-F GAACGCT**GCC**GGCTGGTTCTAGTAAC
P12A-R AACCAGC**CGG**CAGCGTTCCAGTCG
P12C-F GAACGCT**TGC**GGCTGGTTCTAGTAAC
P12C-R AACCAGC**CGA**AGCGTTCCAGTCG
G13A-F CTCCCG**CT**TGGTTCTAGTAACTCGATC

G13A-R	ACTAGAACCA A GCGGGAGCGTTCC
G13S-R	CTCCC A GCTGGTTCTAGTAACTCGATC
G13S-R	ACTAGAACC A GCTGGGAGCGTTCC
W14A-F	CCGGC G CGTTCTAGTAACTCGATCAG
W14A-R	GTTACTAGA A CGCGCCGGGAGCGTTC
W14F-F	CCGGC T CTTCTAGTAACTCGATCAGCAGGAG
W14F-R	GTTACTAGA A GAAGCCGGGAGCGTTCCAGTC
W14Y-F	CCGGC T ACTTCTAGTAACTCGATCAGCAGGAG
W14Y-R	GTTACTAGA A GTAGCCGGGAGCGTTCCAGTC
W14R-F	CCGGC C GCTTCTAGTAACTCGATCAGCAG
W14R-R	GTTACTAGA A GCGGCCGGGAGCGTTCCAG
F15A-F	CGGCTGG G CCTAGTAACTCGATCAG
F15A-R	AGTTACTAG G CCCAGCCGGGAGCG
F15Y-F	CGGCTGG T ACTAGTAACTCGATCAGCAGGAGTTG
F15Y-R	GAGTTACTAG T ACCAGCCGGGAGCGTTCCAG
F15W-F	CGGCTGG T GGTAGTAACTCGATCAGCAGGAG
F15W-R	GAGTTACTAC C ACCAGCCGGGAGCGTTCC
F15R-F	CGGCTGG C GCTAGTAACTCGATCAGCAGGAG
F15R-R	GAGTTACTAG C GCCAGCCGGGAGCGTTCC

Table S3. Plasmids and strains used in this study.

Name	Description	References
Plasmids		
p15A- <i>cm-tet^R-tet^O-hyg-ccdB</i>	PCR template to generate a linear vector for direct cloning	7
pSC101-BAD-ETgA-tet	<i>recET</i> expression plasmid for linear plus linear homologous recombination	22
pR6K-oriT-phiC31	plasmid containing the <i>apra</i> -oriT-attP- <i>int</i> cassette	7
pMM2001	p15A- <i>cm-tet^R-tet^O-hyg-ccdB</i> -derived plasmid carrying the <i>stla</i> gene cluster by direct cloning	This study
pMM2002	pMM2001-derived plasmid with chloramphenicol-resistance gene replaced by <i>apra-oriT-attP-int</i> cassette	This study
pMM2003	pMM2002-derived plasmid with <i>Amp-KasOp*</i> cassette cloned into the upstream of the <i>stlaA</i>	This study
pMM2004	pMM2003-derived plasmid with the ampicillin-resistance gene removed by <i>AcII</i> digestion and self-ligated by T4 ligase	This study
pMM2005	Plasmid used as a template for site-directed mutagenesis and constructed by Gibson assembly with p15A- <i>cm</i> cassette derived from p15A- <i>cm-tet^R-tet^O-hyg-ccdB</i> and <i>Amp-KasOp*-stlaA</i> cassette derived from pMM2003	This study
pMM2006	pMM2004-derived plasmid with <i>KasOp*-stlaA</i> cassette replaced by ampicillin-resistance gene flanked with two <i>AcII</i> recognition sites	This study
pMM2007	pMM2006-derived plasmid with the ampicillin-resistance gene removed by <i>AcII</i> digestion and self-ligated by T4 ligase	This study
pMM2008	pMM2007-derived plasmid with <i>Amp-KasOp*-stlaA</i> cassette bearing mutation of L1A inserted upstream of <i>stlaC</i> and then the <i>Amp</i> removed by <i>AcII</i> digestion and self-ligated by T4 ligase	This study
pMM2009	pMM2007-derived plasmid with <i>Amp-KasOp*-stlaA</i> cassette bearing mutation of V2A inserted upstream of <i>stlaC</i> and then the <i>Amp</i> removed by <i>AcII</i> digestion and self-ligated by T4 ligase	This study
pMM2010	pMM2007-derived plasmid with <i>Amp-KasOp*-stlaA</i> cassette bearing mutation of V3A inserted upstream of <i>stlaC</i> and then the <i>Amp</i> removed by <i>AcII</i> digestion and self-ligated by T4 ligase	This study
pMM2011	pMM2007-derived plasmid with <i>Amp-KasOp*-stlaA</i> cassette bearing mutation of I4A inserted upstream of <i>stlaC</i> and then the <i>Amp</i> removed by <i>AcII</i> digestion and self-ligated by T4 ligase	This study
pMM2012	pMM2007-derived plasmid with <i>Amp-KasOp*-stlaA</i> cassette bearing mutation of V5A inserted upstream of <i>stlaC</i> and then the <i>Amp</i> removed by <i>AcII</i> digestion and self-ligated by T4 ligase	This study

pMM2013	pMM2007-derived plasmid with <i>Amp-KasOp</i> *- <i>stlaA</i> cassette bearing mutation of Q6A inserted upstream of <i>stlaC</i> and then the <i>Amp</i> removed by <i>AcII</i> digestion and self-ligated by T4 ligase	This study
pMM2014	pMM2007-derived plasmid with <i>Amp-KasOp</i> *- <i>stlaA</i> cassette bearing mutation of A7G inserted upstream of <i>stlaC</i> and then the <i>Amp</i> removed by <i>AcII</i> digestion and self-ligated by T4 ligase	This study
pMM2015	pMM2007-derived plasmid with <i>Amp-KasOp</i> *- <i>stlaA</i> cassette bearing mutation of D8E inserted upstream of <i>stlaC</i> and then the <i>Amp</i> removed by <i>AcII</i> digestion and self-ligated by T4 ligase	This study
pMM2016	pMM2007-derived plasmid with <i>Amp-KasOp</i> *- <i>stlaA</i> cassette bearing mutation of W9A inserted upstream of <i>stlaC</i> and then the <i>Amp</i> removed by <i>AcII</i> digestion and self-ligated by T4 ligase	This study
pMM2017	pMM2007-derived plasmid with <i>Amp-KasOp</i> *- <i>stlaA</i> cassette bearing mutation of W9R inserted upstream of <i>stlaC</i> and then the <i>Amp</i> removed by <i>AcII</i> digestion and self-ligated by T4 ligase	This study
pMM2018	pMM2007-derived plasmid with <i>Amp-KasOp</i> *- <i>stlaA</i> cassette bearing mutation of W9F inserted upstream of <i>stlaC</i> and then the <i>Amp</i> removed by <i>AcII</i> digestion and self-ligated by T4 ligase	This study
pMM2019	pMM2007-derived plasmid with <i>Amp-KasOp</i> *- <i>stlaA</i> cassette bearing mutation of W9Y inserted upstream of <i>stlaC</i> and then the <i>Amp</i> removed by <i>AcII</i> digestion and self-ligated by T4 ligase	This study
pMM2020	pMM2007-derived plasmid with <i>Amp-KasOp</i> *- <i>stlaA</i> cassette bearing mutation of N10A inserted upstream of <i>stlaC</i> and then the <i>Amp</i> removed by <i>AcII</i> digestion and self-ligated by T4 ligase	This study
pMM2021	pMM2007-derived plasmid with <i>Amp-KasOp</i> *- <i>stlaA</i> cassette bearing mutation of A11G inserted upstream of <i>stlaC</i> and then the <i>Amp</i> removed by <i>AcII</i> digestion and self-ligated by T4 ligase	This study
pMM2022	pMM2007-derived plasmid with <i>Amp-KasOp</i> *- <i>stlaA</i> cassette bearing mutation of P12A inserted upstream of <i>stlaC</i> and then the <i>Amp</i> removed by <i>AcII</i> digestion and self-ligated by T4 ligase	This study
pMM2023	pMM2007-derived plasmid with <i>Amp-KasOp</i> *- <i>stlaA</i> cassette bearing mutation of G13A inserted upstream of <i>stlaC</i> and then the <i>Amp</i> removed by <i>AcII</i> digestion and self-ligated by T4 ligase	This study

pMM2024	pMM2007-derived plasmid with <i>Amp-KasOp</i> *- <i>stlaA</i> cassette bearing mutation of G13S inserted upstream of <i>stlaC</i> and then the <i>Amp</i> removed by <i>AcII</i> digestion and self-ligated by T4 ligase	This study
pMM2025	pMM2007-derived plasmid with <i>Amp-KasOp</i> *- <i>stlaA</i> cassette bearing mutation of W14A inserted upstream of <i>stlaC</i> and then the <i>Amp</i> removed by <i>AcII</i> digestion and self-ligated by T4 ligase	This study
pMM2026	pMM2007-derived plasmid with <i>Amp-KasOp</i> *- <i>stlaA</i> cassette bearing mutation of W14R inserted upstream of <i>stlaC</i> and then the <i>Amp</i> removed by <i>AcII</i> digestion and self-ligated by T4 ligase	This study
pMM2027	pMM2007-derived plasmid with <i>Amp-KasOp</i> *- <i>stlaA</i> cassette bearing mutation of W14F inserted upstream of <i>stlaC</i> and then the <i>Amp</i> removed by <i>AcII</i> digestion and self-ligated by T4 ligase	This study
pMM2028	pMM2007-derived plasmid with <i>Amp-KasOp</i> *- <i>stlaA</i> cassette bearing mutation of W14Y inserted upstream of <i>stlaC</i> and then the <i>Amp</i> removed by <i>AcII</i> digestion and self-ligated by T4 ligase	This study
pMM2029	pMM2007-derived plasmid with <i>Amp-KasOp</i> *- <i>stlaA</i> cassette bearing mutation of F15A inserted upstream of <i>stlaC</i> and then the <i>Amp</i> removed by <i>AcII</i> digestion and self-ligated by T4 ligase	This study
pMM2030	pMM2007-derived plasmid with <i>Amp-KasOp</i> *- <i>stlaA</i> cassette bearing mutation of F15R inserted upstream of <i>stlaC</i> and then the <i>Amp</i> removed by <i>AcII</i> digestion and self-ligated by T4 ligase	This study
pMM2031	pMM2007-derived plasmid with <i>Amp-KasOp</i> *- <i>stlaA</i> cassette bearing mutation of F15Y inserted upstream of <i>stlaC</i> and then the <i>Amp</i> removed by <i>AcII</i> digestion and self-ligated by T4 ligase	This study
pMM2032	pMM2007-derived plasmid with <i>Amp-KasOp</i> *- <i>stlaA</i> cassette bearing mutation of F15W inserted upstream of <i>stlaC</i> and then the <i>Amp</i> removed by <i>AcII</i> digestion and self-ligated by T4 ligase	This study
pMM2033	pMM2007-derived plasmid with <i>Amp-KasOp</i> *- <i>stlaA</i> cassette bearing double mutation of L1C/A11C inserted upstream of <i>stlaC</i> and then the <i>Amp</i> removed by <i>AcII</i> digestion and self-ligated by T4 ligase	This study
pMM2034	pMM2007-derived plasmid with <i>Amp-KasOp</i> *- <i>stlaA</i> cassette bearing double mutation of V2C/A11C inserted upstream of <i>stlaC</i> and then the <i>Amp</i> removed by <i>AcII</i> digestion and self-ligated by T4 ligase	This study

pMM2035	pMM2007-derived plasmid with <i>Amp-KasOp</i> *- <i>stlaA</i> cassette bearing double mutation of V3C/P12C inserted upstream of <i>stlaC</i> and then the <i>Amp</i> removed by <i>AcII</i> digestion and self-ligated by T4 ligase	This study
pMM2036	pMM2007-derived plasmid with <i>Amp-KasOp</i> *- <i>stlaA</i> cassette bearing double mutation of A7C/P12C inserted upstream of <i>stlaC</i> and then the <i>Amp</i> removed by <i>AcII</i> digestion and self-ligated by T4 ligase	This study
pMM2037	pMM2007-derived plasmid with <i>Amp-KasOp</i> *- <i>stlaA</i> cassette bearing mutation of I4C inserted upstream of <i>stlaC</i> and then the <i>Amp</i> removed by <i>AcII</i> digestion and self-ligated by T4 ligase	This study
<i>E. coli</i> strains		
GB2005	Host strain of general clone	7
GB05RedTrfA	Host strain containing the Red $\alpha\beta$ system for linear plus circular homologous recombination	7
ET12567/pUZ8002	Donor strain for conjugation	23
<i>Streptomyces</i> strains		
<i>S. sp.</i> PKU-MA01240	Wild-type strain bearing gene cluster <i>stla</i>	This study
<i>S. coelicolor</i> A3(2)	Recipient strain for heterologous expression	24
<i>S. lividans</i> K4-114	Recipient strain for heterologous expression	25
MM20001	<i>S. coelicolor</i> A3(2) with the plasmid pMM2002 integrated	This study
MM20002	<i>S. lividans</i> K4-114 with the plasmid pMM2002 integrated	This study
MM20003	<i>S. coelicolor</i> A3(2) with the plasmid pMM2004 integrated	This study
MM20004	<i>S. lividans</i> K4-114 with the plasmid pMM2004 integrated	This study
MM20005	<i>S. coelicolor</i> A3(2) with the plasmid pMM2008 integrated	This study
MM20006	<i>S. coelicolor</i> A3(2) with the plasmid pMM2009 integrated	This study
MM20007	<i>S. coelicolor</i> A3(2) with the plasmid pMM2010 integrated	This study
MM20008	<i>S. coelicolor</i> A3(2) with the plasmid pMM2011 integrated	This study
MM20009	<i>S. coelicolor</i> A3(2) with the plasmid pMM2012 integrated	This study
MM20010	<i>S. coelicolor</i> A3(2) with the plasmid pMM2013 integrated	This study
MM20011	<i>S. coelicolor</i> A3(2) with the plasmid pMM2014 integrated	This study
MM20012	<i>S. coelicolor</i> A3(2) with the plasmid pMM2015 integrated	This study
MM20013	<i>S. coelicolor</i> A3(2) with the plasmid pMM2016 integrated	This study
MM20014	<i>S. coelicolor</i> A3(2) with the plasmid pMM2017 integrated	This study
MM20015	<i>S. coelicolor</i> A3(2) with the plasmid pMM2018 integrated	This study
MM20016	<i>S. coelicolor</i> A3(2) with the plasmid pMM2019 integrated	This study
MM20017	<i>S. coelicolor</i> A3(2) with the plasmid pMM2020 integrated	This study
MM20018	<i>S. coelicolor</i> A3(2) with the plasmid pMM2021 integrated	This study
MM20019	<i>S. coelicolor</i> A3(2) with the plasmid pMM2022 integrated	This study
MM20020	<i>S. coelicolor</i> A3(2) with the plasmid pMM2023 integrated	This study
MM20021	<i>S. coelicolor</i> A3(2) with the plasmid pMM2024 integrated	This study
MM20022	<i>S. coelicolor</i> A3(2) with the plasmid pMM2025 integrated	This study
MM20023	<i>S. coelicolor</i> A3(2) with the plasmid pMM2026 integrated	This study

MM20024	<i>S. coelicolor</i> A3(2) with the plasmid pMM2027 integrated	This study
MM20025	<i>S. coelicolor</i> A3(2) with the plasmid pMM2028 integrated	This study
MM20026	<i>S. coelicolor</i> A3(2) with the plasmid pMM2029 integrated	This study
MM20027	<i>S. coelicolor</i> A3(2) with the plasmid pMM2030 integrated	This study
MM20028	<i>S. coelicolor</i> A3(2) with the plasmid pMM2031 integrated	This study
MM20029	<i>S. coelicolor</i> A3(2) with the plasmid pMM2032 integrated	This study
MM20030	<i>S. coelicolor</i> A3(2) with the plasmid pMM2033 integrated	This study
MM20031	<i>S. coelicolor</i> A3(2) with the plasmid pMM2034 integrated	This study
MM20032	<i>S. coelicolor</i> A3(2) with the plasmid pMM2035 integrated	This study
MM20033	<i>S. coelicolor</i> A3(2) with the plasmid pMM2036 integrated	This study
MM20034	<i>S. coelicolor</i> A3(2) with the plasmid pMM2037 integrated	This study

Table S4. The HRESIMS data of compounds **1-25**. For most compounds, the negative ion mode gave more clearer signals than the positive mode.

Compounds	Molecular formula	Calculated m/z for $[M-H]^-$	Determined m/z for $[M-H]^-$
stlassin (1)	C ₈₄ H ₁₁₇ N ₁₉ O ₁₉	1694.8694	1694.8662
stlassin V2A (2)	C ₈₂ H ₁₁₃ N ₁₉ O ₁₉	1666.8381	1666.8405
stlassin V3A (3)	C ₈₂ H ₁₁₃ N ₁₉ O ₁₉	1666.8381	1666.8388
stlassin I4A (4)	C ₈₁ H ₁₁₁ N ₁₉ O ₁₉	1652.8225	1652.8242
stlassin V5A (5)	C ₈₂ H ₁₁₃ N ₁₉ O ₁₉	1666.8381	1666.8333
stlassin Q6A (6)	C ₈₂ H ₁₁₄ N ₁₈ O ₁₈	1637.8480	1637.8478
stlassin N10A (7)	C ₈₃ H ₁₁₆ N ₁₈ O ₁₈	1651.8636	1651.8573
stlassin A11G (8)	C ₈₃ H ₁₁₅ N ₁₉ O ₁₉	1680.8538	1680.8490
stlassin P12A (9)	C ₈₂ H ₁₁₅ N ₁₉ O ₁₉	1668.8538	1668.8528
stlassin L1A (10)	C ₈₁ H ₁₁₁ N ₁₉ O ₁₉	1652.8225	1652.8276
stlassin A7G (11)	C ₈₃ H ₁₁₅ N ₁₉ O ₁₉	1680.8538	1680.8539
stlassin W9F (12)	C ₈₂ H ₁₁₆ N ₁₈ O ₁₉	1655.8585	1655.8507
stlassin W9Y (13)	C ₈₂ H ₁₁₆ N ₁₈ O ₂₀	1671.8534	1671.8504
stlassin W14F (14)	C ₈₂ H ₁₁₆ N ₁₈ O ₁₉	1655.8585	1655.8571
stlassin W14Y (15)	C ₈₂ H ₁₁₆ N ₁₈ O ₂₀	1671.8534	1671.8534
stlassin F15Y (16)	C ₈₄ H ₁₁₇ N ₁₉ O ₂₀	1710.8643	1710.8608
stlassin F15W (17)	C ₈₆ H ₁₁₈ N ₂₀ O ₁₉	1733.8803	1733.8746
stlassin I4C (21)	C ₈₁ H ₁₁₁ N ₁₉ O ₁₉ S	1684.7945	1684.7978
stlassin I4C-I (22)	C ₈₇ H ₁₂₁ N ₁₉ O ₂₄ S	1846.8474	1846.8480
stlassin I4C-III (24)	C ₈₇ H ₁₁₄ N ₂₀ O ₂₁ S	1805.8109	1805.8148
Compounds	Molecular formula	Calculated m/z for $[M+H]^+$	Determined m/z for $[M+H]^+$
Stlassin I4C-IV (25)	C ₈₁ H ₁₀₉ N ₁₉ O ₁₉	1652.8225	1652.8258
Compounds	Molecular formula	Calculated m/z for $[M-2H]^{2-}$	Determined m/z for $[M-2H]^{2-}$
stlassin V2C/A11C (18)	C ₈₂ H ₁₁₁ N ₁₉ O ₁₉ S ₂	863.8794	863.8757
stlassin V3C/P12C (19)	C ₈₀ H ₁₀₉ N ₁₉ O ₁₉ S ₂	850.8716	850.8723
stlassin F15Y-I (20)	C ₉₀ H ₁₂₇ N ₁₉ O ₂₅	935.9547	935.9551
stlassin I4C-II (23)	C ₁₆₂ H ₂₂₀ N ₃₈ O ₃₈ S ₂	1683.7868	1683.7888
Stlassin D8E	C ₈₅ H ₁₁₉ N ₁₉ O ₁₉	853.9386	853.9380

Table S5. Assignment of ^1H , ^{13}C and ^{15}N signals (ppm) of stlassin (**1**). The signals were assigned based on TOCSY, NOESY, ^1H - ^{13}C HSQC and ^1H - ^{15}N HSQC spectra

Residue	Atom	δ_{H}	$\delta_{\text{C}}/\delta_{\text{N}}$	Residue	Atom	δ_{H}	$\delta_{\text{C}}/\delta_{\text{N}}$
Leu1	NH	8.48	119.33	Trp9	NH	6.40	110.55
	α	4.45	55.15		N ϵ		131.14
	β	1.62, 1.72	44.18		α	4.16	59.89
	γ	1.45	27.39		β	3.13, 3.22	29.00
	δ	0.76	23.53		δ	7.28	
		0.98		ϵ	7.57	120.66	
Val2	NH	8.55	125.88			10.55	
	α	4.20	61.57	ζ	7.28	122.65	
	β	1.78	29.76		7.63	115.34	
	γ	0.77	22.13	η	7.36	125.24	
		1.12	25.73	Asn10	NH	7.43	113.38
Val3	NH	8.10	118.92		α	4.83	
	α	4.34	66.58	β	2.32, 2.34	40.79	
	β	2.12	36.23	Ala11	NH	7.93	125.73
	γ	0.93	22.21		α	4.65	20.78
		0.93	22.21	β	1.38		
Ile4	NH	9.71	123.36	Pro12	α	4.23	64.63
	α	4.44	61.42		β	1.92, 2.37	32.78
	β	1.89	40.55		γ	1.90, 2.03	27.58
	γ	1.10	18.35		δ	3.65, 3.75	51.16
			1.25, 1.63	27.59	Gly13	NH	6.81
δ	0.91	13.26	α	2.92, 4.82		44.33	
Val5	NH	8.60	119.92	Trp14	NH	8.46	120.65
	α	3.42	66.88		N ϵ		130.24
	β	3.48	29.28		α	4.29	59.07
	γ	1.08	22.20		β	2.17, 2.30	31.84
		1.25	22.33	δ	6.77	127.49	
Gln6	NH	8.64	126.87	ϵ	7.55	121.11	
	N ϵ		112.03		9.93		
	α	4.69		ζ	6.95	121.50	
	β	2.04, 2.10	29.67		7.30	115.07	
	γ	2.58, 2.61	34.20	η	6.87	123.73	
	ϵ	6.92, 7.69		Phe15	NH	9.20	123.03
Ala7	NH	7.13	124.76		α	4.85	
	α	3.86	53.81		β	2.73, 3.46	42.35
	β	1.34	24.13	δ	7.36		
Asp8	NH	5.63					
	α	3.00	50.29				
	β	1.60, 2.18	38.12				

Table S6. Assignment of ^1H , ^{13}C and ^{15}N signals (ppm) of stlassin V3A (**3**). The signals were assigned based on TOCSY, NOESY, ^1H - ^{13}C HSQC and ^1H - ^{15}N HSQC spectra

Residue	Atom	δ_{H}	$\delta_{\text{C}}/\delta_{\text{N}}$	Residue	Atom	δ_{H}	$\delta_{\text{C}}/\delta_{\text{N}}$
Leu1	NH	8.48		Asp8	NH	5.81	114.99
	α	4.39			α	3.08	50.23
	β	1.67		β	1.57, 2.10		
		1.57		Trp9	NH	6.51	111.54
	γ	1.43			α	4.15	
	δ	0.74			β	3.12, 3.18	
	0.95		δ		7.25		
Val2	NH	8.41	124.85	ϵ	10.48		
	α	4.10	61.82	ζ	7.59	115.13	
	β	1.67	29.80	Asn10	NH	7.45	113.89
	γ	0.76			α	4.75	
	1.01		β	2.30, 2.30	40.52		
Ala3	NH	8.17	124.37	δ	6.52, 7.17		
	α	4.60		Ala11	NH	7.90	125.29
	β	1.45	23.10		α	4.64	
Ile4	NH	9.73	121.94	β	1.32		
	α	4.39		Pro12	α	4.21	
	β	1.89			β	1.88, 2.34	32.75
	γ	1.06			γ	1.90, 2.01	27.62
		1.21, 1.55			δ	3.64, 3.73	
	δ	1.06		Gly13	NH	6.67	100.55
			α		2.93, 4.71		
Val5	NH	8.63	120.53	Trp14	NH	8.45	
	α	3.42	66.93		α	4.23	
	β	3.46			β	2.16, 2.28	
	γ	1.24			δ	6.69	127.39
	1.07		ϵ	9.89			
Gln6	NH	8.66	126.69	ζ	7.15		
	α	4.62		Phe15	NH	9.24	123.01
	β	2.02, 2.05	29.62		α	4.83	
	γ	2.57	34.11		β	2.75, 3.45	42.25
Ala7	NH	7.15	124.68	δ	7.36	132.54	
	α	3.85	53.82				
	β	1.32					

Table S7. Assignment of ^1H , ^{13}C and ^{15}N signals (ppm) of stlassin I4A (**4**). The signals were assigned based on TOCSY, NOESY, ^1H - ^{13}C HSQC and ^1H - ^{15}N HSQC spectra

Residue	Atom	δ_{H}	$\delta_{\text{C}}/\delta_{\text{N}}$	Residue	Atom	δ_{H}	$\delta_{\text{C}}/\delta_{\text{N}}$
Leu1	NH	8.12	120.61	Trp9	NH	7.70	
	α	4.54			N ϵ		130.02
	β	1.50, 1.66	44.81		α	4.39	59.72
	γ	1.44	27.35		β	3.14, 3.31	29.03
	δ	0.77	23.69		δ	7.25	
Val2		0.87	25.27	ϵ	7.56		
	NH	7.91	120.04		10.24		
	α	4.31	60.95	ζ	7.12	122.16	
	β	1.83	31.98		7.48		
	γ	0.63	20.47	η	7.22		
Val3		0.93	23.15	Asn10	NH	7.88	
	NH	7.75	119.01		α	4.70	
	α	3.99	64.35	β	2.23, 2.30	40.29	
	β	2.05	33.44	δ	6.55, 7.12		
	γ	0.89	21.42	Ala11	NH	8.08	124.25
	0.90	21.37	α		4.68		
Ala4	NH	7.09		β	1.29	20.25	
	α	3.86		Pro12	α	4.53	
	β	1.33			β	2.09, 2.20	31.24
Val5	α	3.93			γ	1.99, 1.99	27.76
	β	2.51	31.74	δ	3.59, 3.64	50.50	
	γ	0.96	21.62	Gly13	NH	7.39	
	0.96	21.62	α		4.07, 3.31	46.04	
Gln6	NH	8.13	119.29	Trp14	NH	8.32	119.65
	α	4.30	56.19		N ϵ		129.50
	β	2.09, 2.13	28.97		α	4.68	
	γ	2.21, 2.21	33.94		β	2.99, 3.44	31.35
	ϵ	6.65, 7.16			δ	6.57	126.92
Ala7	NH	7.83	122.75	ϵ	7.54		
	α	4.23			10.12		
	β	1.38	20.49	ζ	7.13	122.06	
	Asp8	NH	7.94			7.48	114.82
α		4.81		η	7.22		
β		2.75, 2.89	39.46	Phe15	NH	7.71	
			α		4.45	58.57	
			β		2.83, 3.08	41.06	
			δ		7.10		
			ϵ		7.22		

Table S8. Assignment of ^1H signals (ppm) of stlassin W14F (**14**). The signals were assigned based on TOCSY, NOESY and ^1H - ^{13}C HSQC spectra

Residue	Atom	δ_{H}	Residue	Atom	δ_{H}	
Leu1	NH	8.34	Asp8	NH	6.00	
	α	4.47		α	4.30	
	β	1.56, 1.71		β	2.13, 3.20	
	γ	1.49	Trp9	NH	7.50	
	δ	0.68		α	4.28	
	0.93	β		3.06, 3.41		
Val2	NH	8.55	δ	7.30		
	α	4.17	ϵ	7.55		
	β	1.72		10.26		
	γ	0.71	ζ	7.13		
		1.07		7.47		
Val3	NH	8.09	η	7.21		
	α	4.30	Asn10	NH	7.33	
	β	2.10		α	4.72	
	γ	0.90		β	1.87, 1.95	
	0.90	δ		6.43, 6.94		
Ile4	NH	9.66	Ala11	NH	7.96	
	α	4.40		α	4.63	
	β	1.86		β	1.37	
	γ	1.07		Pro	α	4.24
		1.22, 1.61			β	1.93, 2.35
δ	0.87	γ	1.96, 2.01			
Val5	NH	8.57	δ	3.63, 3.74		
	α	3.39	Gly13	NH	6.82	
	β	3.45		α	2.89, 4.82	
	γ	1.06	Phe14	NH	8.47	
	1.23	α		4.30		
β	2.02, 2.07	β		2.03, 2.11		
Gln6	NH	8.54	δ	6.92		
	α	4.62	ϵ	7.21		
	β	2.02, 2.07	Phe15	NH	9.21	
	γ	2.57, 2.57		α	4.79	
		β		2.72, 3.42		
Ala7	NH	6.79	δ	7.32		
	α	3.87	ϵ	7.17		
	β	1.36				

Table S9. Assignment of ^1H signals (ppm) of stlassin F15Y (**16**). The signals were assigned based on TOCSY, NOESY and ^1H - ^{13}C HSQC spectra

Residue	Atom	δ_{H}	Residue	Atom	δ_{H}
Leu1	NH	8.46	Trp9	NH	6.43
	α	4.44		α	4.15
	β	1.60, 1.70		β	3.12, 3.20
	γ	1.45		δ	7.27
	δ	0.75		ϵ	7.55
Val2	NH	8.54			10.54
	α	4.19	ζ	7.27	
	β	1.76		7.61	
	γ	0.75	η	7.34	
		1.08	Asn10	NH	7.42
Val3	NH	7.95	α	4.81	
	α	4.33	β	2.30, 2.30	
	β	2.10	Ala11	NH	7.92
	γ	0.91	α	4.63	
Ile4	NH	9.50	β	1.37	
	α	4.42	Pro12	α	4.21
	β	1.83	β	1.90, 2.35	
	γ	1.05	γ	1.91, 2.00	
		1.20, 1.59	δ	3.64, 3.73	
Val5	NH	8.57	Gly13	NH	6.81
	α	3.39	α	2.89, 4.80	
	β	3.39	Trp14	NH	8.46
	γ	1.05	α	4.33	
		1.20	β	2.32, 2.40	
Gln6	NH	8.61	δ	6.77	
	α	4.67	ϵ	7.56	
	β	2.03, 2.07		9.93	
	γ	2.56	ζ	6.94	
		2.58		7.30	
Ala7	NH	7.11	η	6.86	
	α	3.86	Tyr15	NH	9.11
	β	1.33	α	4.79	
			β	2.63, 3.32	
Asp8	NH	5.70	δ	7.18	
	α	3.08	ϵ	6.75	
	β	1.65, 2.23			

Table S10. Assignment of ^1H signals and ^{13}C signals (ppm) of stlassin V2C/A11C (**18**). The signals were assigned based on TOCSY, NOESY and ^1H - ^{13}C HSQC spectra.

Residue	Atom	δ_{H}	$\delta_{\text{C}}/\delta_{\text{N}}$	Residue	Atom	δ_{H}	$\delta_{\text{C}}/\delta_{\text{N}}$	
Leu1	NH	7.98		Trp9	NH	9.09		
	α	4.30	49.93		α	4.10	55.91	
	β	1.60, 1.22	40.95		β	2.97, 3.22	26.19	
	γ	1.22	23.57		δ	7.13		
	δ	0.71, 0.32	21.32		ϵ	7.51	117.89	
Cys2	NH	8.24				10.81		
	α	4.24	50.65	ζ	6.96	118.22		
	β	3.04, 3.71	32.51		7.31	111.23		
Val3	NH	8.55		η	7.03	120.86		
	α	3.95	58.91	Asn10	NH	8.03		
	β	1.57	25.48		α	4.42	51.85	
	γ	0.43	19.90		β	2.53, 2.58	36.89	
	0.83	23.01	δ		7.25, 6.85			
Ile4	NH	8.38		Cys11	NH	6.85		
	α	4.33	60.06		α	4.43	49.76	
	β	2.22	36.57		β	2.57, 3.38	34.81	
	γ	0.81	15.72		Pro12	α	4.39	61.67
		0.97, 1.39	25.13			β	1.69, 2.16	29.57
δ	0.81	10.20	γ	1.87, 1.99		24.91		
Val5	NH	9.62		δ	3.75, 3.44	47.15		
	α	4.57	57.38	Gly13	NH	6.55		
	β	1.67	32.47		α	3.99, 3.22	42.00	
	γ	0.82		Trp14	NH	8.38		
Gln6	NH	8.59			α	4.12	56.64	
	α	3.69	55.91		β	2.98, 3.41	27.51	
	β	2.39, 2.86	24.01		δ	6.21	123.15	
	γ	2.22, 2.39	32.74		ϵ	7.71	119.06	
	ϵ	6.99, 7.45			10.42			
Ala7	NH	8.19		ζ	6.96	118.22		
	α	4.23	49.10		7.22	110.36		
	β	1.11	17.73	η	6.98	120.01		
Asp8	NH	7.77		Phe15	NH	8.01		
	α	4.46	48.92		α	4.20	54.38	
	β	3.61, 2.41	37.85		β	2.92, 2.87	38.02	
			δ		7.12	127.57		
			ϵ		7.12	129.69		
			ζ		7.04	125.31		

Table S11. The Optical density (OD) values and inhibition ratios (% in parentheses) from parallel ELISA experiments for each stlassins against the binding of LPS to TLR4. N1–N4 represent four control experiments.

Compounds or controls	OD ₄₅₀ values (inhibition ratios (%)) from three or four parallel experiments				SD
N1	0.039	0.034	0.045		0.0056
N2	0.042	0.053	0.066		0.0120
N3	0.041	0.035	0.036		0.0034
N4	0.042	0.036	0.035		0.0036
DMSO	0.837	0.807	0.792	0.822	0.0643
TAK-242	0.464 (44.56)	0.453 (43.87)	0.441 (44.32)	0.430 (47.69)	0.0251
stlassin (1)	0.563 (32.74)	0.549 (31.97)	0.535 (32.45)	0.521 (36.62)	0.0184
L1A (10)	0.839 (-0.24)	0.821 (-1.74)	0.803 (-1.39)	0.785 (4.50)	0.0232
V2A (2)	0.840 (-0.36)	0.804 (0.37)	0.786 (0.76)	0.822 (0.00)	0.0232
V3A (3)	0.828 (1.08)	0.824 (-2.11)	0.820 (-3.54)	0.816 (0.73)	0.0052
I4A (4)	0.508 (39.31)	0.489 (39.41)	0.469 (40.78)	0.450 (45.26)	0.0246
I4C (21)	0.507 (39.43)	0.496 (38.54)	0.484 (38.89)	0.473 (42.46)	0.0146
I4C-III (24)	0.489 (41.58)	0.483 (40.15)	0.477 (39.77)	0.471 (42.70)	0.0073
V5A (5)	0.823 (1.67)	0.811 (-0.50)	0.805 (-1.64)	0.817 (0.61)	0.0077
Q6A (6)	0.710 (15.17)	0.699 (13.38)	0.687 (13.26)	0.676 (17.76)	0.0150
A7G (11)	0.687 (17.92)	0.673 (16.61)	0.659 (16.69)	0.645 (21.53)	0.0184
N10A (7)	0.840 (-0.36)	0.839 (-3.97)	0.839 (-5.93)	0.838 (-1.95)	0.0012
A11G (8)	0.709 (15.29)	0.691 (14.35)	0.673 (15.03)	0.655 (20.33)	0.0232
P12A (9)	0.690 (17.56)	0.672 (16.73)	0.654 (17.42)	0.636 (22.63)	0.0234
W9F (12)	0.838 (-0.12)	0.834 (-3.36)	0.830 (-4.80)	0.826 (-0.49)	0.0052
W14F (14)	0.884 (-5.62)	0.865 (-7.19)	0.845 (-6.69)	0.826 (-0.49)	0.0246
W14Y (15)	0.842 (-0.60)	0.831 (-2.97)	0.819 (-3.41)	0.808 (1.70)	0.0146
F15Y (16)	0.423 (49.46)	0.417 (48.33)	0.411 (48.11)	0.405 (50.73)	0.0073
F15Y-I (20)	0.419 (49.94)	0.420 (47.96)	0.400 (49.49)	0.404 (50.85)	0.0073
V2C/A11C (18)	0.669 (20.07)	0.664 (17.72)	0.658 (16.92)	0.653 (20.56)	0.0065
V3C/P12C (19)	0.662 (20.91)	0.661 (18.09)	0.661 (16.54)	0.660 (19.71)	0.0012

Table S12. Inhibition ratios from parallel ELISA experiments for each concentration in dose-response determination.

compounds	Concentration (μM)	Inhibition ratio (%) from three parallel experiments			SD
stlassin (1)	0.01	11.45	8.58	8.87	1.580
	0.05	9.79	6.72	9.70	1.747
	0.50	41.95	38.28	40.41	1.843
	2.00	67.07	67.06	68.07	0.580
	10.00	85.64	82.04	85.87	2.148
	100.00	89.26	87.87	91.15	1.646
I4A (4)	0.01	10.15	10.92	11.57	0.711
	0.05	31.21	33.02	34.80	1.795
	0.50	38.92	38.085	40.56	1.259
	2.00	51.00	50.18	52.61	1.236
	10.00	59.08	57.91	60.39	1.241
	100.00	71.29	67.93	71.53	2.013
I4C (21)	0.01	3.44	3.77	4.37	0.471
	0.05	11.15	11.82	13.93	1.451
	0.50	31.95	29.84	29.86	1.212
	2.00	46.00	47.91	49.93	1.965
	10.00	59.85	58.70	59.24	0.575
	100.00	74.57	74.21	75.30	0.555
I4C-III (24)	0.01	5.65	4.47	5.11	0.591
	0.05	25.36	26.91	26.72	0.845
	0.50	33.91	33.07	35.48	1.223
	2.00	46.12	47.22	48.87	1.384
	10.00	59.61	59.92	61.41	0.962
	100.00	66.54	65.76	68.08	1.181
F15Y (16)	0.01	11.27	12.24	10.16	1.041
	0.05	27.74	28.84	29.43	0.858
	0.50	52.53	52.09	52.13	0.243
	2.00	61.60	59.39	61.67	1.297
	10.00	70.39	68.23	70.16	1.186
	100.00	79.60	79.72	79.28	0.227
F15Y-I (20)	0.01	16.14	12.69	10.86	2.681
	0.05	32.91	29.76	28.57	2.243
	0.50	44.53	44.33	45.54	0.649
	2.00	64.37	62.86	62.28	1.079
	10.00	73.052	72.71	73.87	0.596
	100.00	75.40	74.57	74.97	0.415

Figure S1. The phylogenetic analysis of strain PKU-MA01240 (labeled in red) based on comparison of 16S rRNA sequences. The sequence of 16S rRNA of *Kitasatospora azatica* strain OS-3256 was used as an outgroup. The GenBank accession numbers are shown in parentheses.

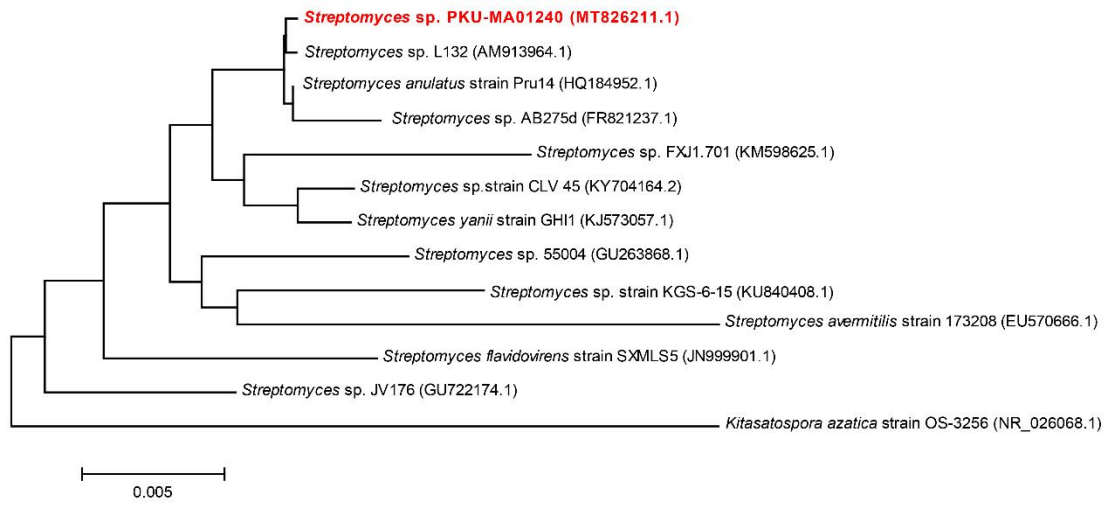


Figure S2. The construction of plasmid pMM2002 for the heterologous expression. (A) The diagram for the construction of pMM2002 using RecET-mediated direct cloning and Red $\alpha\beta$ -mediated recombineering. The black bars labeled with “*Bgl*III” indicate the *Bgl*III restriction sites. (B) The verification of the plasmid pMM2001 construction by *Apa*LI digestion followed by agarose gel electrophoresis analysis. Lane 1-8, the digestion of plasmids extracted from eight *E. coli* single colonies after the RecET-mediated direct cloning; lane M, DNA ladder; lane 9 and lane M', the predicted digestion of pMM2001 by *Apa*LI and predicted DNA ladder, respectively, generated by SnapGene software. (C) The verification of the plasmid pMM2002 construction by *Apa*LI digestion followed by agarose gel electrophoresis analysis. Lane 1, the digestion of pMM2001 as the negative control; lane 2-9, the digestion of plasmids extracted from eight *E. coli* single colonies after the Red $\alpha\beta$ -mediated recombineering; lane M, DNA ladder; lane 10 and lane M', the predicted digestion of pMM2002 by *Apa*LI and predicted DNA ladder, respectively, generated by SnapGene software. The lanes labeled with asterisks represent the digestion of correct plasmids.

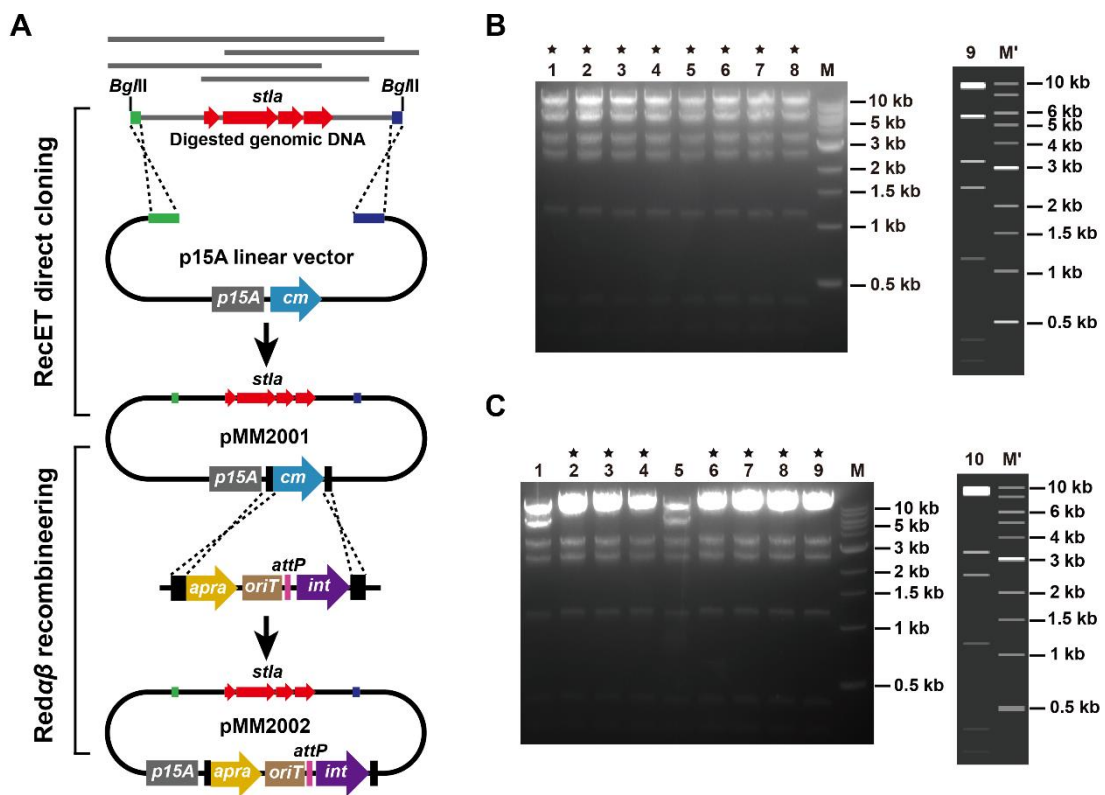


Figure S3. Comparative HPLC analysis of fermentations of heterologous expression strains using three different media. Lane I, fermentation of strain MM20003 using media M2; lane II, fermentation of strain MM20001 using media M2; lane III, fermentation of heterologous host *S. coelicolor* A3(2) using media M2; lane IV, fermentation of strain MM20003 using media M3; lane V, fermentation of strain MM20001 using media M3; lane VI, fermentation of heterologous host *S. coelicolor* A3(2) using media M3; lane VII, fermentation of strain MM20003 using media M4; lane VIII, fermentation of strain MM20001 using media M4; lane IX, fermentation of heterologous host *S. coelicolor* A3(2) using media M4; lane X, fermentation of strain MM20004 using media M2; lane XI, fermentation of strain MM20002 using media M2; lane XII, fermentation of heterologous host *S. lividans* K4-114 using media M2; lane XIII, fermentation of strain MM20004 using media M3; lane XIV, fermentation of strain MM20002 using media M3; lane XV, fermentation of heterologous host *S. lividans* K4-114 using media M3; lane XVI, fermentation of strain MM20004 using media M4; lane XVII, fermentation of strain MM20002 using media M4; lane XVIII, fermentation of heterologous host *S. lividans* K4-114 using media M4. The asterisks indicate the peaks of stlassin (**1**).

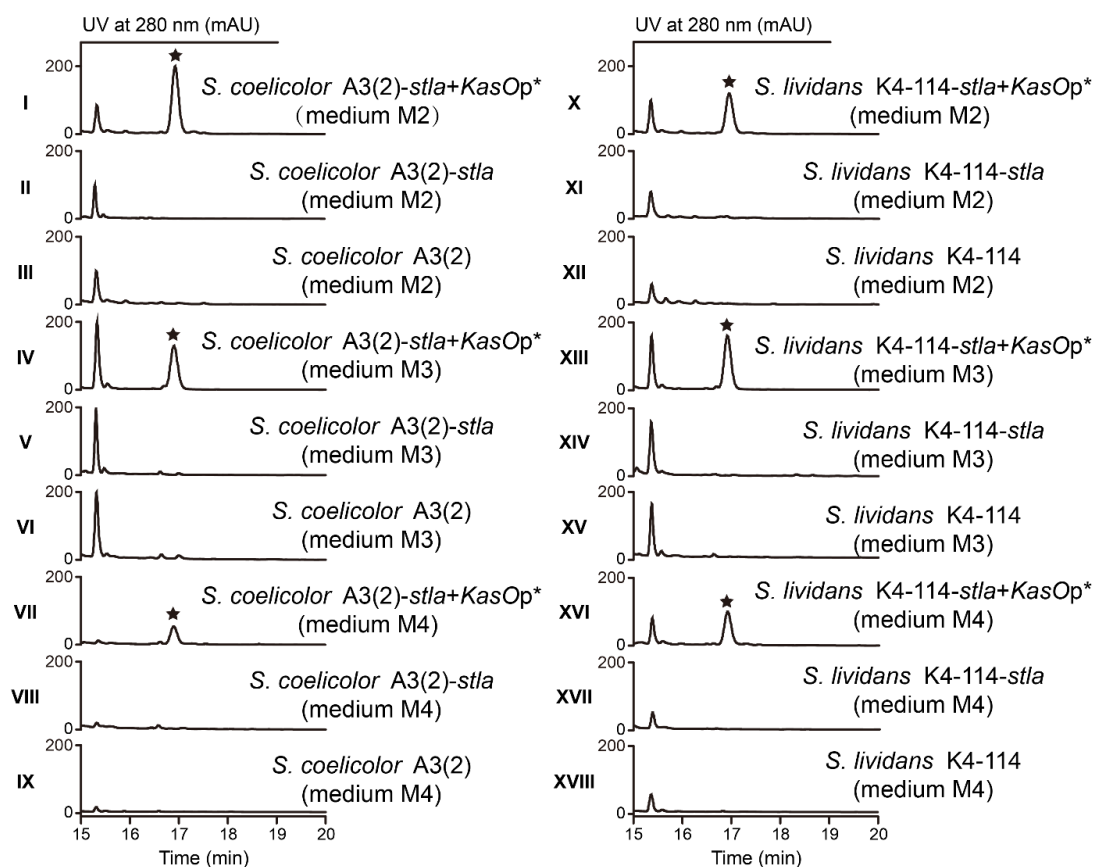


Figure S4. The construction of plasmid pMM2003 and pMM2004. (A) The diagram for the construction of pMM2003 and pMM2004. (B) The verification of the plasmid pMM2003 construction by *Apa*LI digestion followed by agarose gel electrophoresis analysis. Lane 1, the digestion of pMM2002 as the negative control; lane 2-9, the digestion of plasmids extracted from eight *E. coli* single colonies after the Red $\alpha\beta$ -mediated recombineering; lane M, DNA ladder; lane 10 and lane M', the predicted digestion of pMM2003 by *Apa*LI and predicted DNA ladder, respectively, generated by SnapGene software. The lanes labeled with asterisks represent the digestion of correct plasmids. (C) The PCR verification of the construction of pMM2004 with *stla*-2-F and *stla*-2-R as the primers. Lane M, DNA ladder; lane 1, the PCR product using plasmid pMM2002 as the template (negative control); lane 2, the PCR product using plasmid pMM2003 as the template; lane 3, the PCR product using pMM2004 as the template. The amplified regions corresponding to the PCR products in lane 1-3 were labeled in (A).

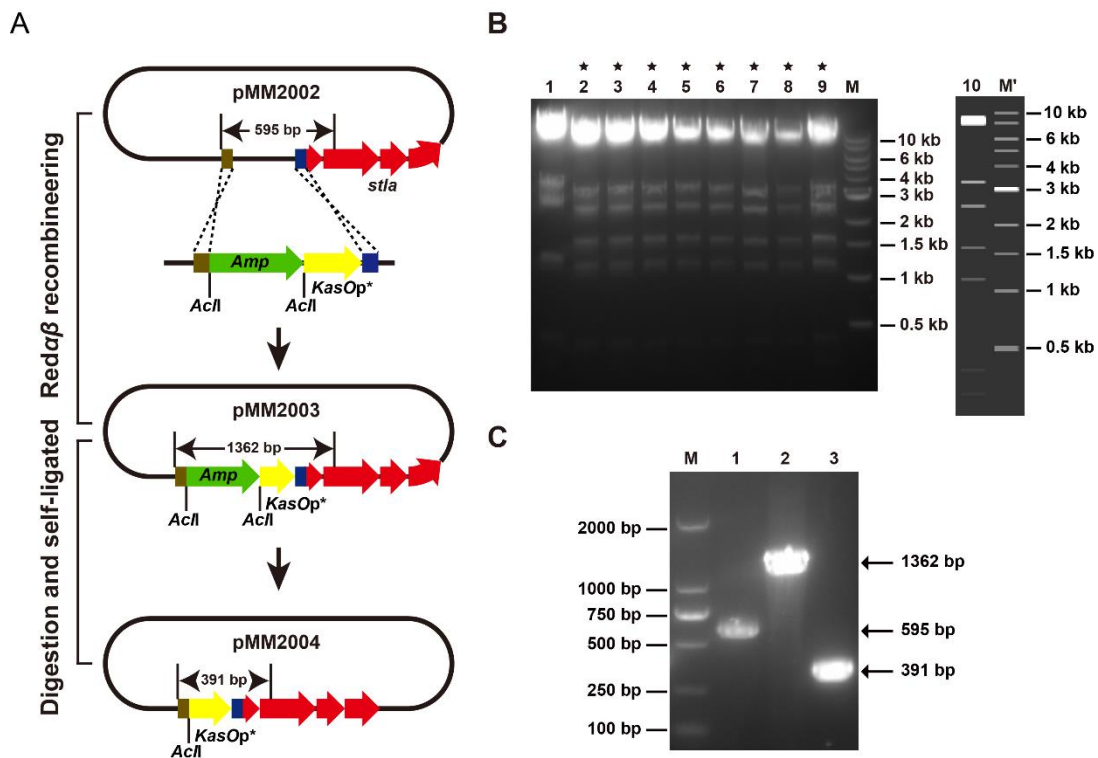


Figure S5. HPLC analysis of stlassin (**1**, labeled with asterisk) in cells and supernatant of the heterologous expression strain MM20003 (*S. coelicolor* A3(2) with pMM2004 integrated) after fermentation using three different media. Lane I, the extract of supernatant of MM20003 using media M2; lane II, the extract of cells of MM20003 using media M2; lane III, the extract of supernatant of MM20003 using media M3; lane IV, the extract of cells of MM20003 using media M3; lane V, the extract of supernatant of strain MM20003 using media M4; lane VI, the extract of cells of MM20003 using media M4.

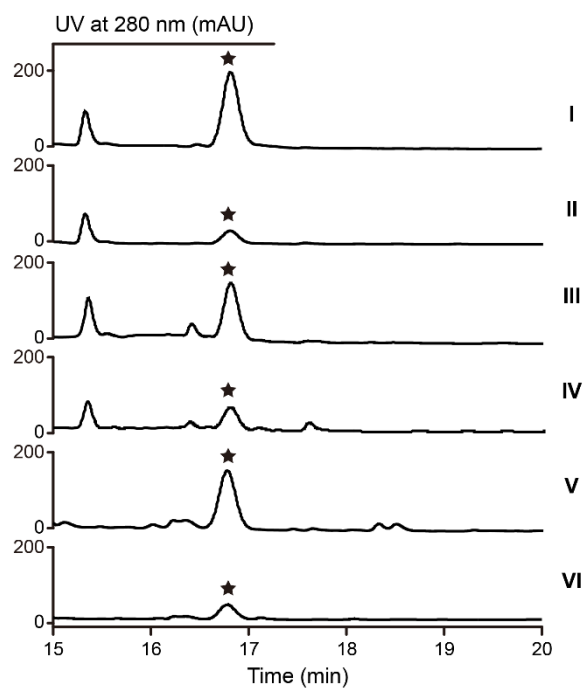


Figure S6. The HPLC analysis of thermal stability and carboxypeptidase-treatment reactions. (A) The heating experiments and carboxypeptidase Y-treatment of stlassin (1). (B) The heating experiments and carboxypeptidase Y-treatment of stlassin V3A (3). (C) The HRESIMS spectra of compound A (unthreaded 3) and compound C (stlassin V3A- Δ C6) purified from the heating experiments of 3. (D) The heating experiments and carboxypeptidase Y-treatment of stlassin I4A (4). (E) The heating experiments and carboxypeptidase Y-treatment of stlassin W14F (14). (F) The heating experiments and carboxypeptidase Y-treatment of stlassin F15Y (16). (G) The heating experiments and carboxypeptidase Y-treatment of stlassin V2C/A11C (18). The "cY" represents carboxypeptidase Y.

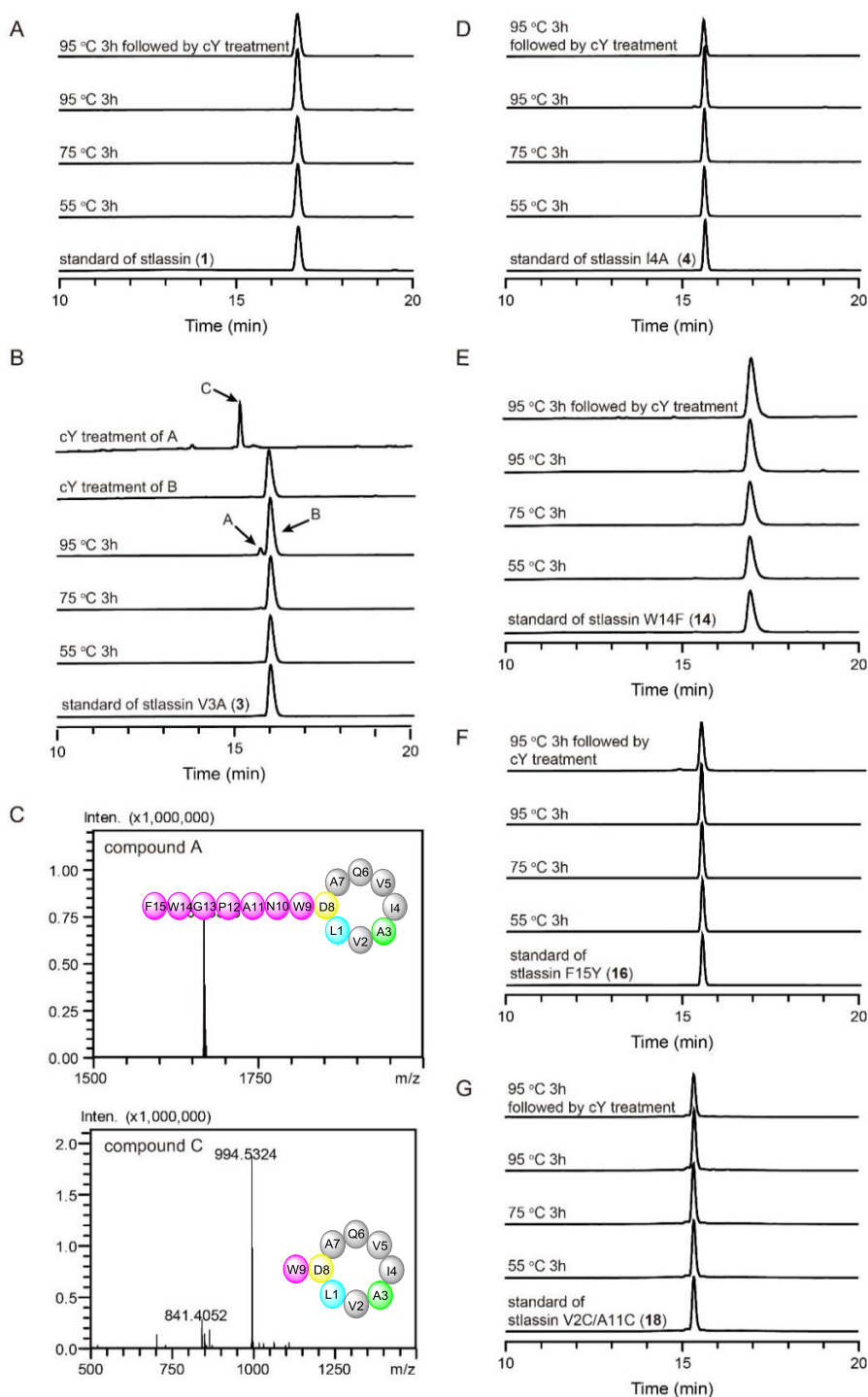


Figure S7. The diagram for site-directed mutagenesis of *stlaA* gene based on the Red $\alpha\beta$ recombinering system. (A) The diagram for construction of the plasmid pMM2007 with the *KasOp*^{*}-*stlaA* cassette deletion. (B) The diagram for preparation of *Amp*-*KasOp*^{*}-*stlaA* cassette bearing mutations for Red $\alpha\beta$ recombinering. (C) The diagram for the construction of the heterologous expression plasmids pMM2008-pMM2037 with different mutated *stlaA*.

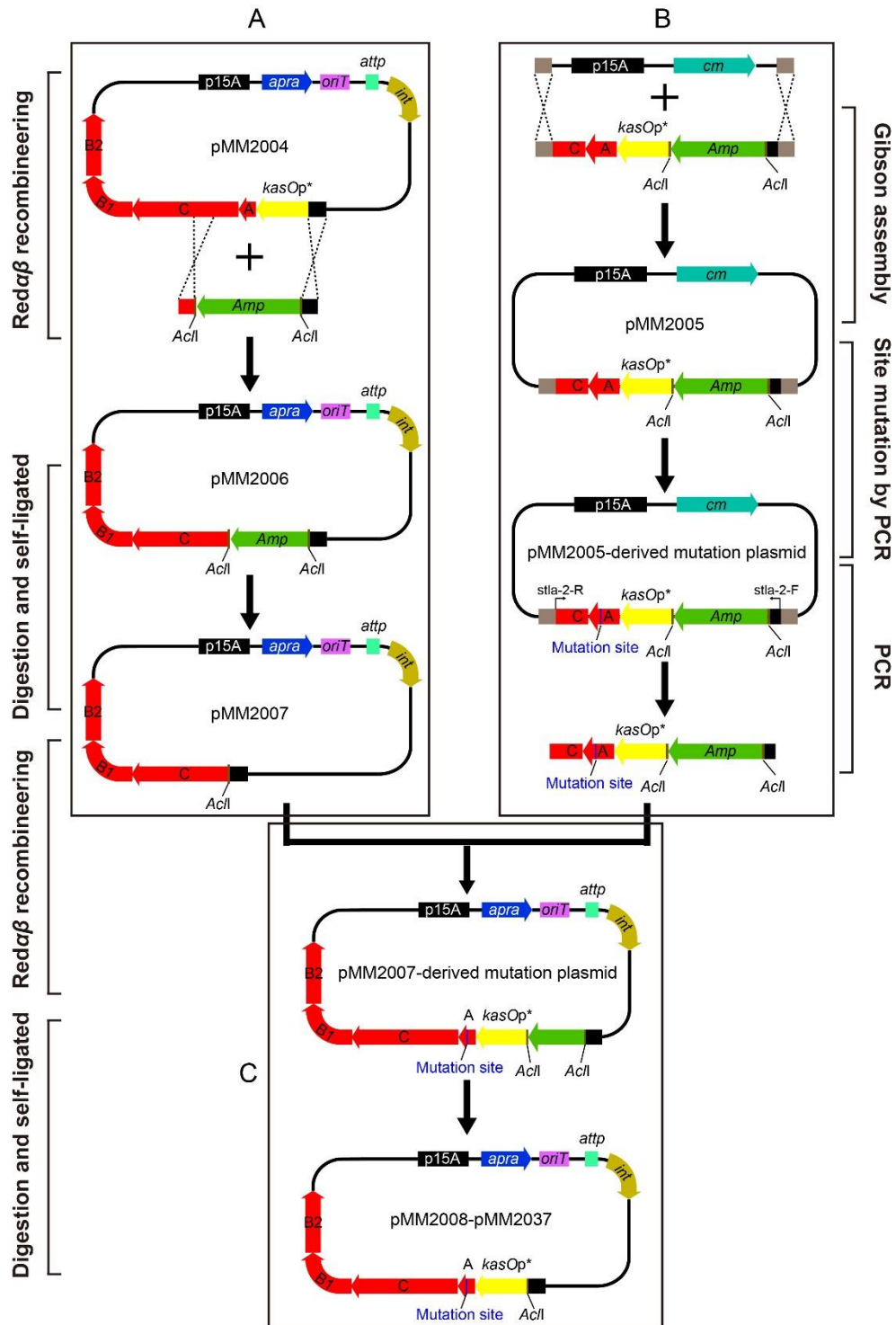


Figure S8. The HPLC analysis of stlassin (**1**) and its derivatives produced in the crude extracts of different strains. The specific mutations are shown in parentheses under the strain names.

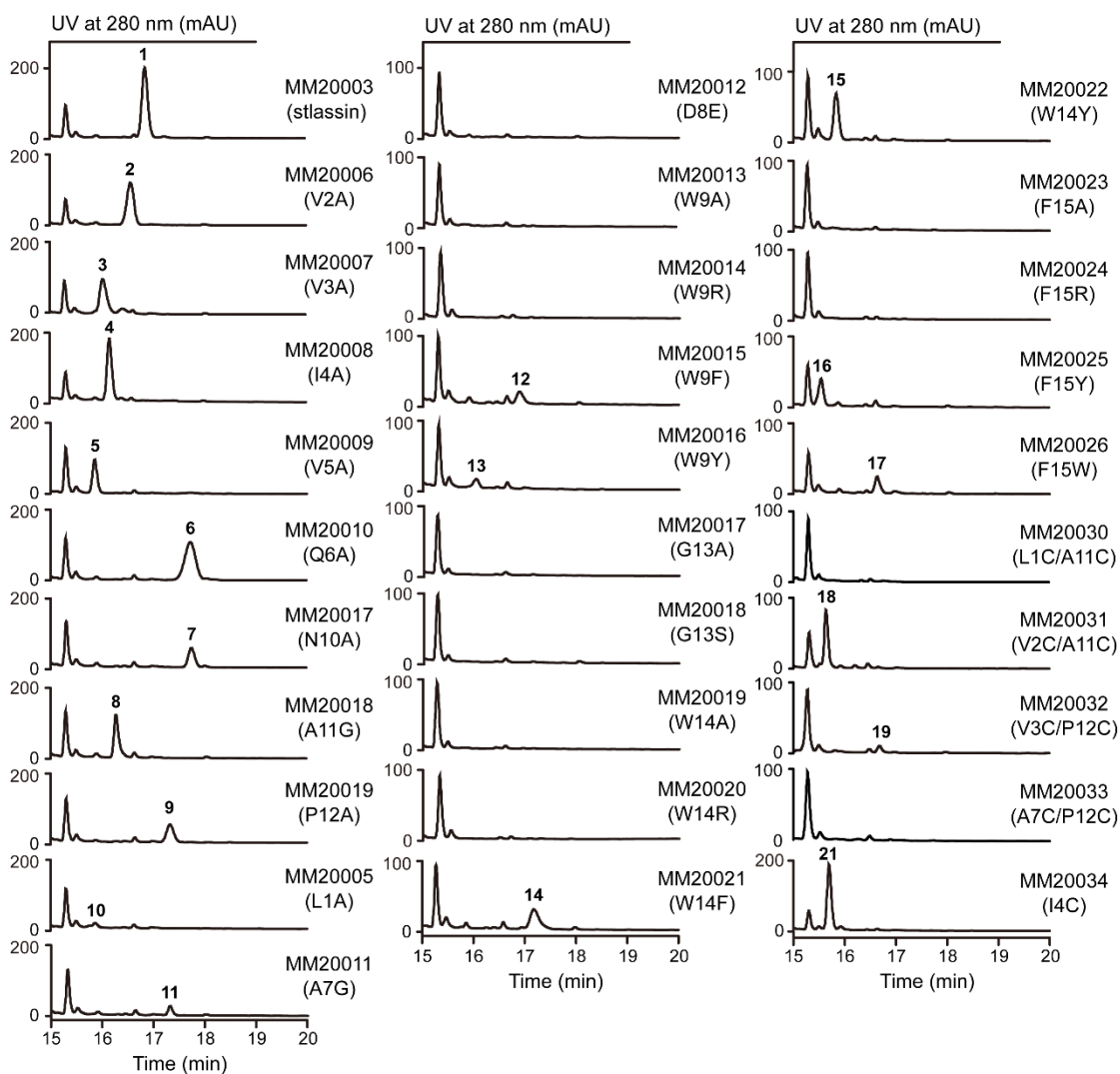


Figure S9. The design of double mutations for introducing two cysteine residues. The four pairs of Leu1/Ala11, Val2/Ala11, Val3/Pro12 and Ala7/Pro12 that were selected for disulfide bond formation based on the superimposition of solution NMR structures of **1**, **3**, **4**, **14** and **16**. The distances between the β -carbons, which are within 5.71 Å, are indicated in yellow dashed lines.

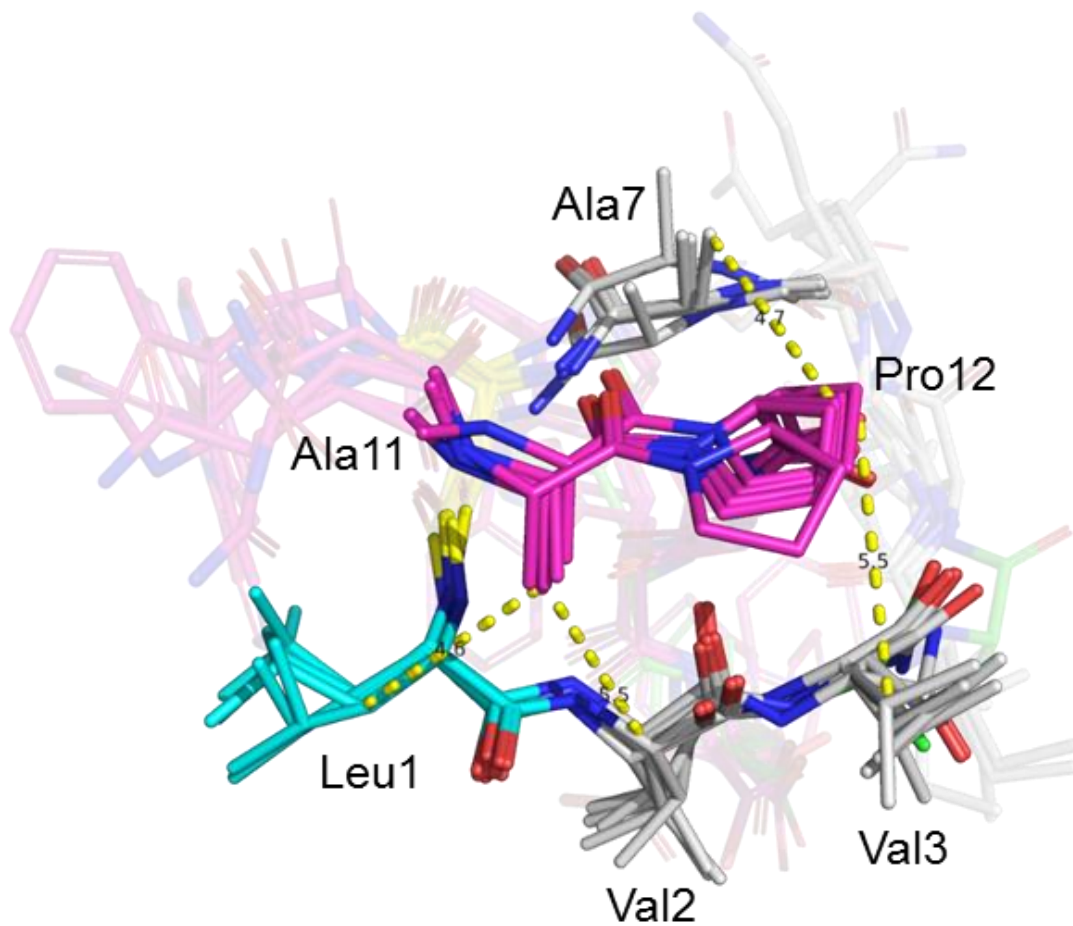


Figure S10. The lasso presentation of the structures of compounds **1-27**. The amino acid residues were shown in spheres with different colors. For all structure, the N-terminal macrolactam residues were labeled in grey except Leu1 was labeled in cyan and Asp8 was labeled in yellow, the C-terminal Trp9-Phe15 were labeled in magenta, and the residues from mutations were labeled in green.

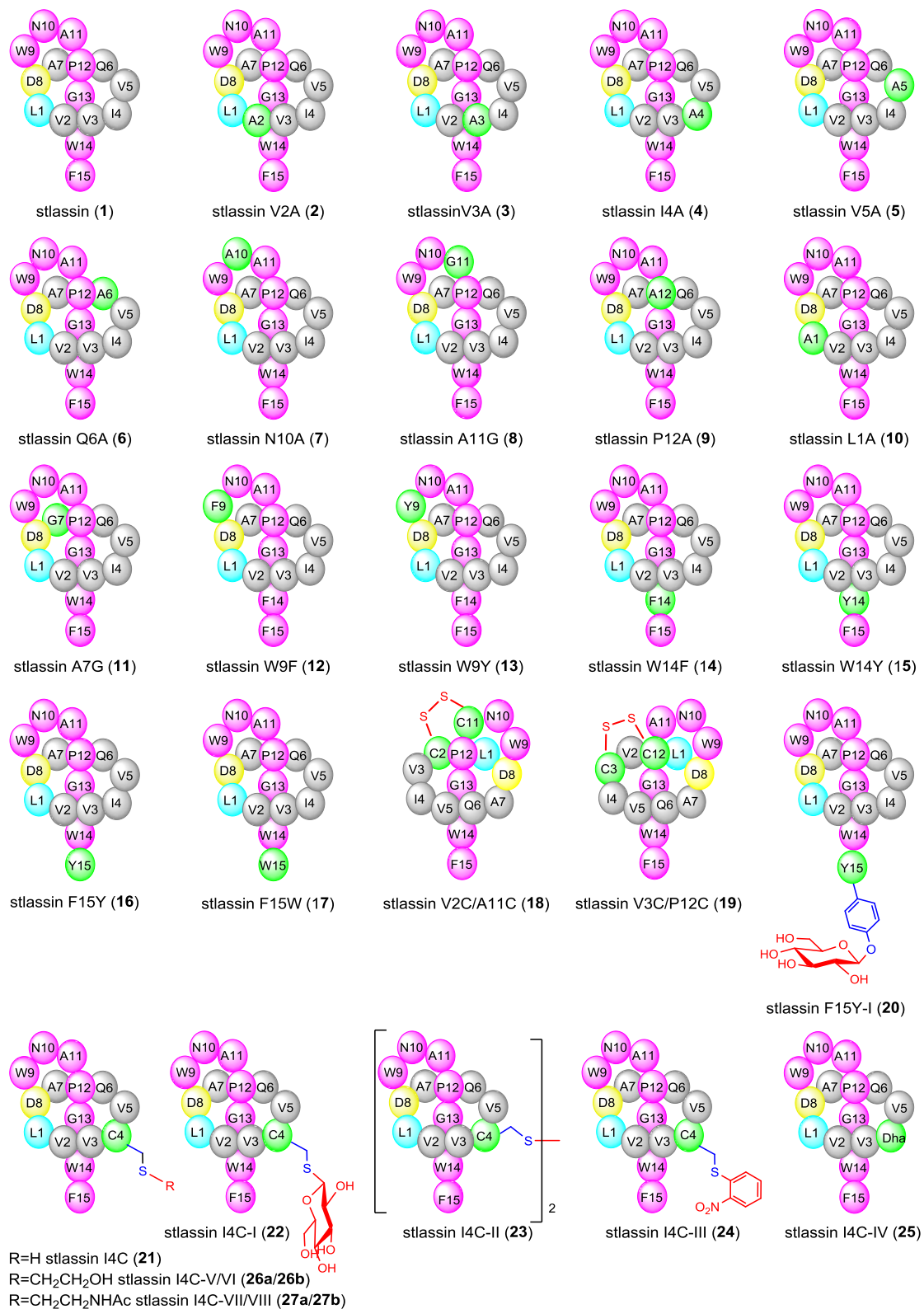


Figure S11. The superimposition of the 20 solution structures with the lowest total energy of stlassin (**1**), stlassin V3A (**3**), stlassin I4A (**4**), stlassin W14F (**14**), stlassin F15Y (**16**) and stlassin V2C/A11C (**18**). For all structures, the N-terminal macrolactam residues were labeled in grey except Leu1 was labeled in cyan and Asp8 was labeled in yellow, the C-terminal Trp9-Phe15 were labeled in magenta, and the residues from mutations were labeled in green.

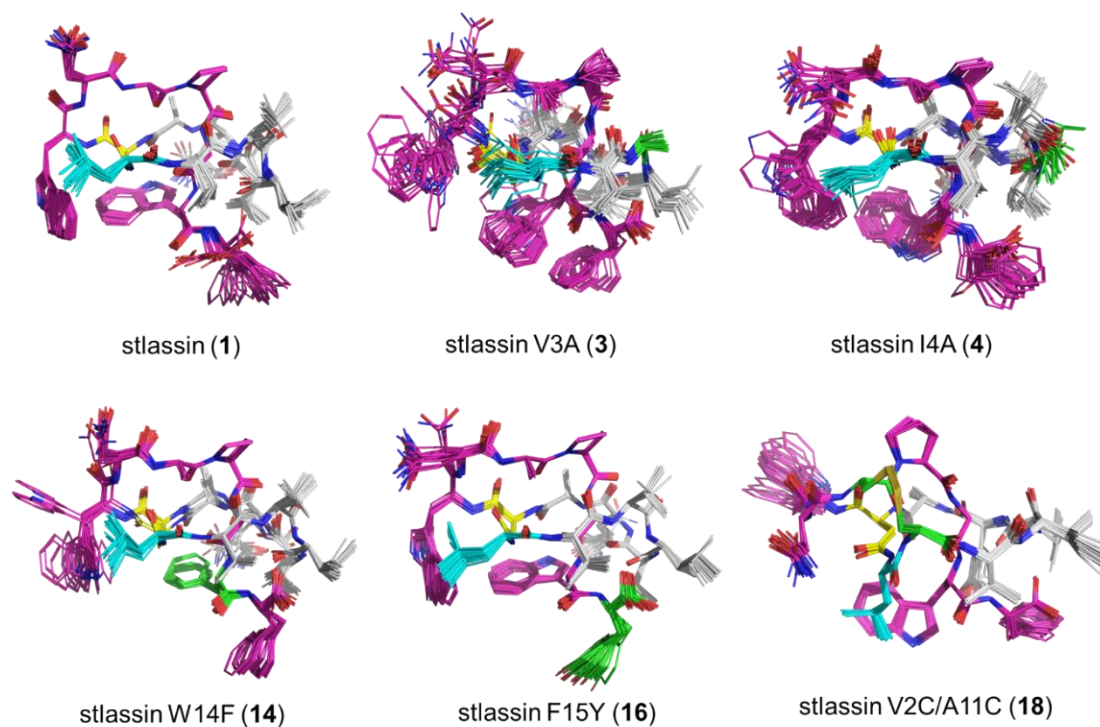


Figure S12. The superimposition of solution NMR structures. (A) The main chains superimposition of solution NMR structures of **1**, **3**, **4**, **14** and **16**. (B) The superimposition of solution NMR structures of **1**, **3**, **4**, **14** and **16**. (C) The superimposition of **1** (blue, partial) and **18**, with the residues' names labeled in black for **18** and red for **1**. For all structures except **1** in (C), the N-terminal macrolactam residues are shown in gray except Leu1 in cyan and Asp8 in yellow, the C-terminal residues are shown in magenta and the residues from mutation are shown in green.

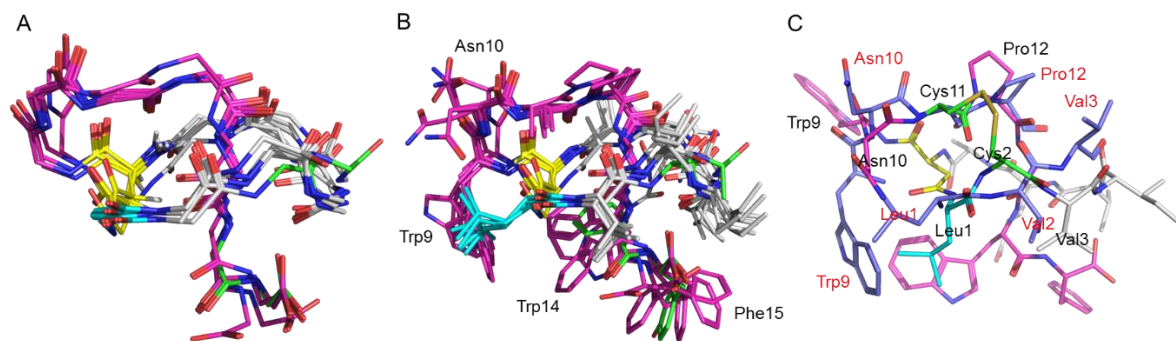


Figure S13. Amplified region of NOESY spectra of **1**, **3**, **4**, **14** and **16** showing the correlations (indicated with circles) between Val3 (or Ala3) and Pro12. More NOE correlations can be observed between V3 and P12 in **1**, **4**, **14**, and **16**, whereas only one can be observed between A3 and P12 in **3**.

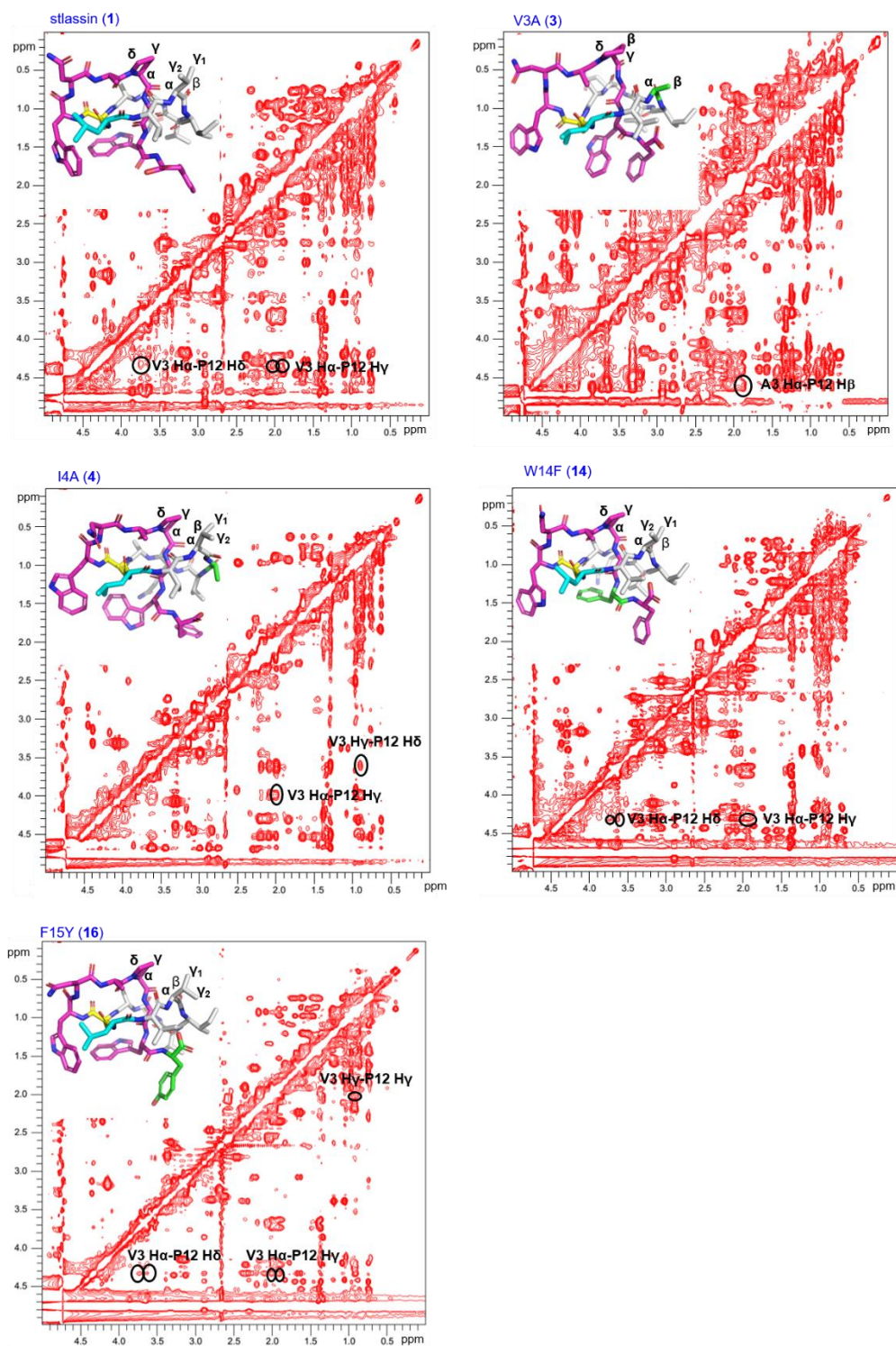


Figure S14. The OD values of four control ELISA experiments (N1–N4) compared to that of DMSO control. Compared to the complete ELISA procedures for antagonistic activities assays, N1 only omits the mouse anti-human TLR4 antibody in the coating step; N2 only omits the addition of the NCM460 proteins; N3 uses biotin instead of biotin-labeled LPS; N4 uses LPS instead of biotin-labeled LPS; DMSO control uses DMSO instead of compounds.

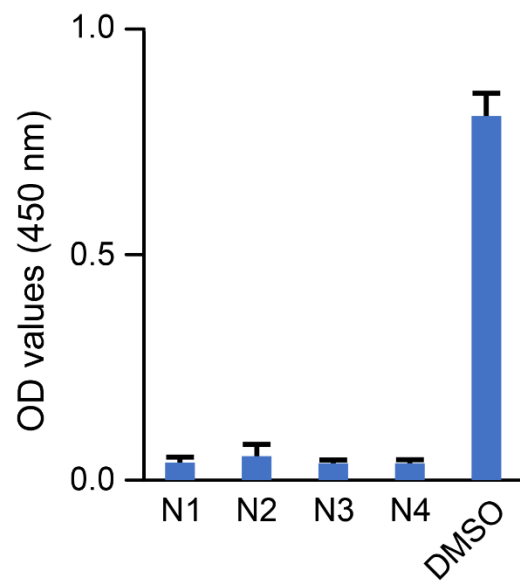


Figure S15. The antagonistic activities of stlassins against the binding of LPS to TLR4 at different concentrations. (A) The inhibition ratios of stlassin and variants against the binding of LPS to TLR4 with concentration of 1 $\mu\text{g/mL}$, using TAK-242 as the positive control. These inhibition ratios were generated from the same sets of data used for the OD value determinations in Figure 6 in the main text. The inhibition ratios and error bars were generated based on the calculation of mean \pm standard deviation from four parallel experiments. (B) The inhibition ratios of stlassin (1) and variants I4A (4), I4C (21), I4C-III (24), F15Y (16), and F15Y-I (20) at different concentrations. The inhibition ratios and error bars were generated based on the calculation of mean \pm standard deviation from three parallel experiments. The IC_{50} values were determined based on the dose-response curves using GraphPad Prism 7.0.

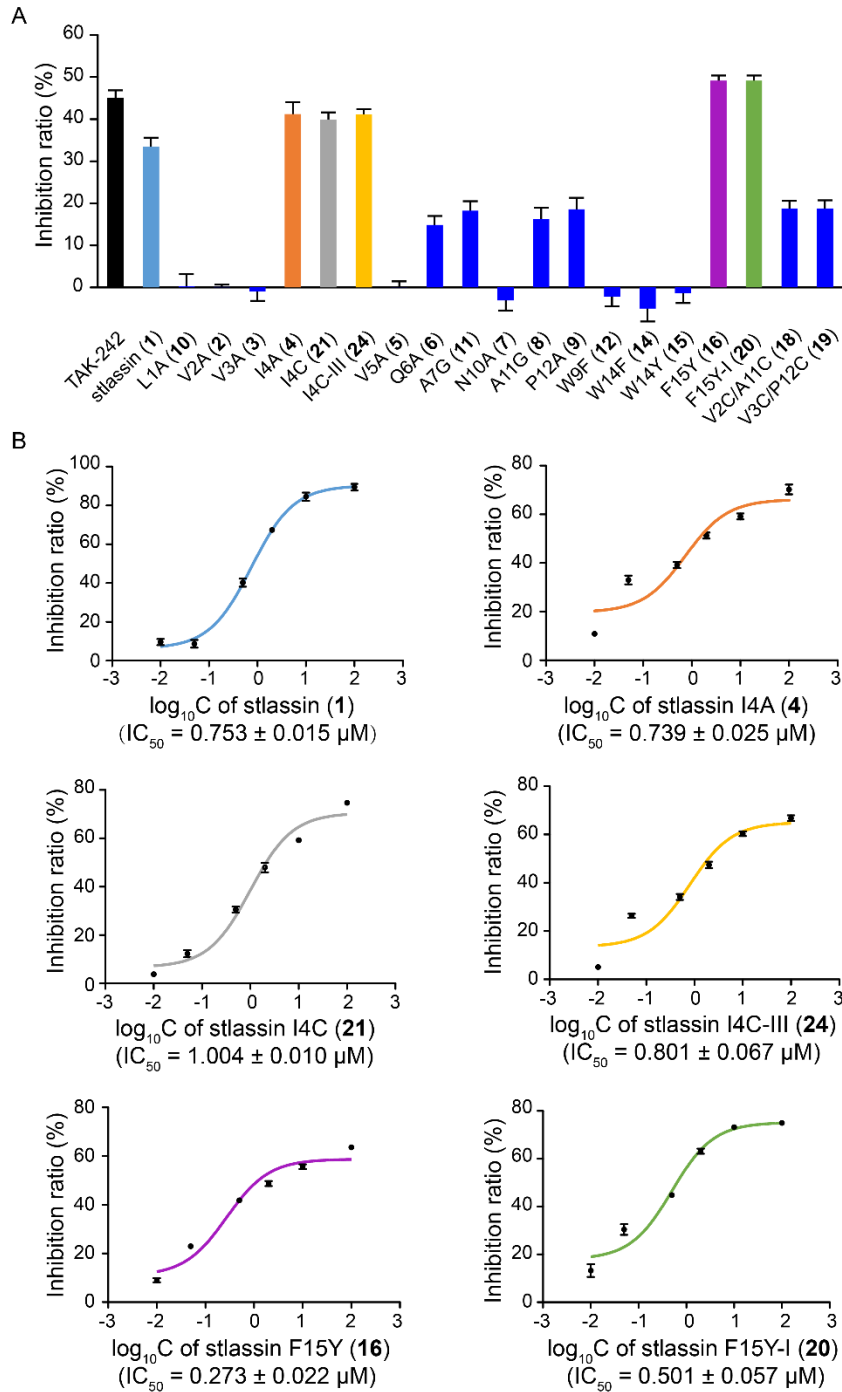


Figure S16. The HRESIMS spectrum of stlassin (1).

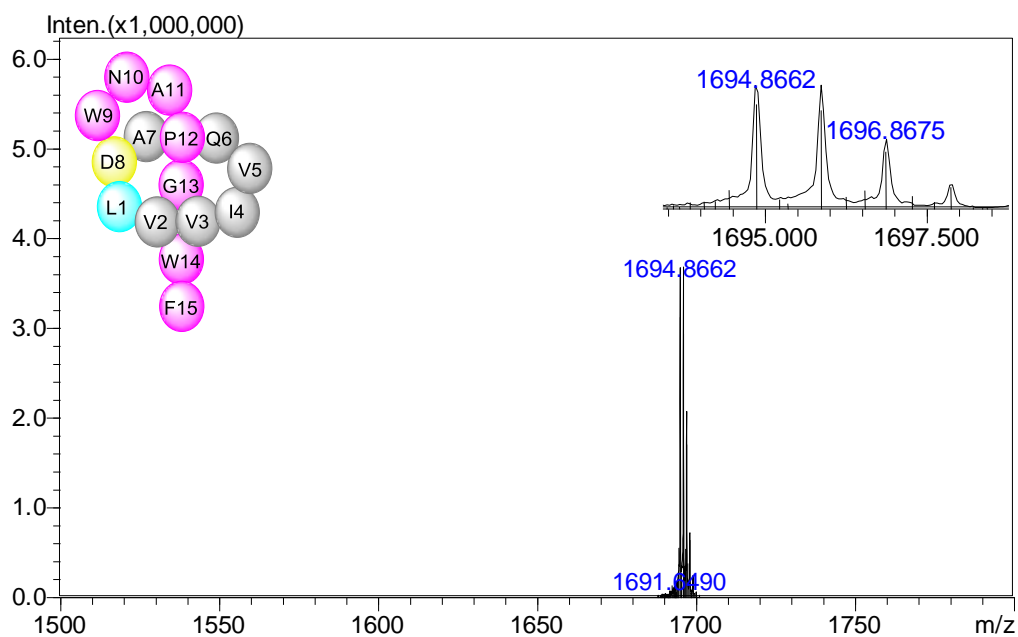


Figure S17. The HRESIMS spectrum of stlassin V2A (2).

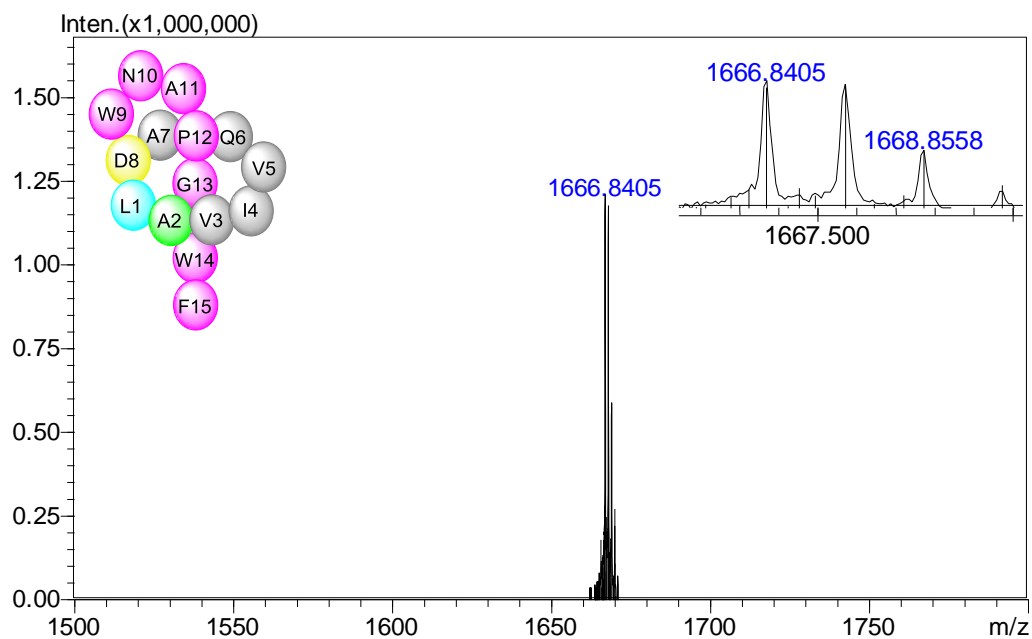


Figure S18. The HRESIMS spectrum of stlassin V3A (**3**).

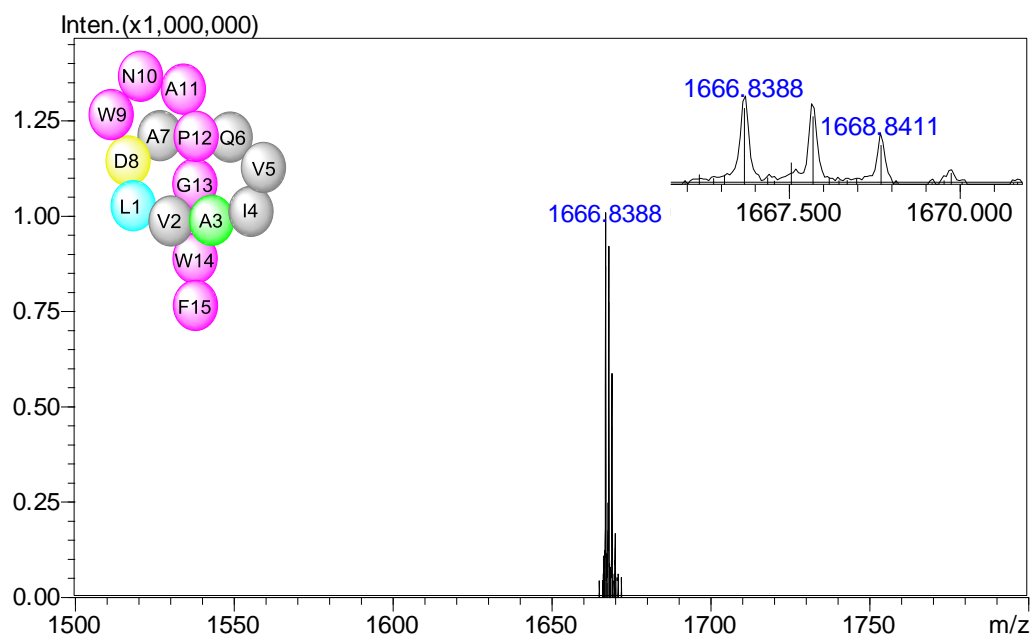


Figure S19. The HRESIMS spectrum of stlassin I4A (**4**).

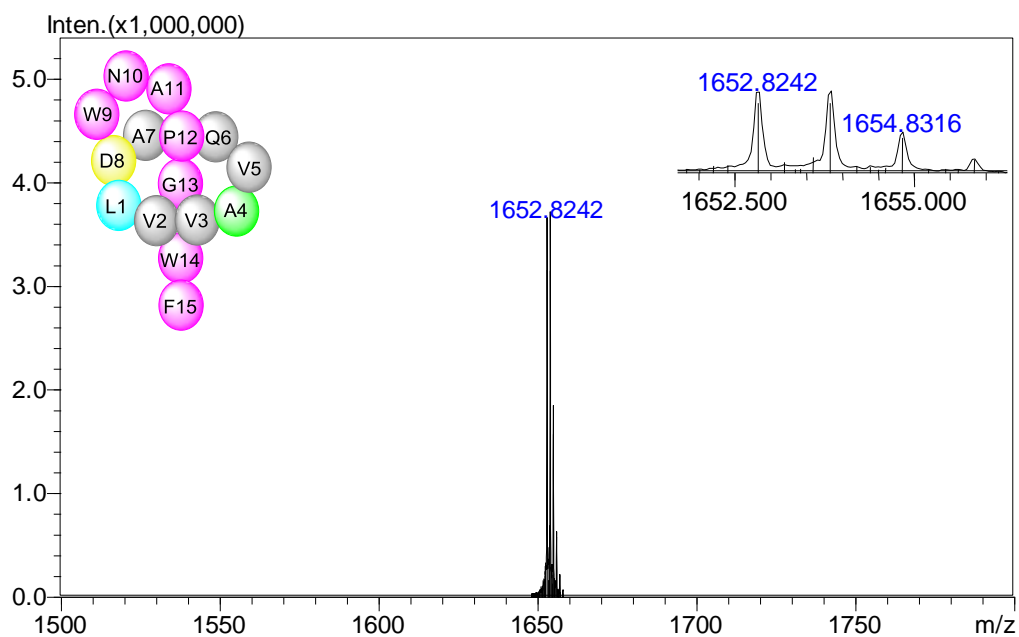


Figure S20. The HRESIMS spectrum of stlassin V5A (5).

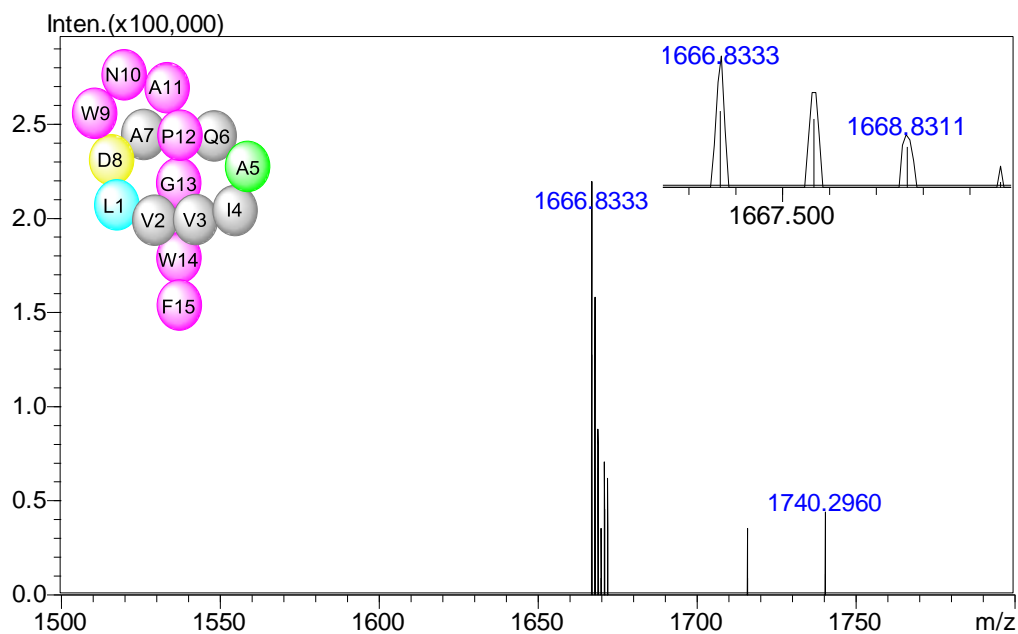


Figure S21. The HRESIMS spectrum of stlassin Q6A (6).

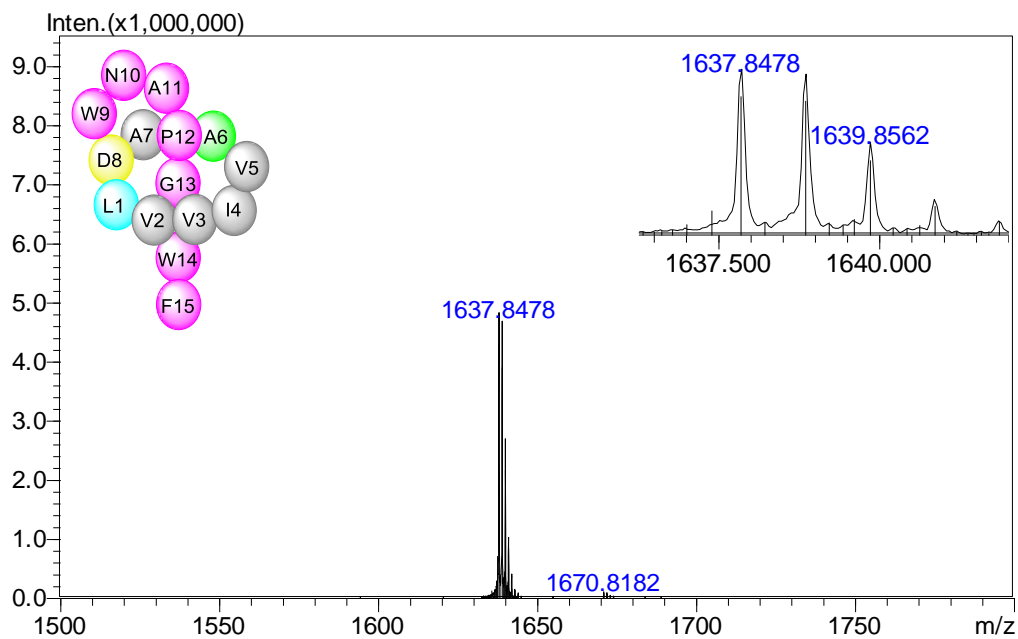


Figure S22. The HRESIMS spectrum of stlassin N10A (7).

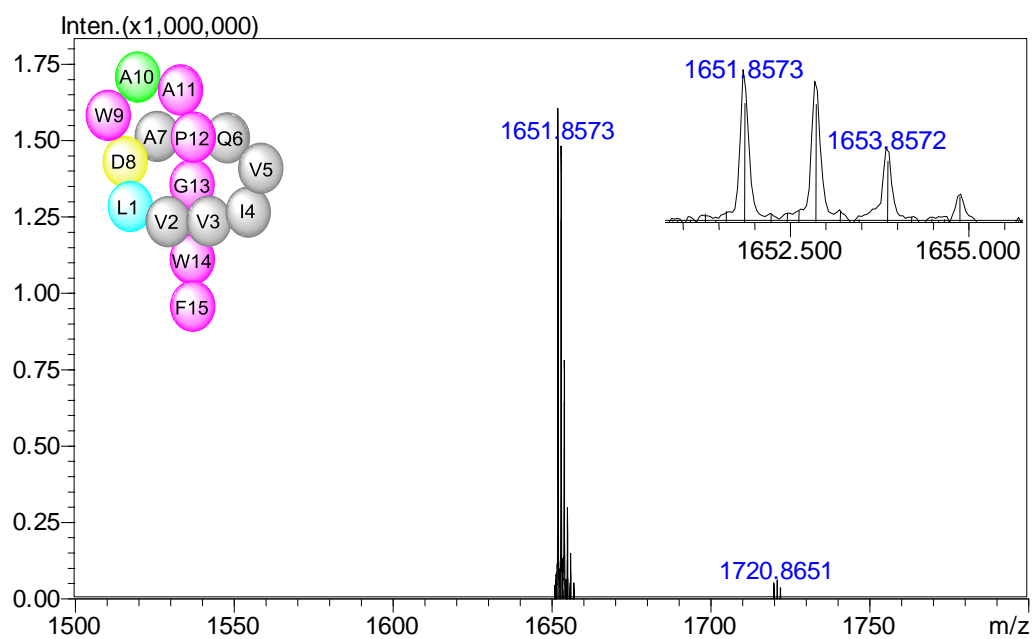


Figure S23. The HRESIMS spectrum of stlassin A11G (8).

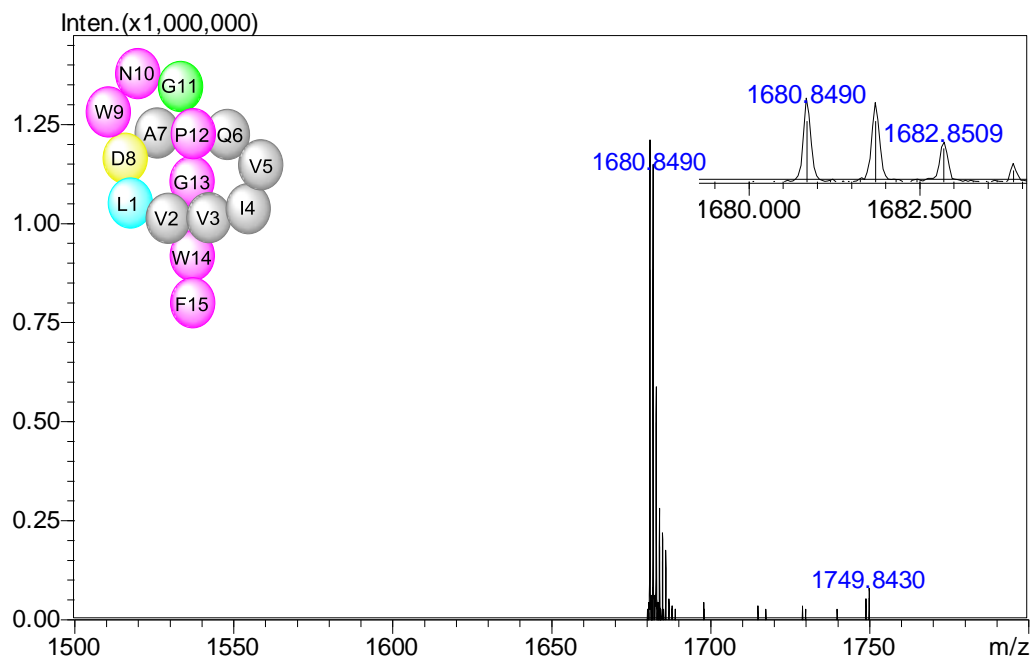


Figure S24. The HRESIMS spectrum of stlassin P12A (**9**).

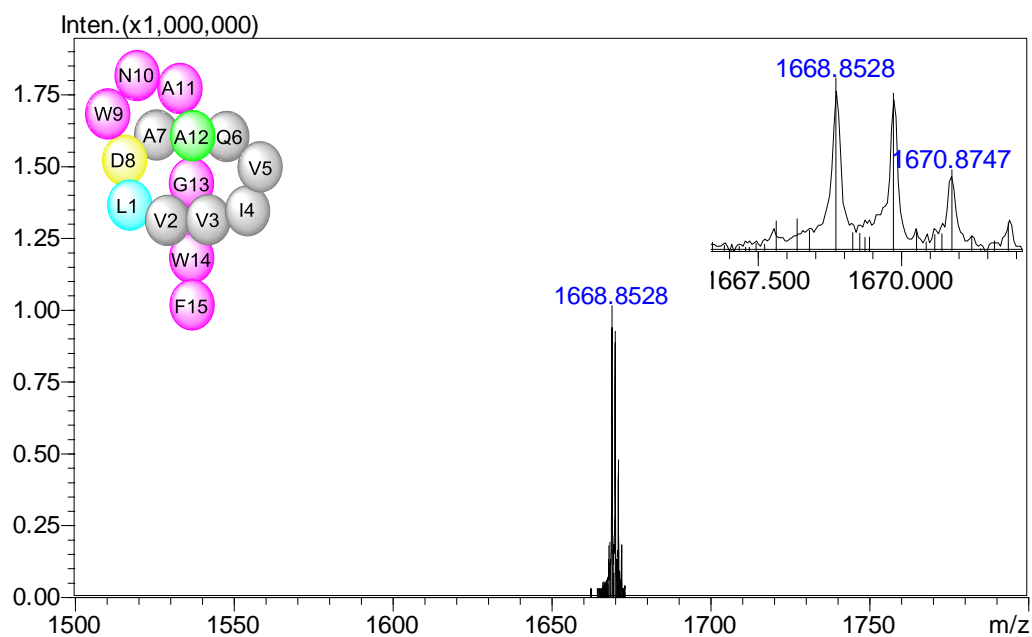


Figure S25. The HRESIMS spectrum of stlassin L1A (**10**).

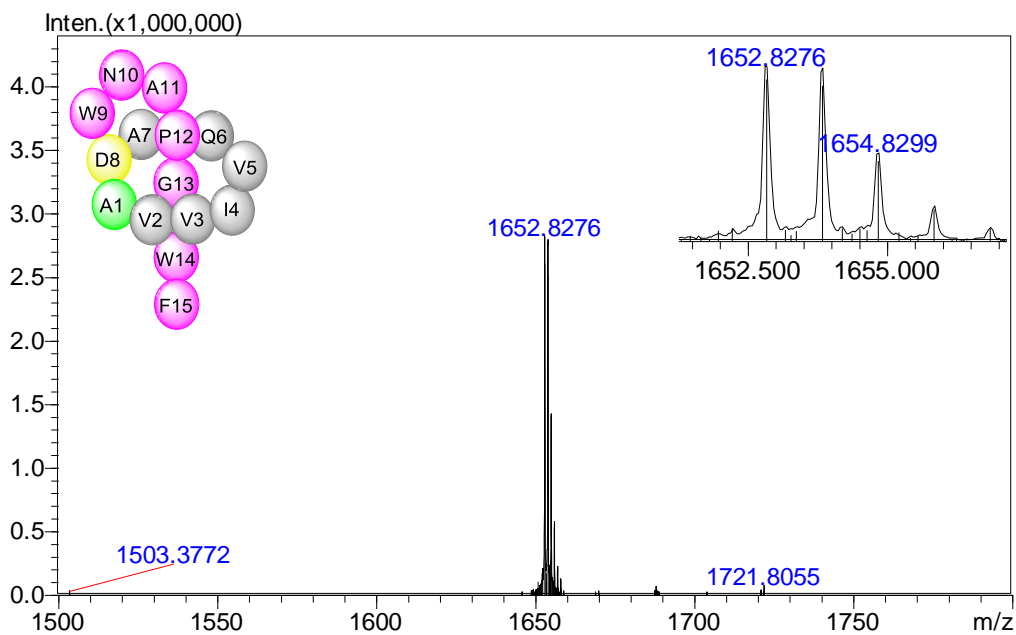


Figure S26. The HRESIMS spectrum of stlassin A7G (11).

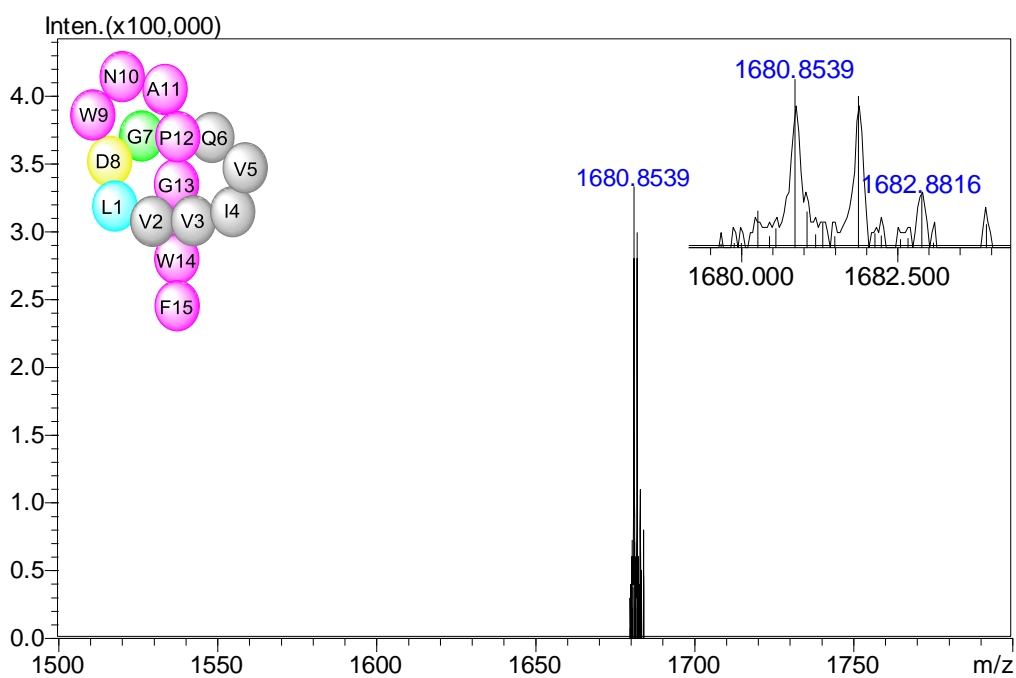


Figure S27. The HRESIMS spectrum of stlassin D8E.

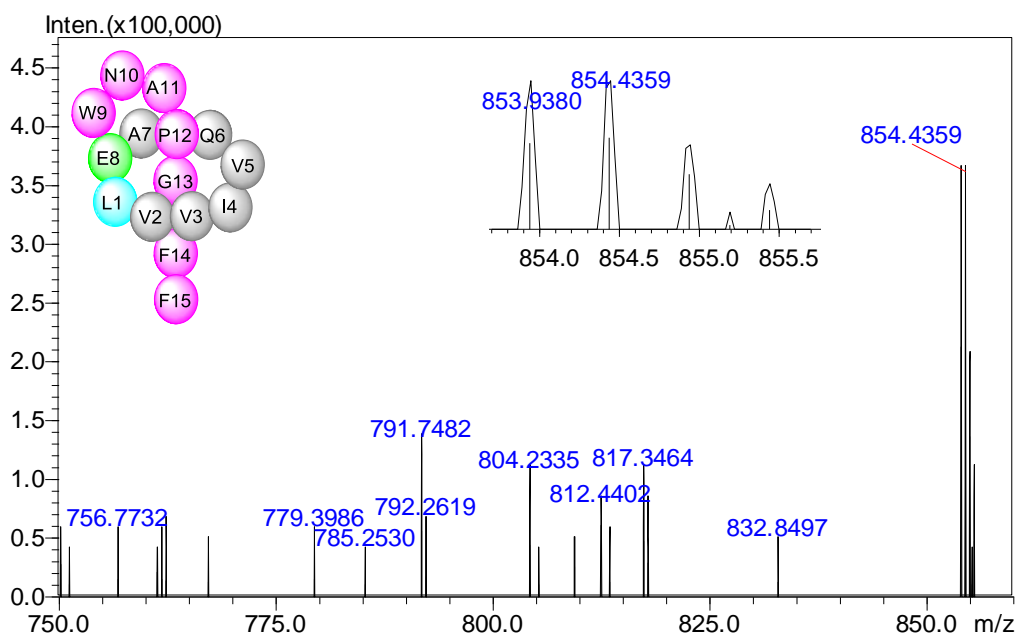


Figure S28. The HRESIMS spectrum of stlassin W9F (**12**).

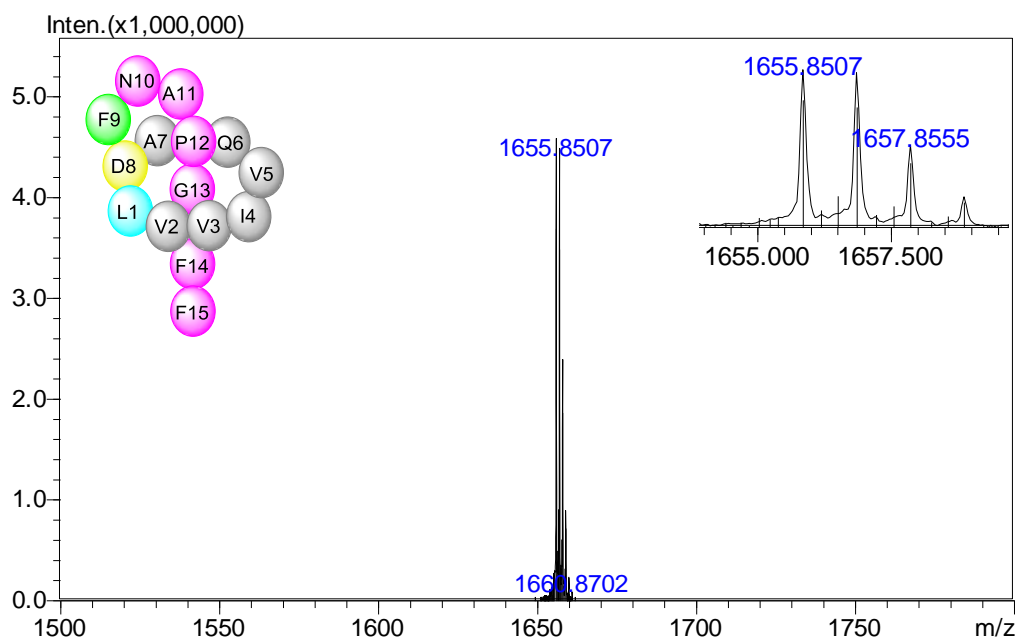


Figure S29. The HRESIMS spectrum of stlassin W9Y (**13**).

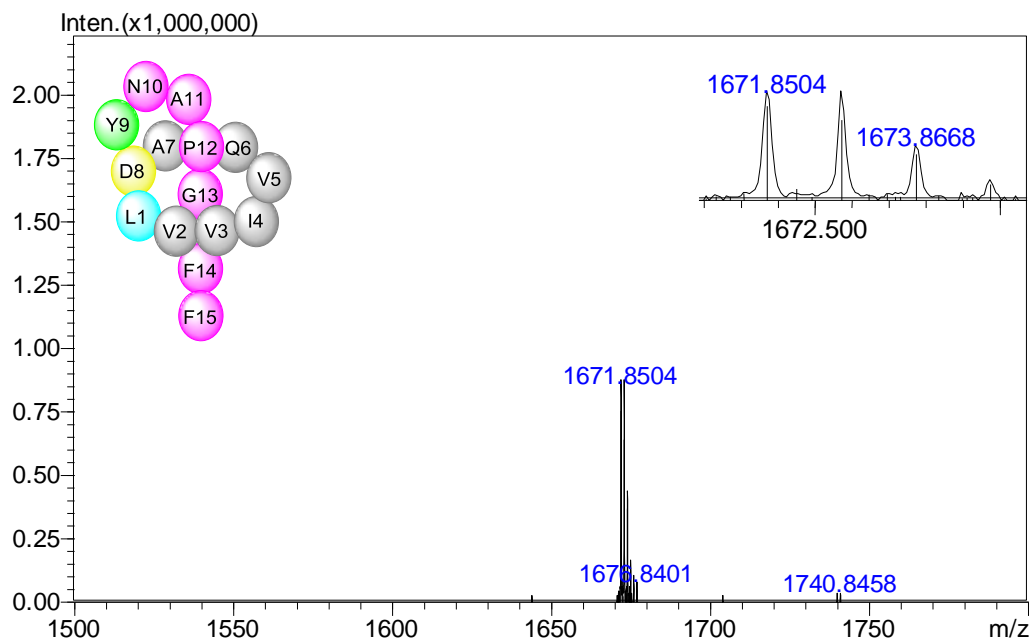


Figure S30. The HRESIMS spectrum of stlassin W14F (**14**).

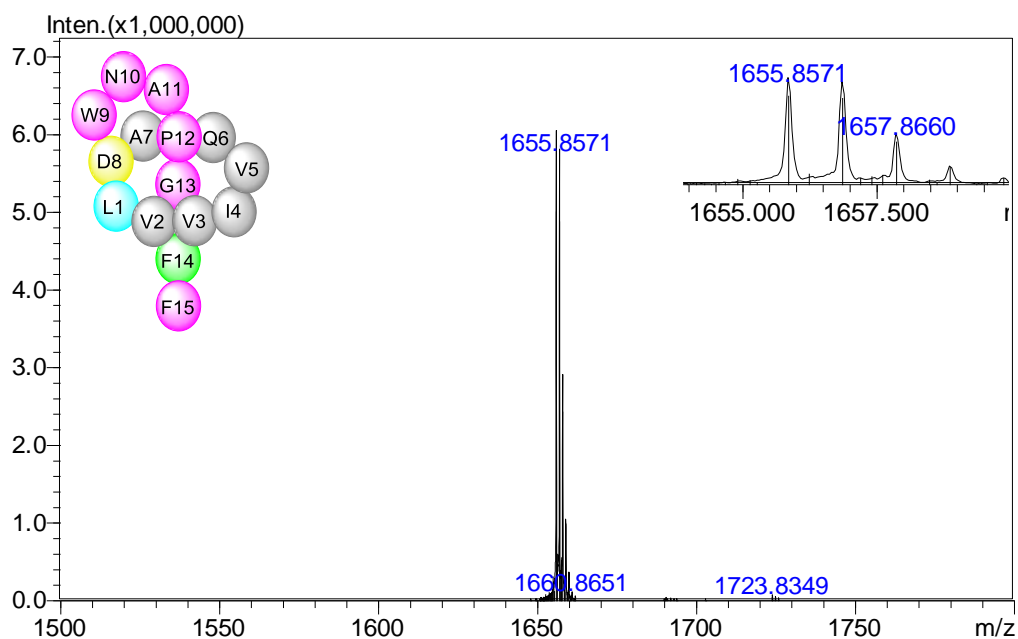


Figure S31. The HRESIMS spectrum of stlassin W14Y (**15**).

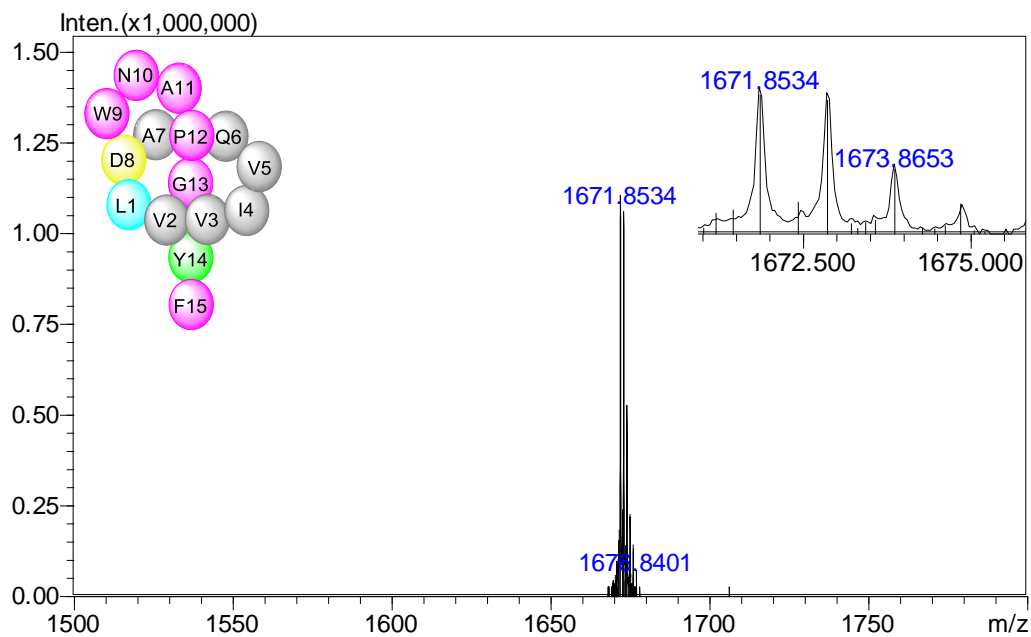


Figure S32. The HRESIMS spectrum of stlassin F15Y (**16**).

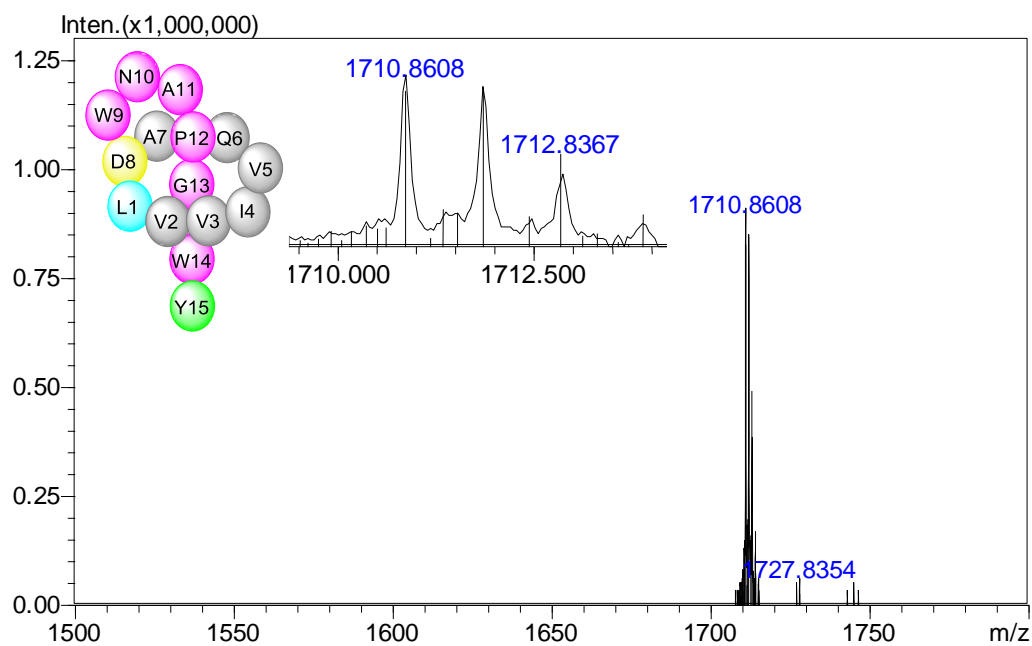


Figure S33. The HRESIMS spectra of stlassin F15W (**17**).

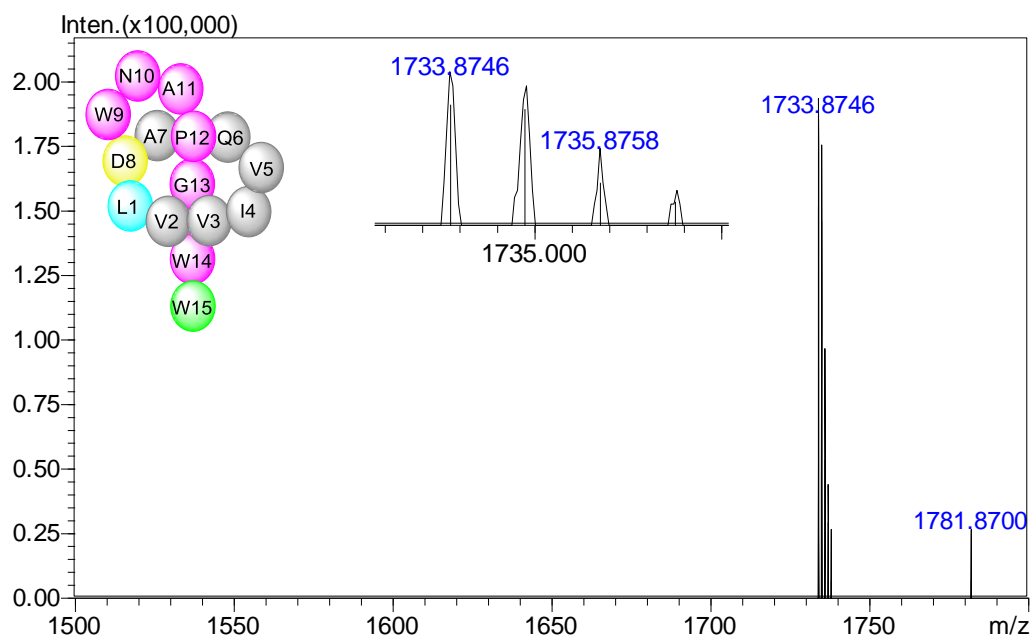


Figure S34. The HRESIMS spectra of stlassin V2C/A11C (**18**).

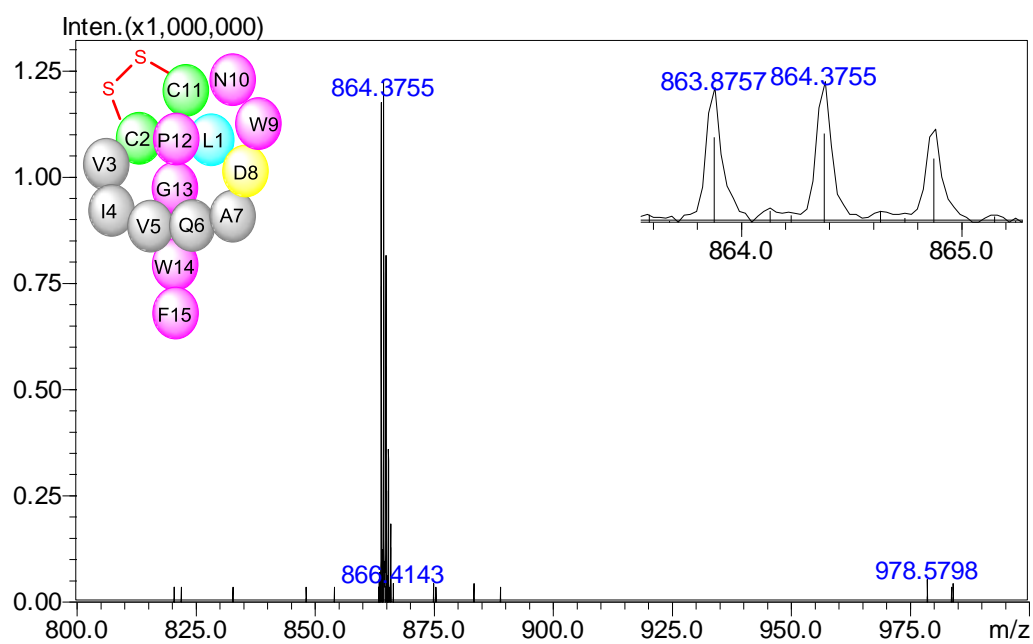


Figure S35. The HRESIMS spectra of stlassin V3C/ P12C (**19**).

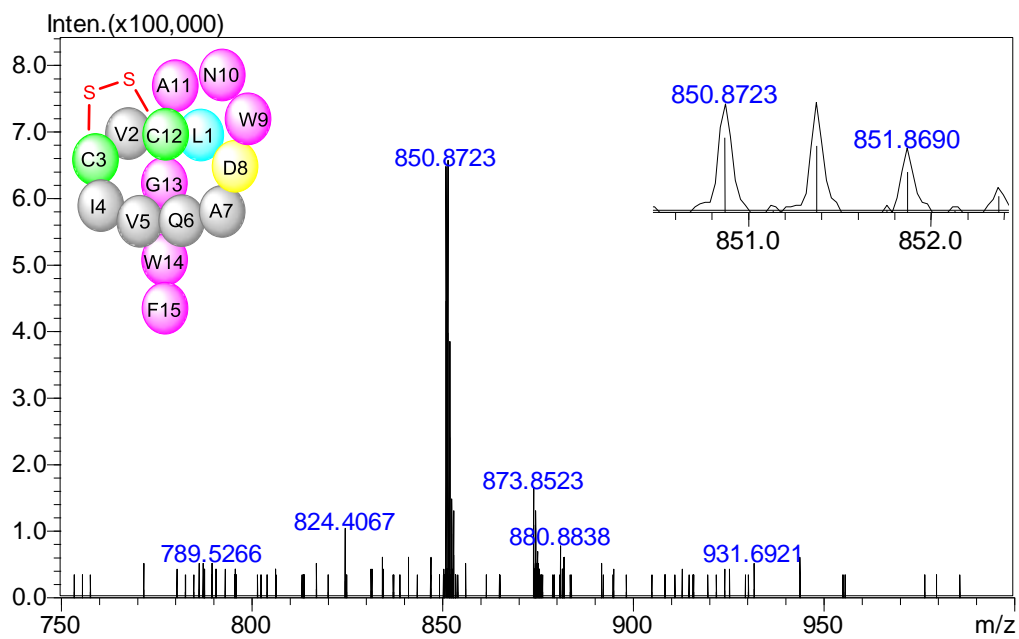


Figure S36. The HRESIMS spectra of stlassin F15Y- I (**20**).

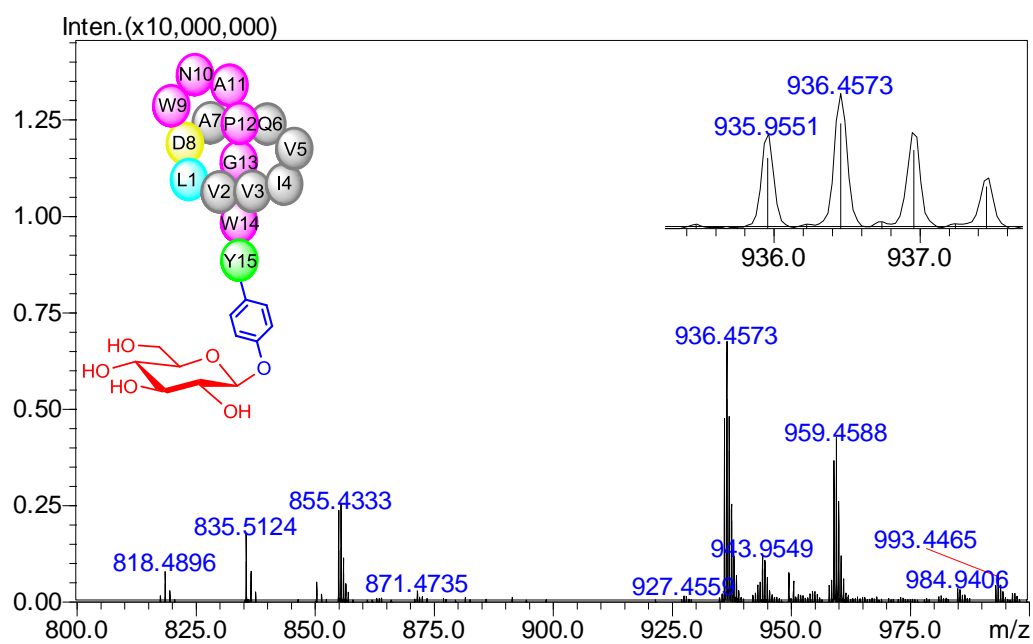


Figure S37. The HRESIMS spectrum of stlassin I4C (**21**).

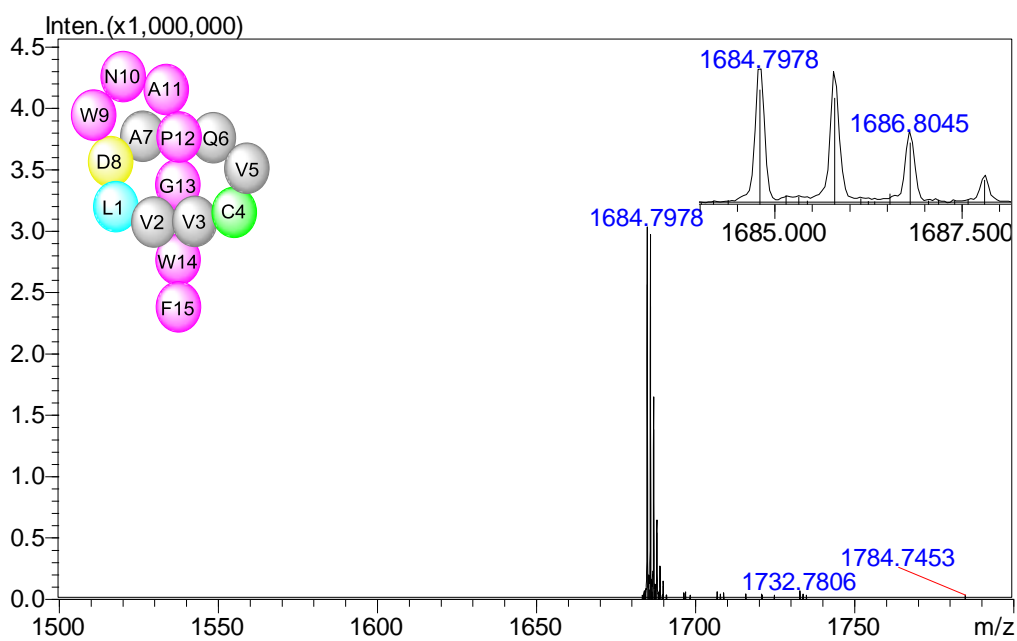


Figure S38. The HRESIMS spectrum of stlassin I4C-I (**22**).

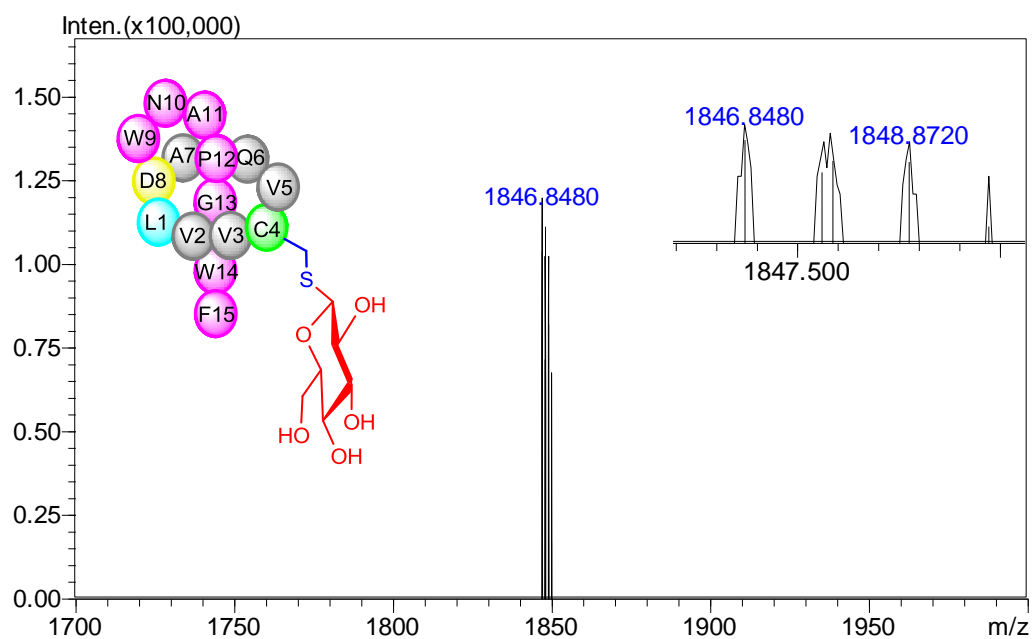


Figure S39. The HRESIMS spectra of stlassin I4C-II (**23**).

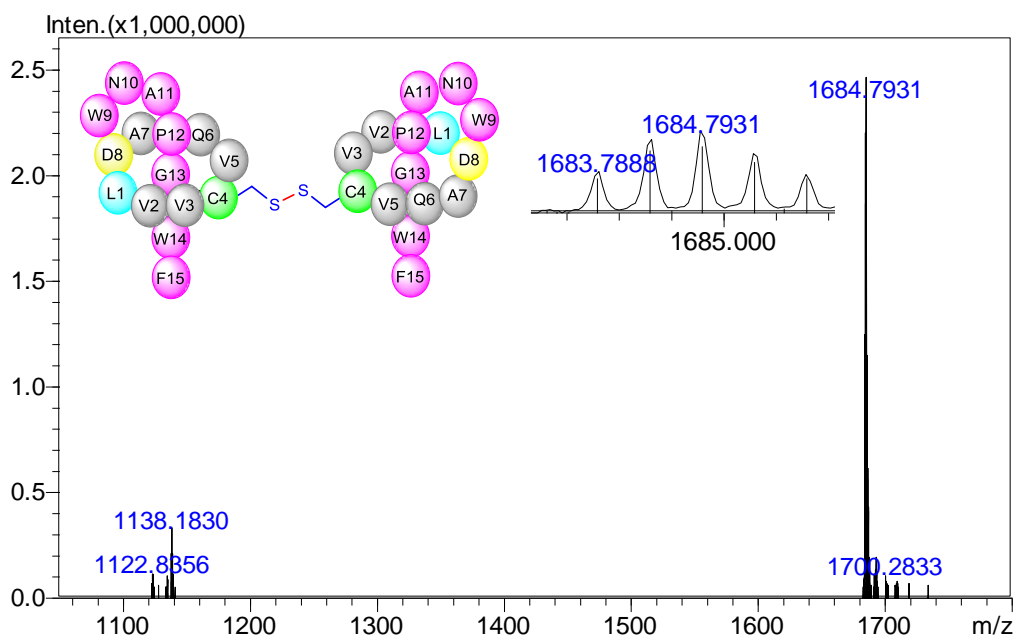


Figure S40. The HRESIMS spectrum of stlassin I4C-III (**24**).

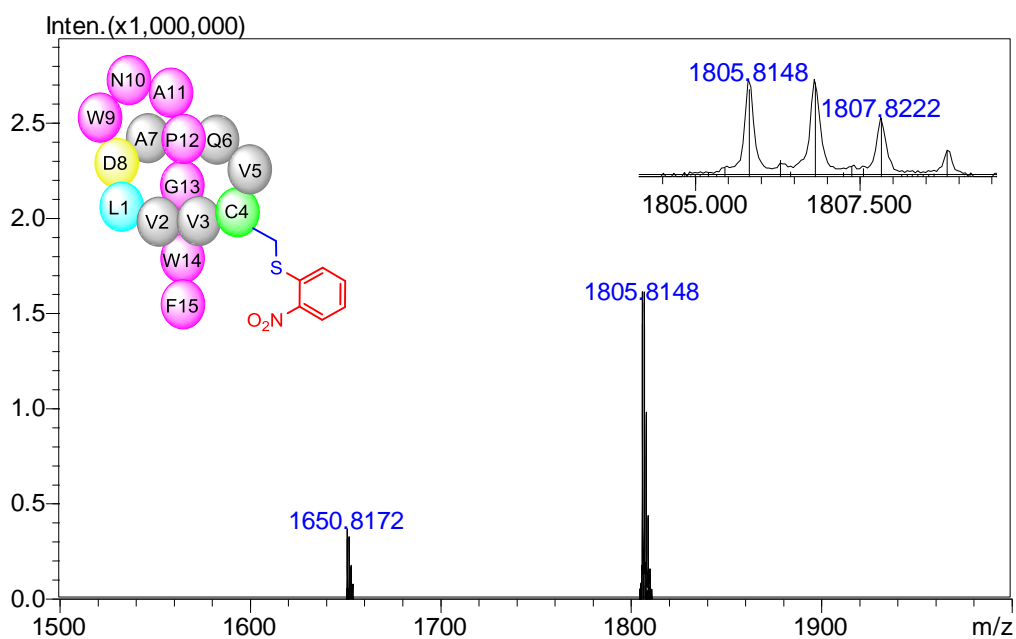


Figure S41. The HRESIMS spectrum of stlassin I4C-IV (**25**).

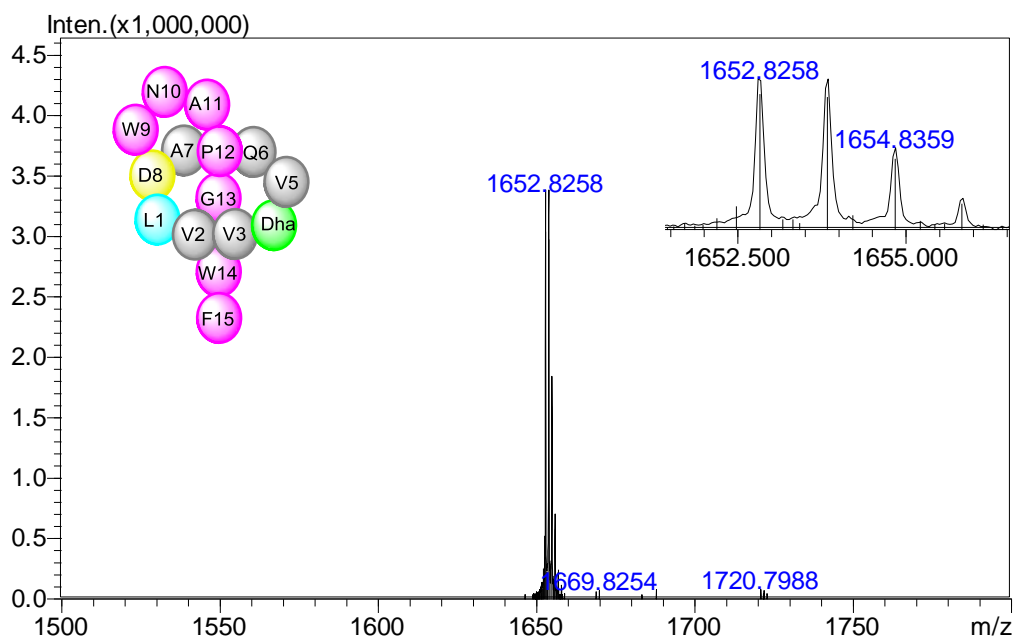


Figure S42. The HRESIMS spectrum of stlassin I4C-V (**26a**).

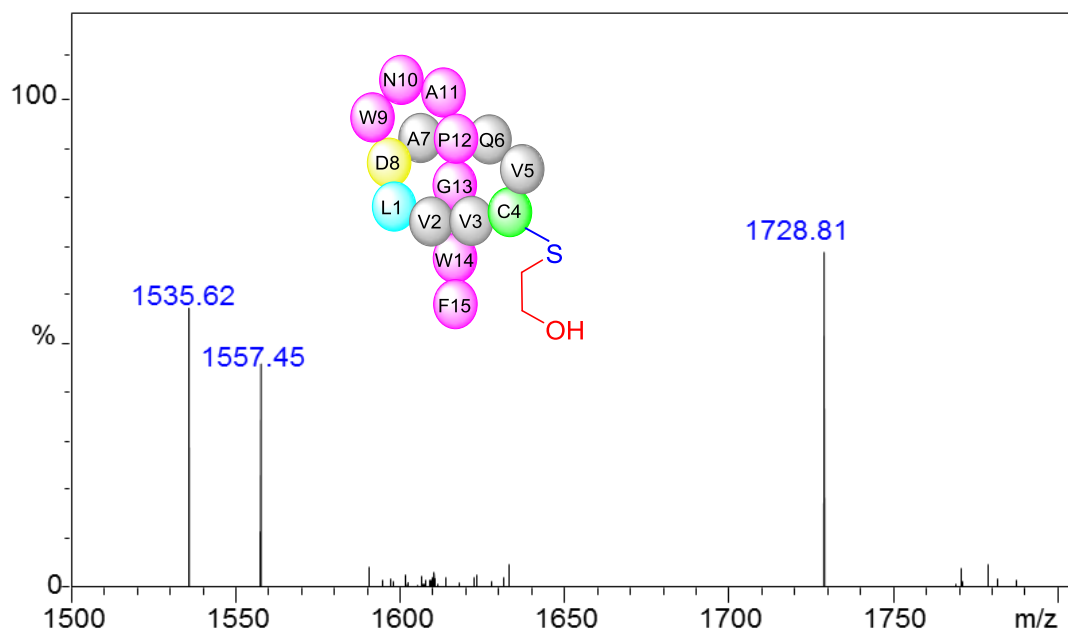


Figure S43. The HRESIMS spectrum of stlassin I4C- VI (**26b**)

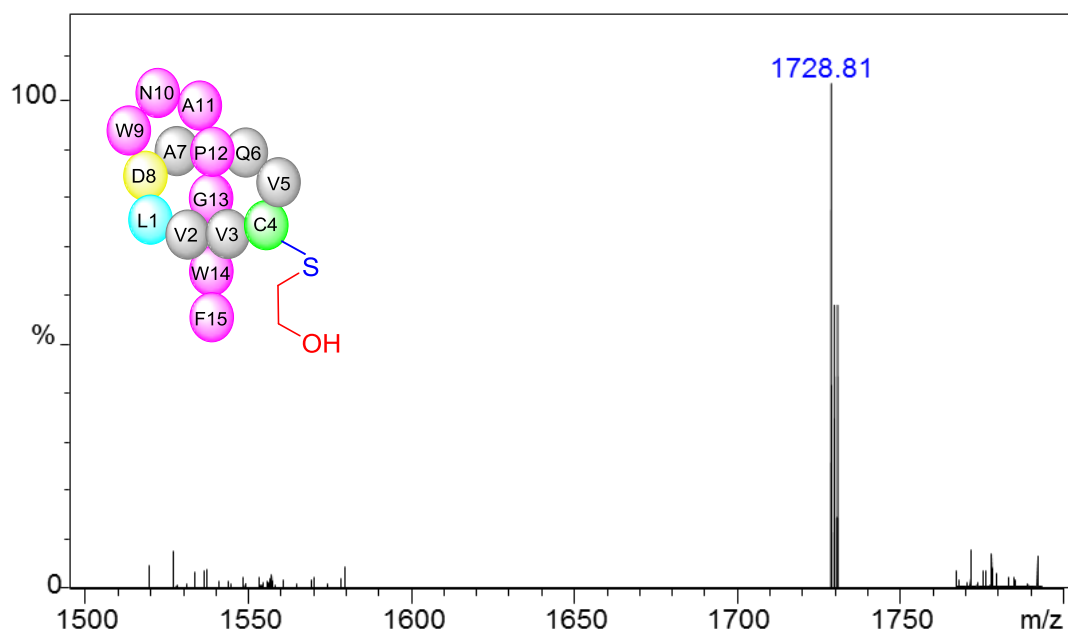


Figure S44. The ESIMS spectrum of stlassin I4C-VII (**27a**).

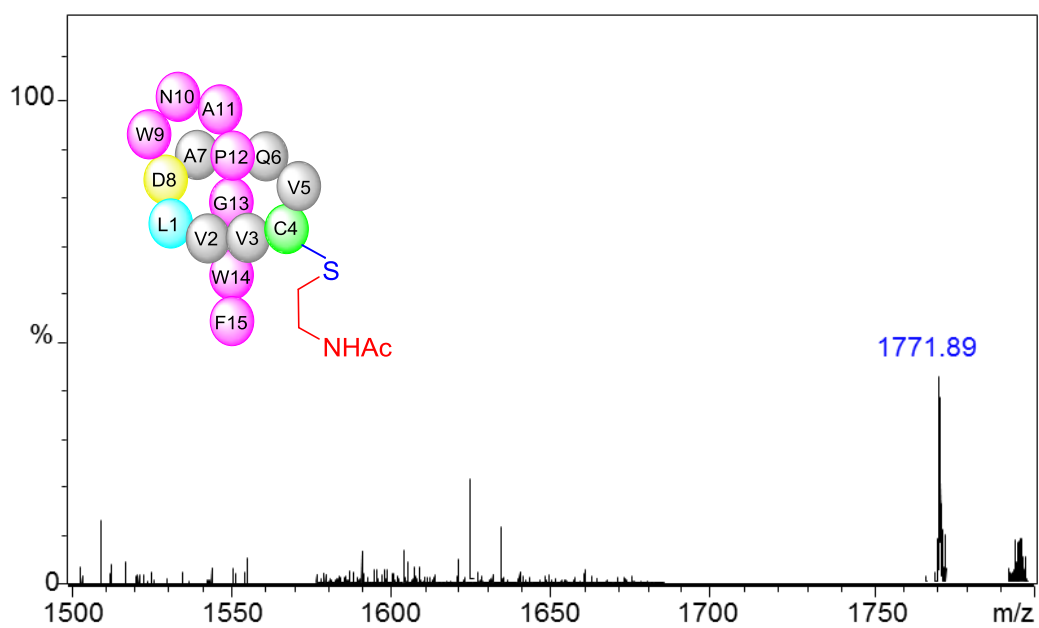


Figure S45. The ESIMS spectrum of stlassin I4C-VIII (**27b**).

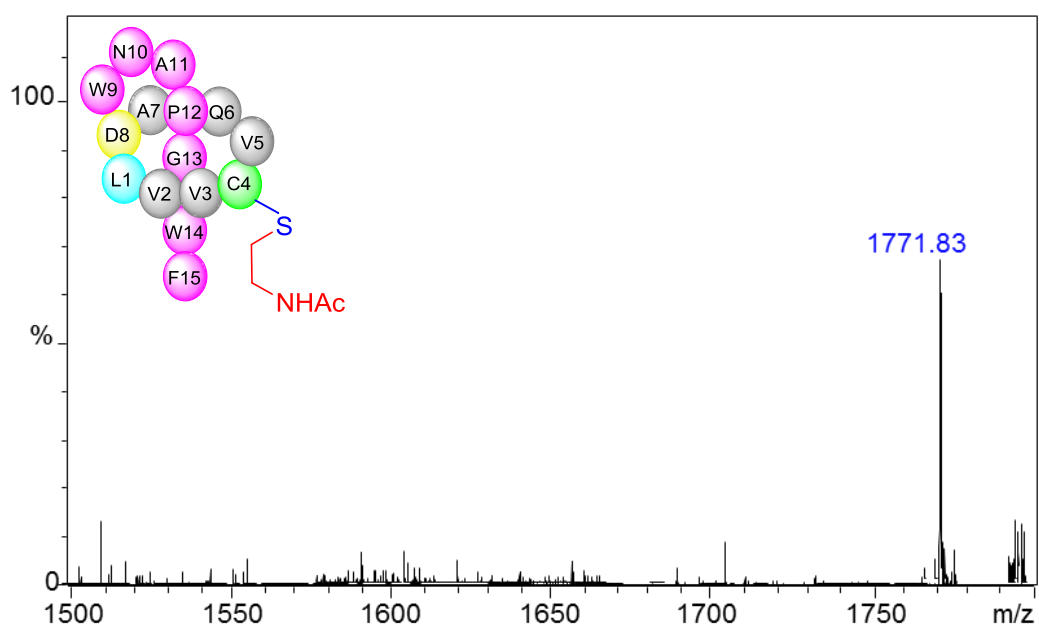


Figure S46. The TOCSY spectrum (blue, mixing time: 70 ms) and NOESY spectrum (red, mixing time: 300 ms) of stlassin (**1**) in H₂O/DMSO-*d*₆ (8:2) with 100 mM NaCl at 298 K.

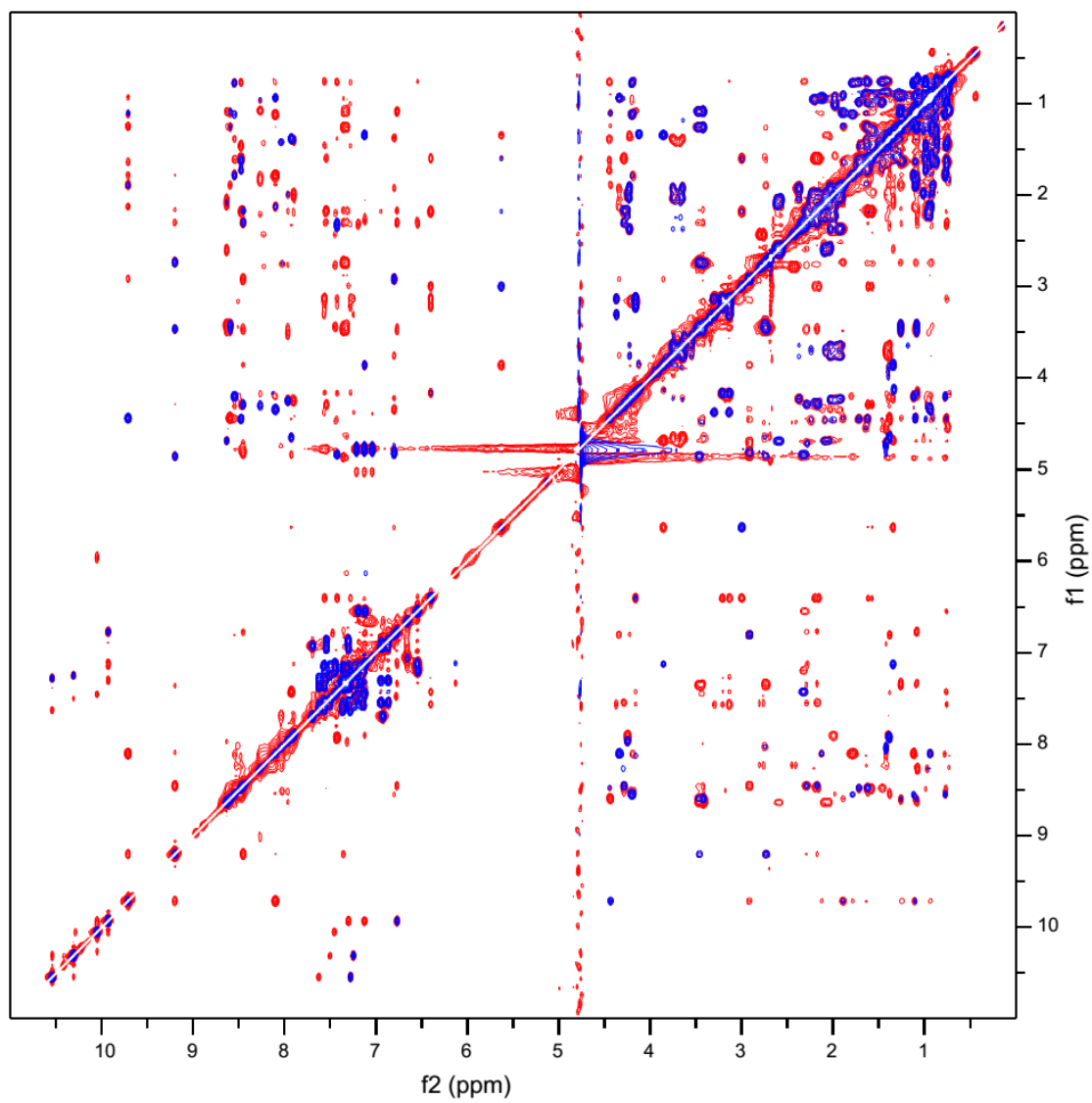


Figure S47. The ^1H - ^{13}C HSQC spectrum of stlassin (**1**) in $\text{H}_2\text{O}/\text{DMSO-}d_6$ (8:2) with 100 mM NaCl at 298 K.

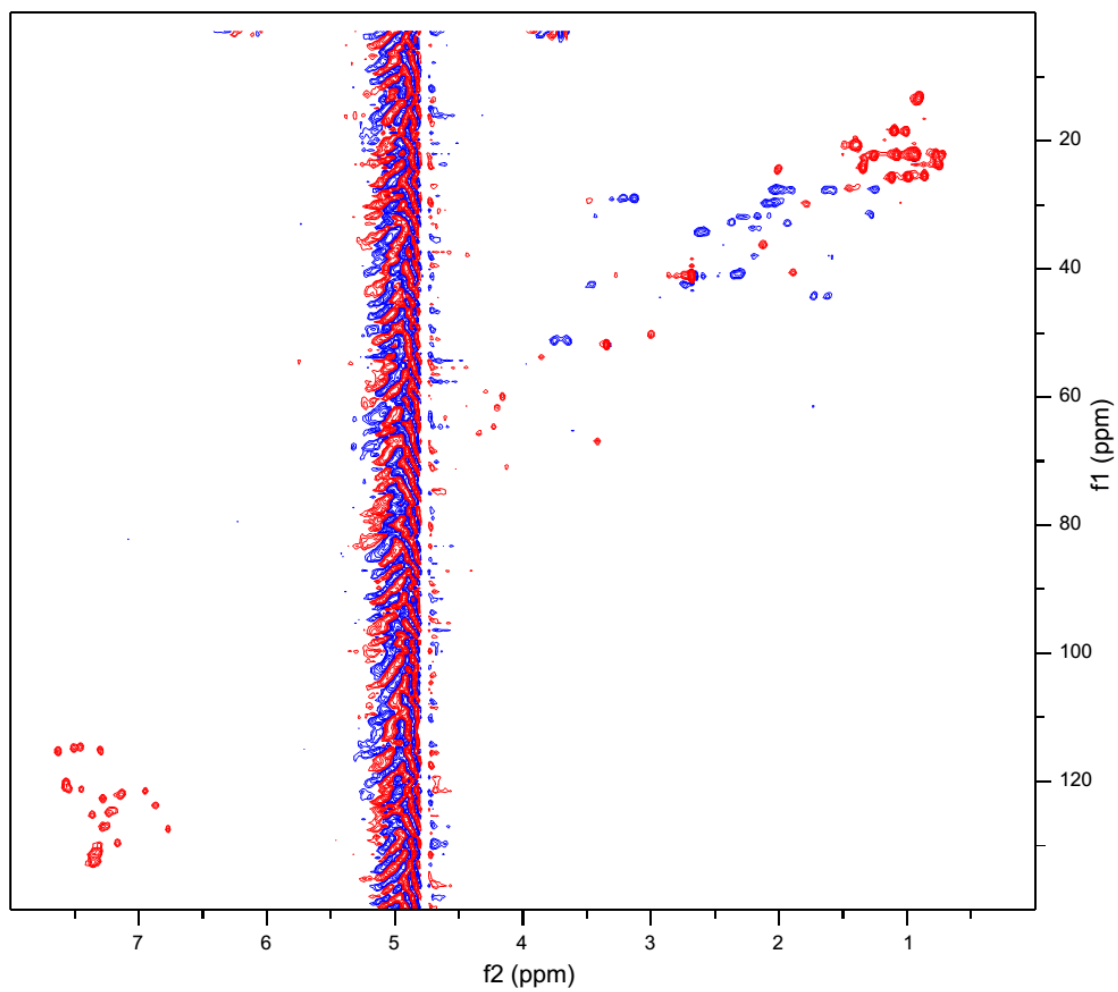


Figure S48. The ^1H - ^{15}N HSQC spectrum of stlassin (**1**) in $\text{H}_2\text{O}/\text{DMSO-}d_6$ (8:2) with 100 mM NaCl at 298 K.

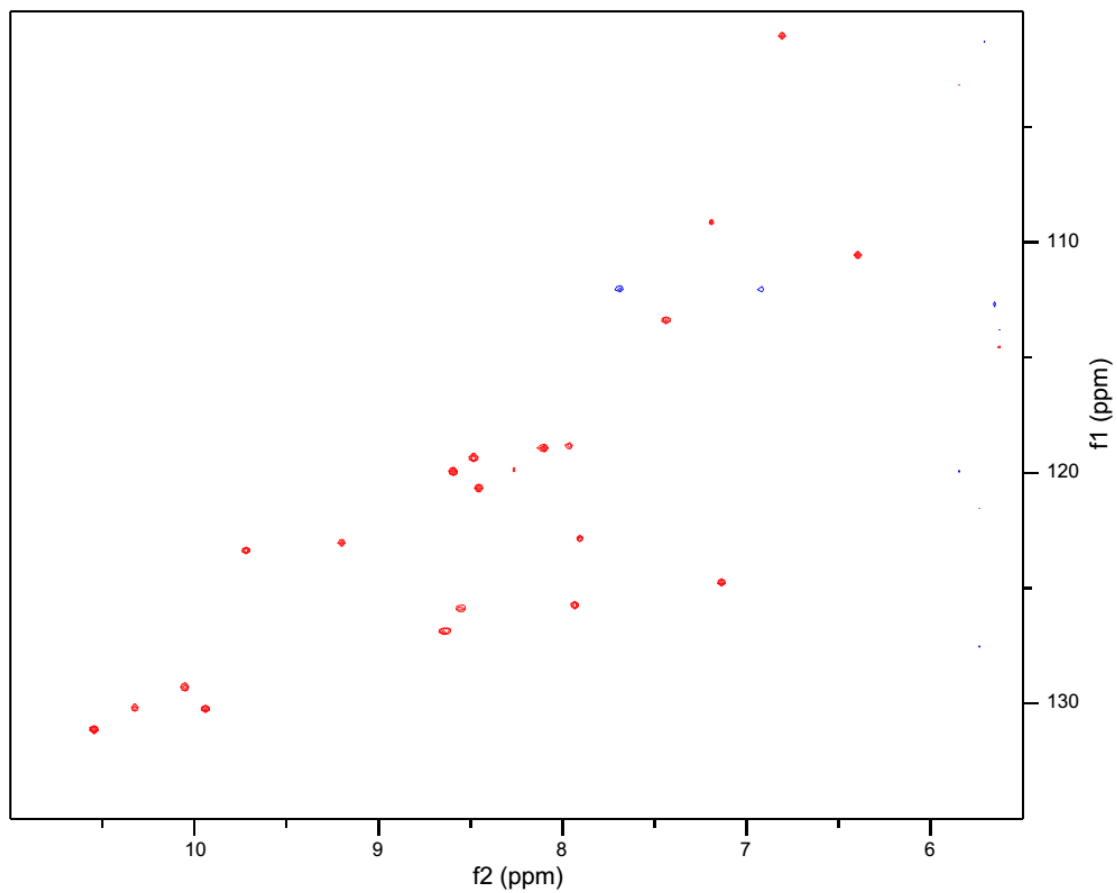


Figure S49. The TOCSY spectrum (blue, mixing time: 70 ms) and NOESY spectrum (red, mixing time: 300 ms) of stlassin V3A (**3**) in H₂O/DMSO-*d*₆ (8:2) with 100 mM NaCl at 298 K.

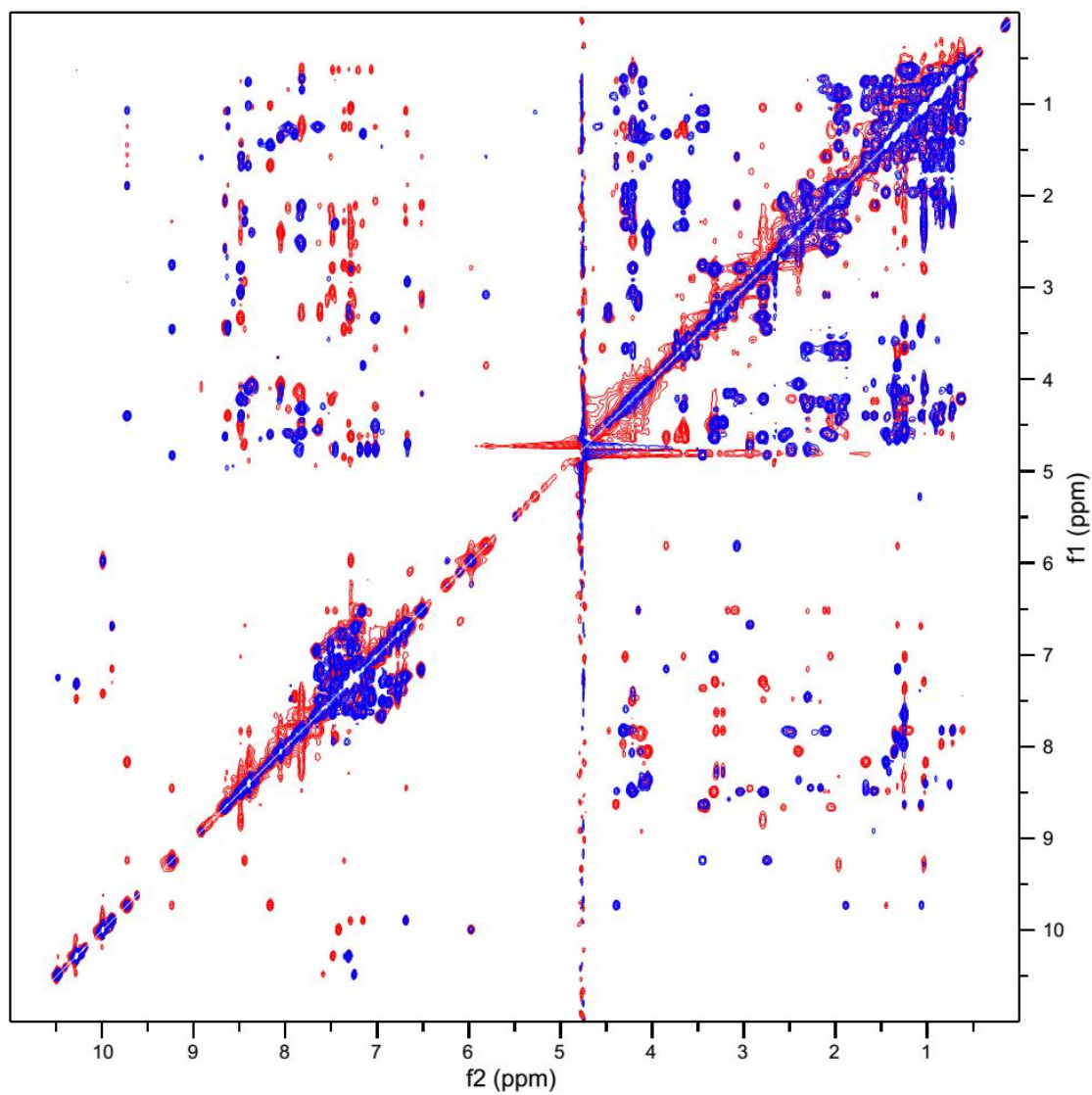


Figure S50. The ^1H - ^{13}C HSQC spectrum of stlassin V3A (**3**) in $\text{H}_2\text{O}/\text{DMSO-}d_6$ (8:2) with 100 mM NaCl at 298 K.

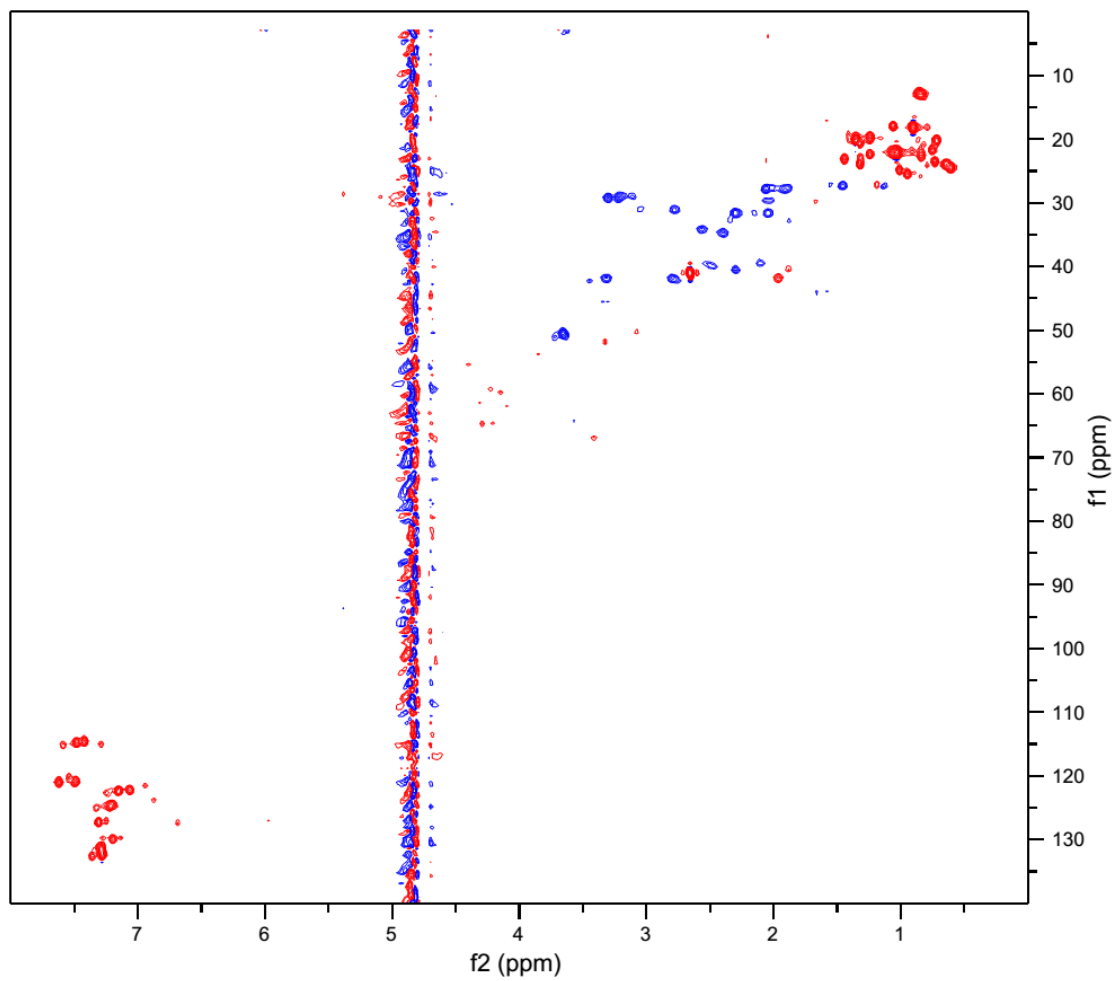


Figure S51. The ^1H - ^{15}N HSQC spectrum of stlassin V3A (**3**) in $\text{H}_2\text{O}/\text{DMSO-}d_6$ (8:2) with 100 mM NaCl at 298 K.

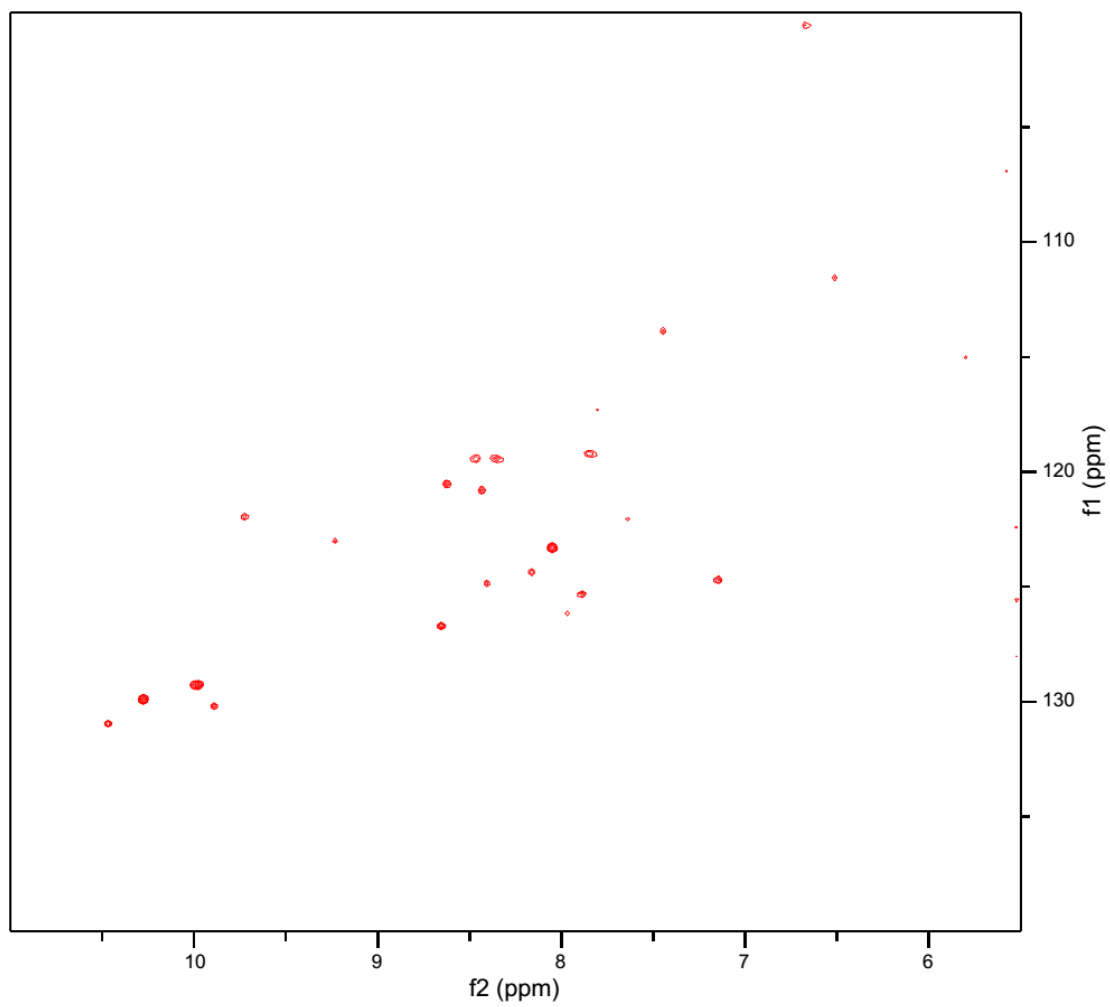


Figure S52. The TOCSY spectrum (blue, mixing time: 70 ms) and NOESY spectrum (red, mixing time: 300 ms) of stlassin I4A (**4**) in H₂O/DMSO-*d*₆ (8:2) with 100 mM NaCl at 298 K.

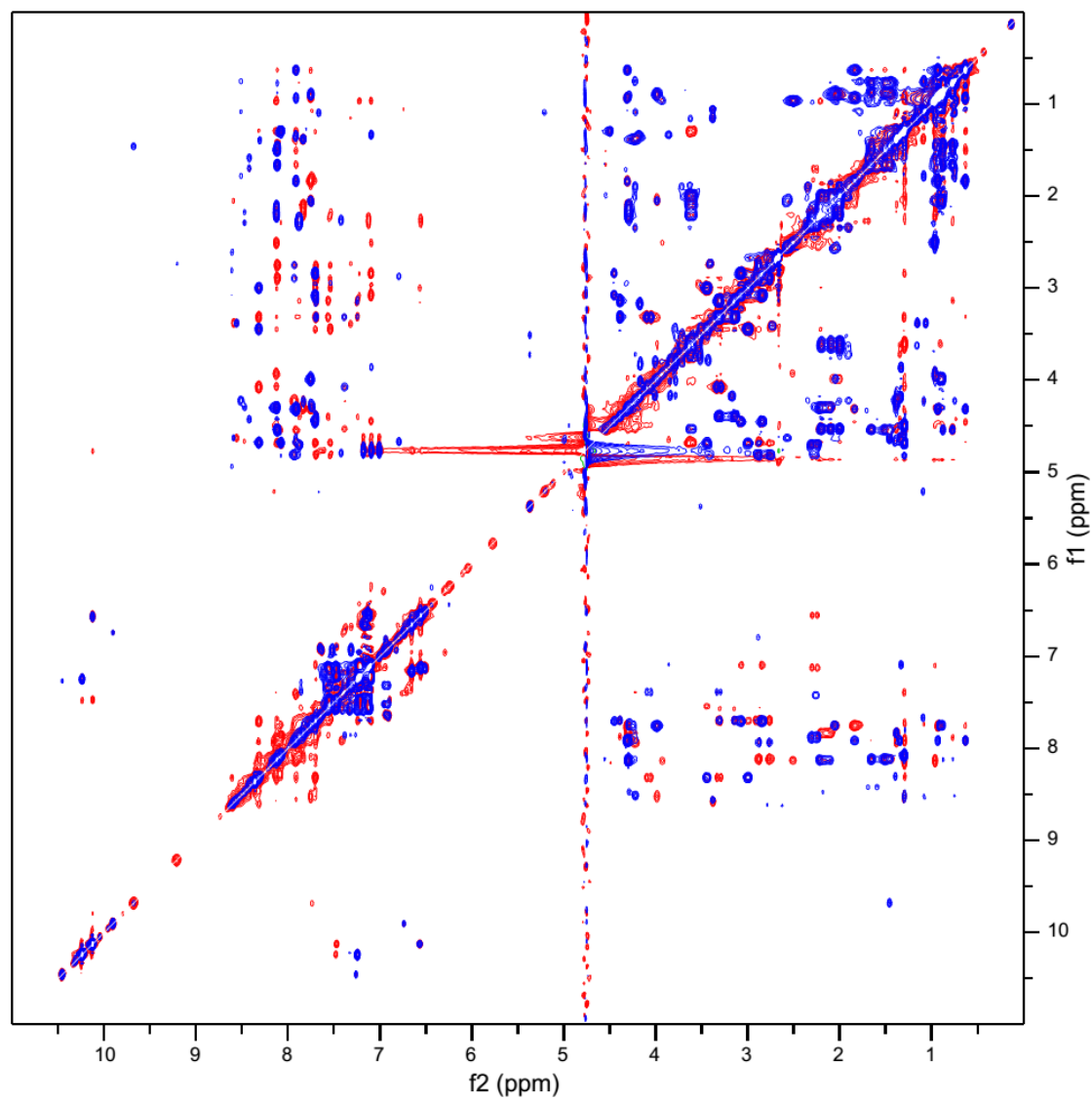


Figure S53. The ^1H - ^{13}C HSQC spectrum of stlassin I4A (**4**) in $\text{H}_2\text{O}/\text{DMSO-}d_6$ (8:2) with 100 mM NaCl at 298 K.

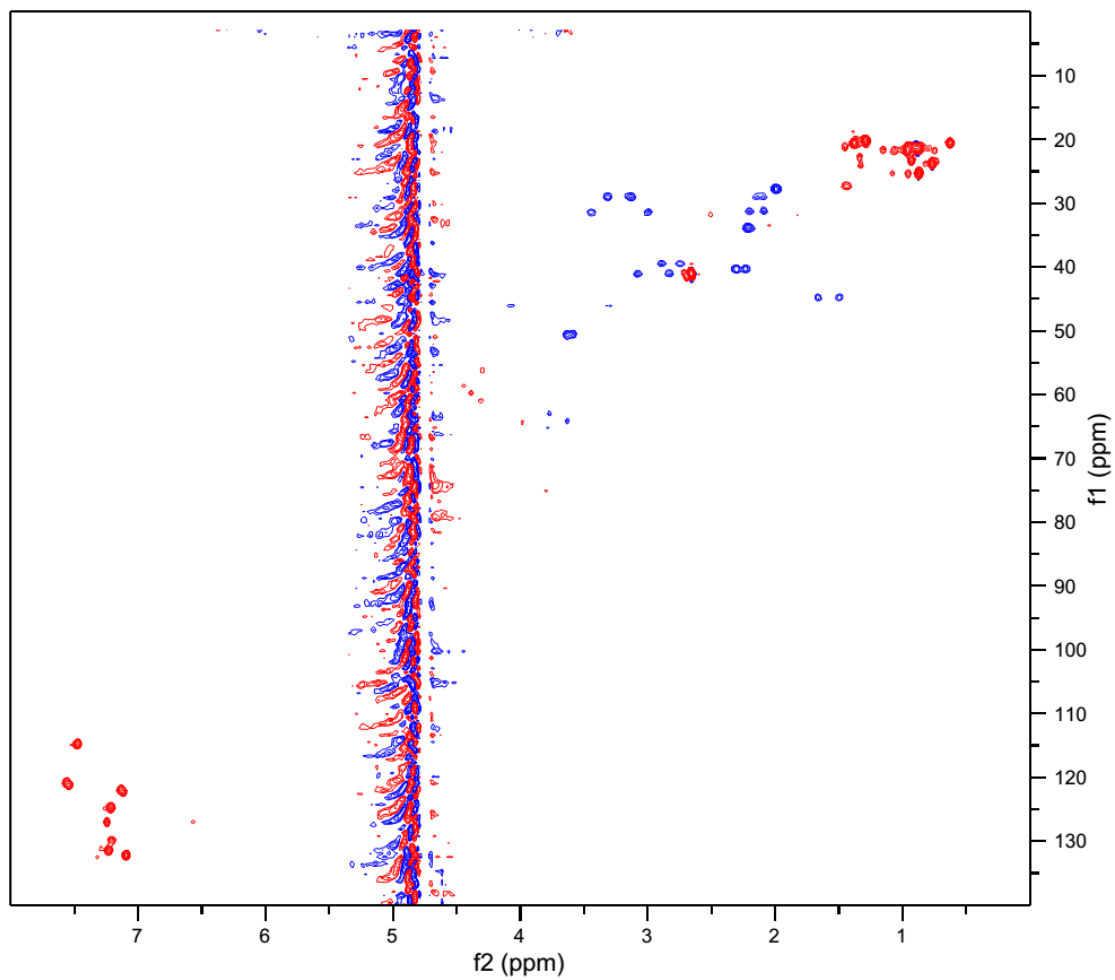


Figure S54. The ^1H - ^{15}N HSQC spectrum of stlassin I4A (**4**) in $\text{H}_2\text{O}/\text{DMSO-}d_6$ (8:2) with 100 mM NaCl at 298 K.

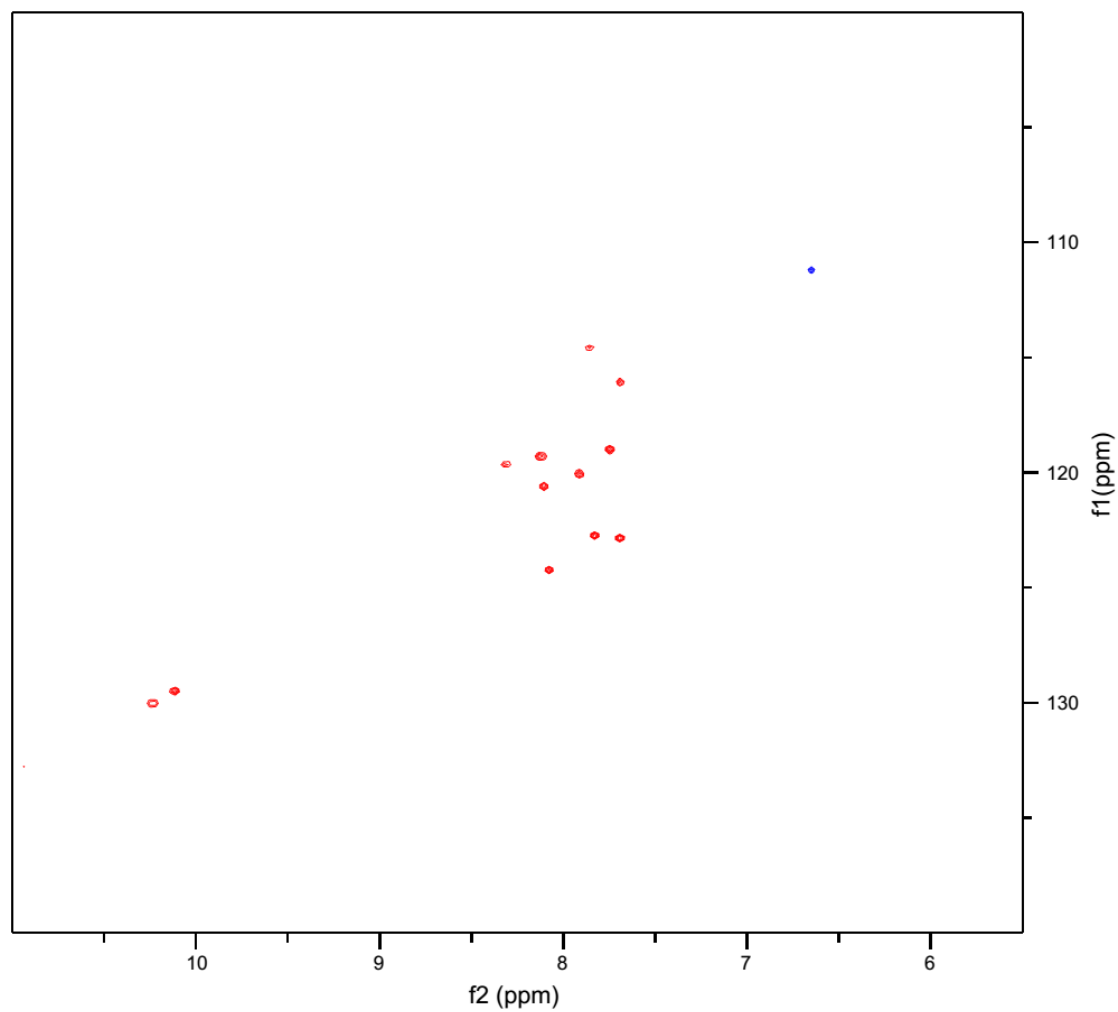


Figure S55. The TOCSY spectrum (blue, mixing time: 70 ms) and NOESY spectrum (red, mixing time: 300 ms) of stlassin W14F (**14**) in H₂O/DMSO-*d*₆ (8:2) with 100 mM NaCl at 298 K.

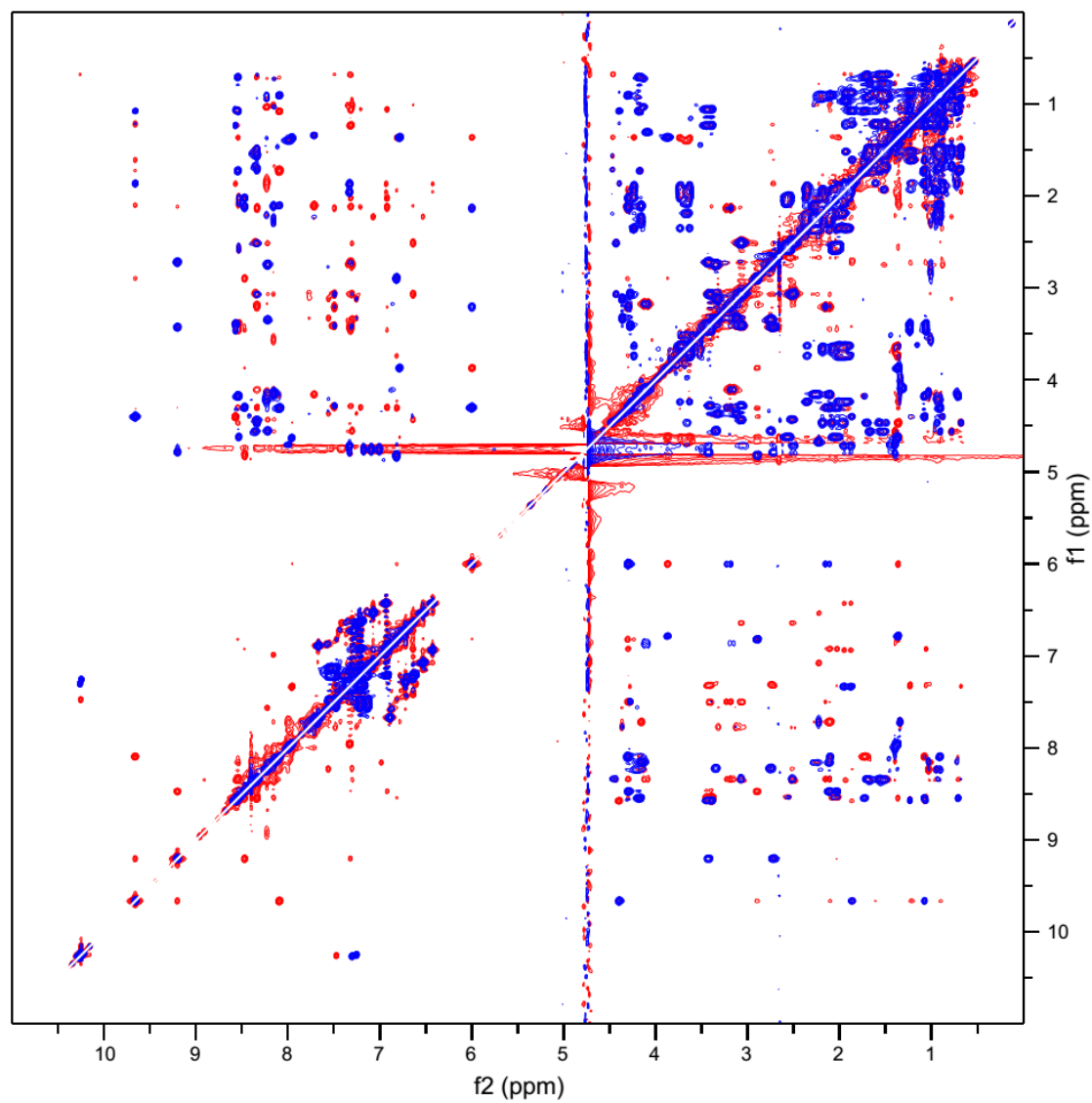


Figure S56. The ^1H - ^{13}C HSQC spectrum of stlassin W14F (**14**) in $\text{H}_2\text{O}/\text{DMSO-}d_6$ (8:2) with 100 mM NaCl at 298 K.

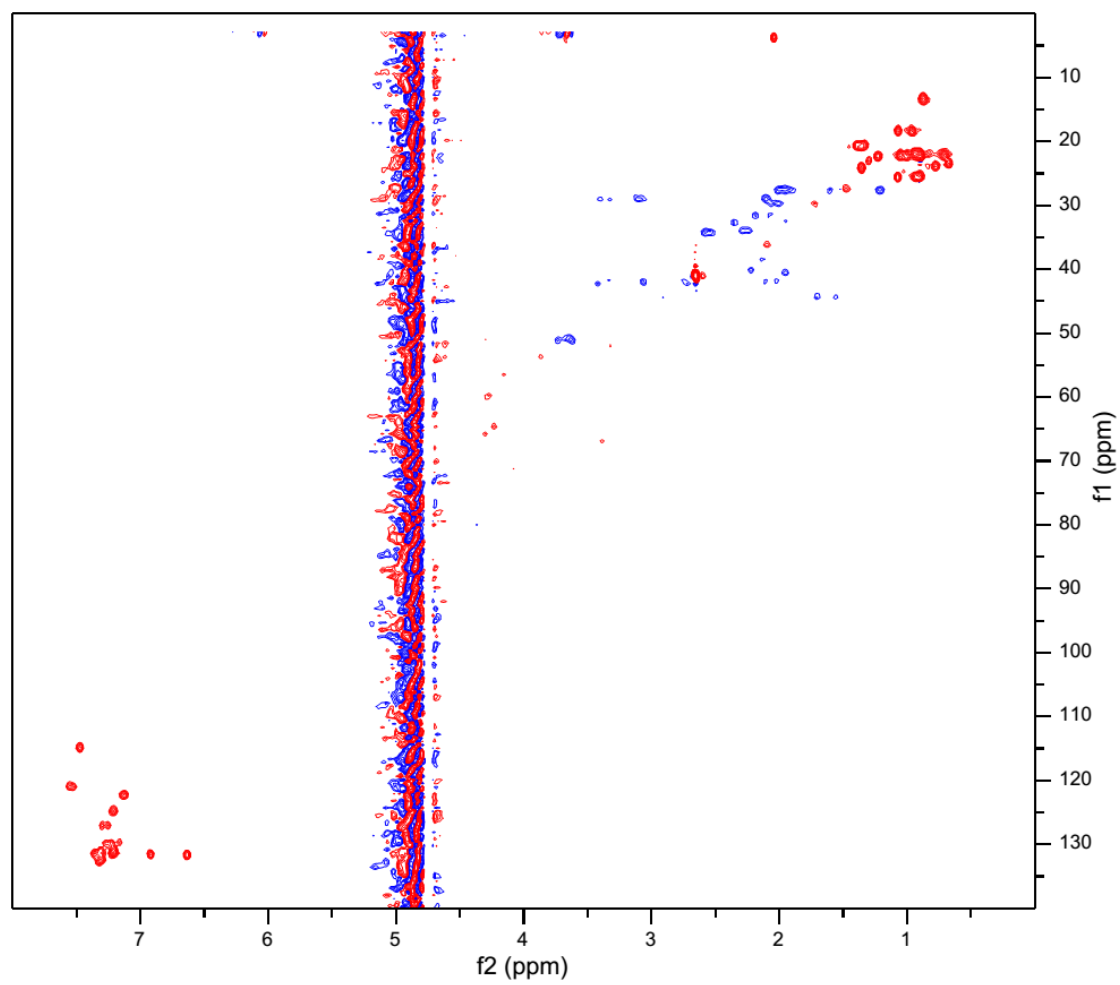


Figure S57. The TOCSY spectrum (blue, mixing time: 70 ms) and NOESY spectrum (red, mixing time: 300 ms) of stlassin F15Y (**16**) in H₂O/DMSO-*d*₆ (8:2) with 100 mM NaCl at 298 K.

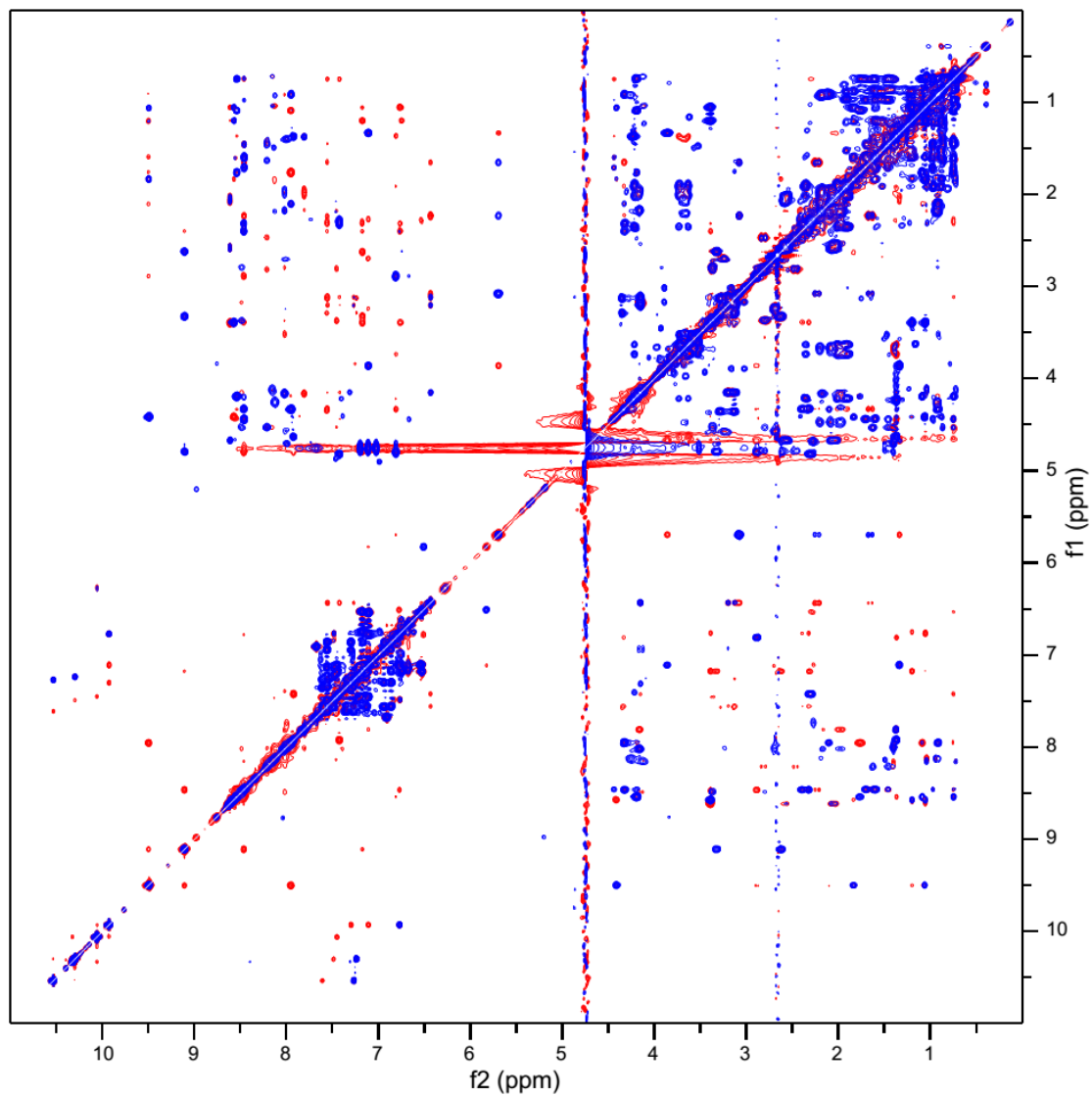


Figure S58. The ^1H - ^{13}C HSQC spectrum of stlassin F15Y (**16**) in $\text{H}_2\text{O}/\text{DMSO-}d_6$ (8:2) with 100 mM NaCl at 298 K.

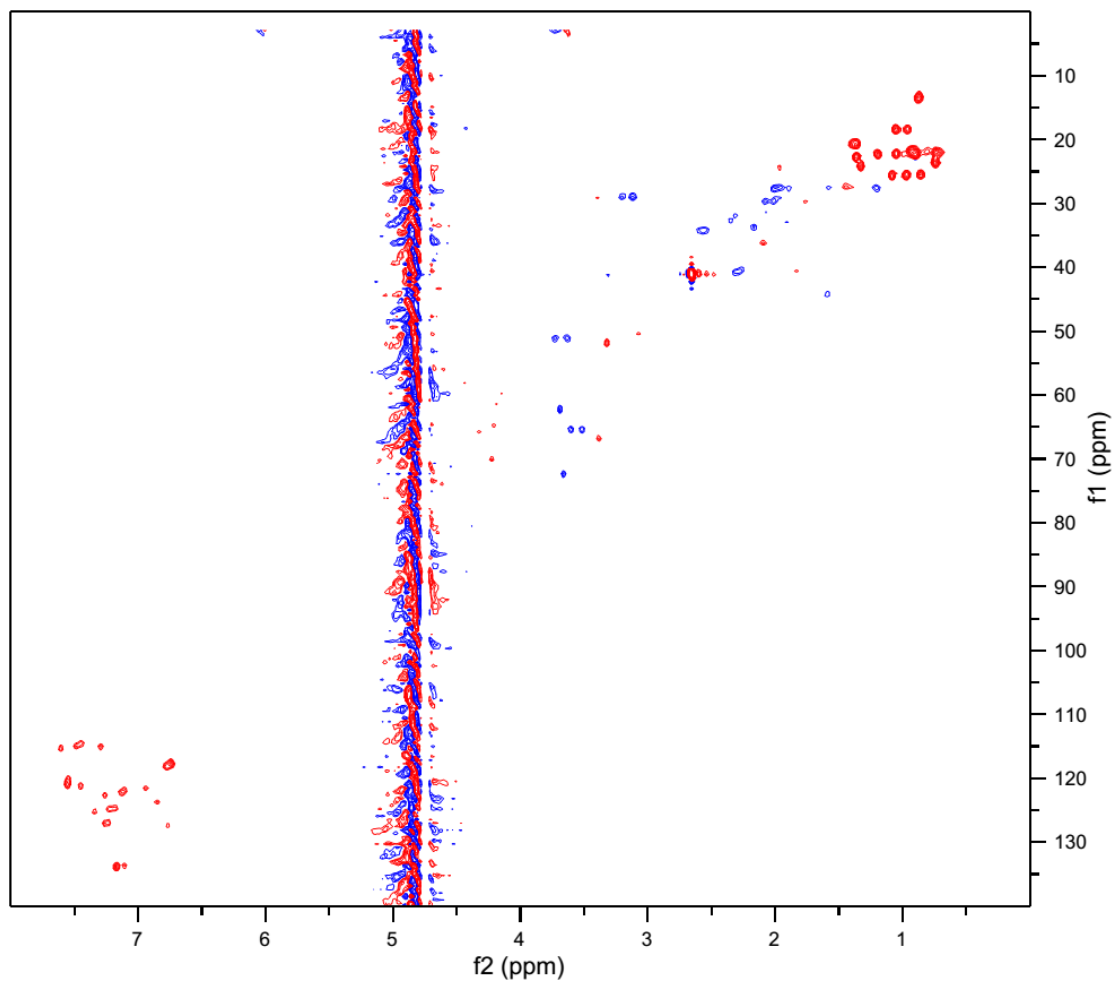


Figure S59. The TOCSY spectrum (blue, mixing time: 70 ms) and NOESY spectrum (red, mixing time: 300 ms) of stlassin V2C/A11C (**18**) in DMSO-*d*₆ at 298 K.

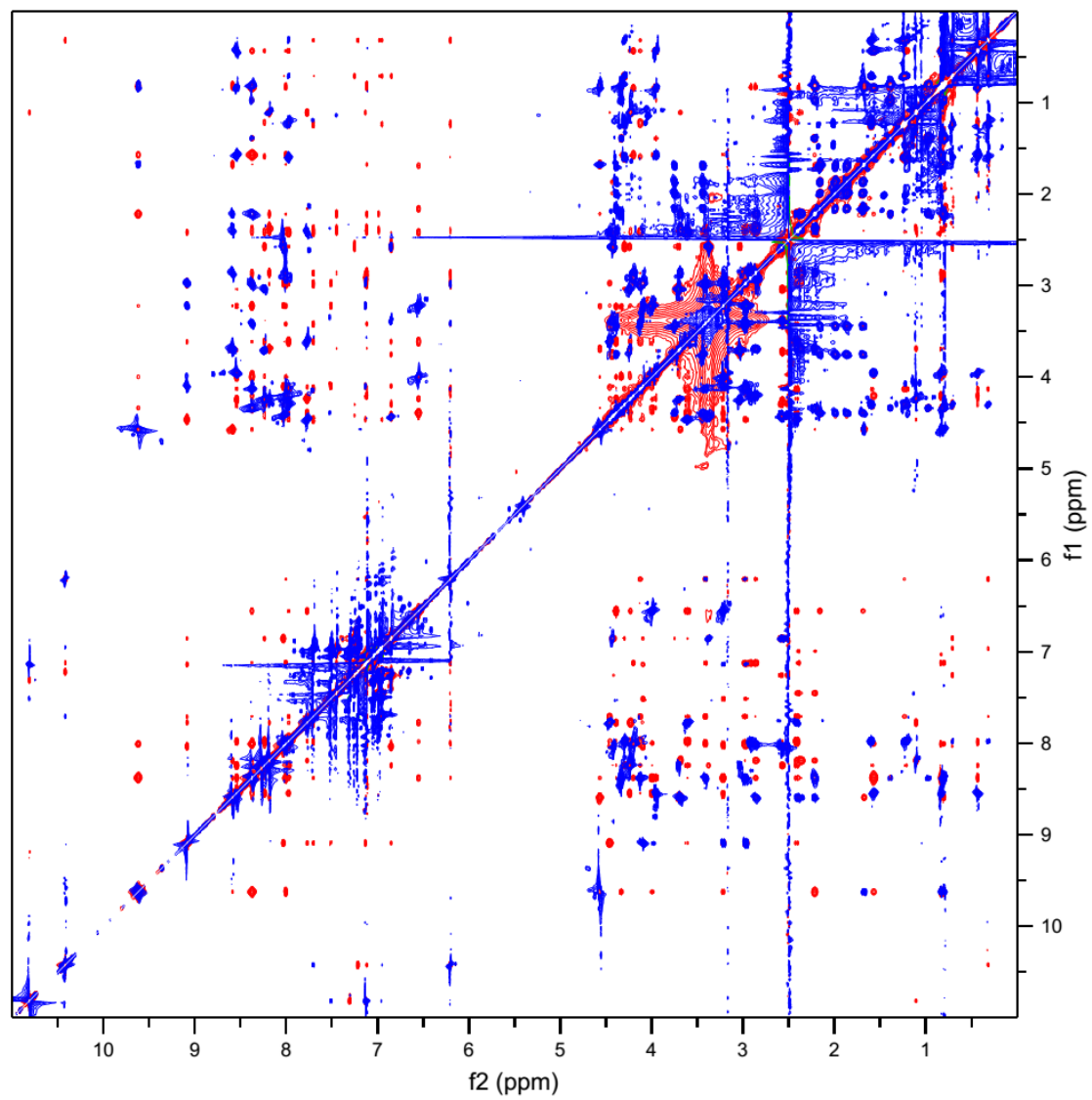
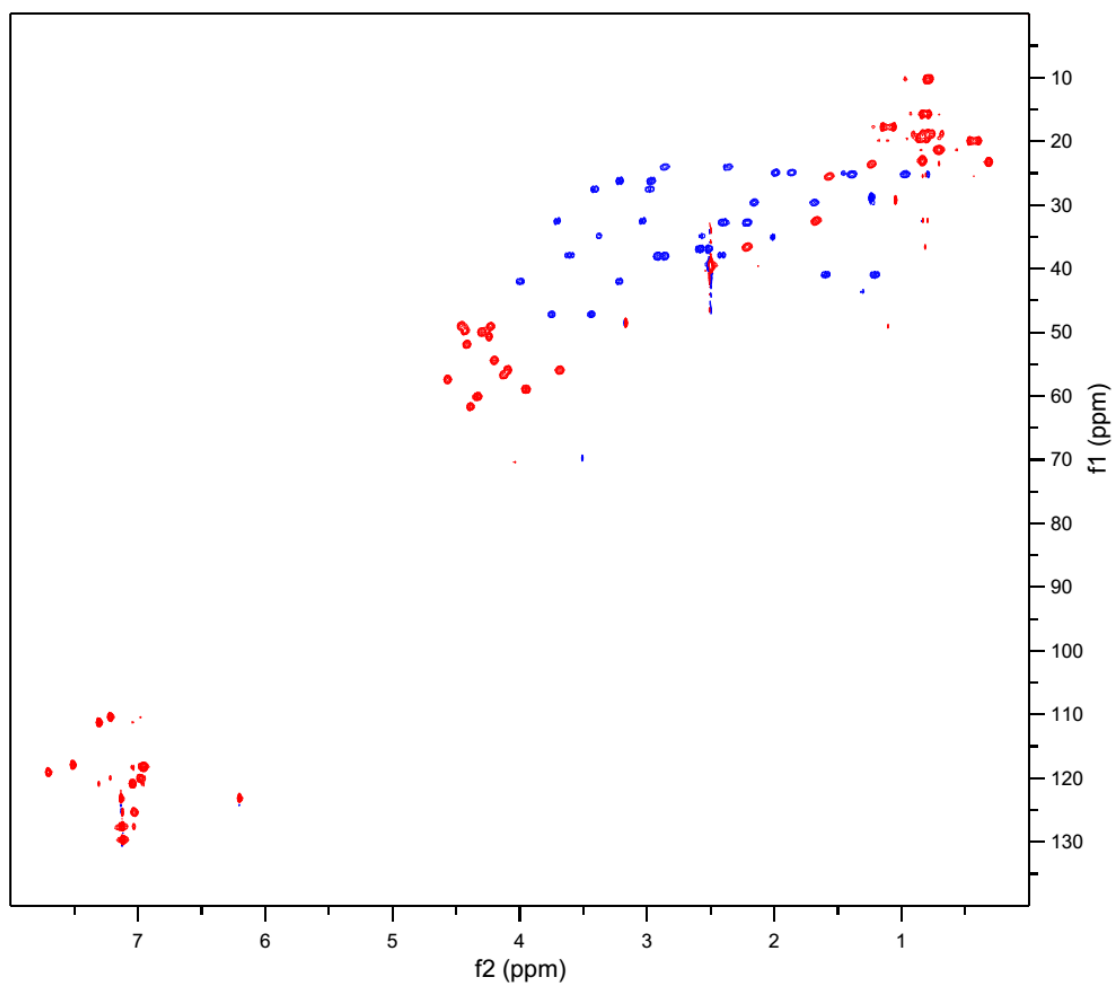


Figure S60. The ^1H - ^{13}C HSQC spectrum of stlassin V2C/A11C (**18**) in $\text{DMSO-}d_6$ at 298 K.



References

- (1) Ge, Y. J.; Wang, G. Y.; Jin, J.; Liu, T.; Ma, X. Y.; Zhang, Z. Y.; Geng, T. T.; Song, J.; Ma, X. J.; Zhang, Y. T.; Yang, D. H.; Ma, M. Discovery and Biosynthesis of Peptidocinnamins G-M Featuring Three Enzymes-Catalyzed Nonproteinogenic Amino Acid Formation. *J. Org. Chem.* **2020**, *85*, 8673-8682.
- (2) Kieser, T.; Bibb, M.; Buttner, M.; Chater, K.; Hopwood, D. *Practical Streptomyces Genetics*. The John Innes Foundation, Norwich, **2000**, 406-422.
- (3) Heuer, H.; Krsek, M.; Baker, P.; Smalla, K.; Wellington, E. M. Analysis of Actinomycete Communities by Specific Amplification of Genes Encoding 16S rRNA and Gel-Electrophoretic Separation in Denaturing Gradients. *Appl. Environ. Microbiol.* **1997**, *63*, 3233-3241.
- (4) Blin, K.; Shaw S.; Steinke K.; Villebro R.; Ziemert N.; Lee S. Y.; Medema M. H.; Weber T. antiSMASH 5.0: updates to the secondary metabolite genome mining pipeline. *Nucleic Acids Res.* **2019**, *47*, W81-W87.
- (5) Madeira F; Park Y. M.; Lee J.; Buso N.; Gur T.; Madhusoodanan N.; Basutkar P.; Tivey A. R. N.; Potter S. C.; Finn R. D.; Lopez R. The EMBL-EBI search and sequence analysis tools APIs in 2019. *Nucleic Acids Res.* **2019**, *47*, W636-W641.
- (6) Liu, T.; Jin, J.; Yang, X.; Song, J.; Yu, J.; Geng, T.; Zhang, Z.; Ma, X.; Wang, G.; Xiao, H.; Ge, Y.; Sun, X.; Xing, B.; Ma, X.; Chi, C.; Kuang, Y.; Ye, M.; Wang, H.; Zhang, Y.; Yang, D.; Ma, M. Discovery of a Phenylamine-Incorporated Angucyclinone from Marine *Streptomyces* sp. PKU-MA00218 and Generation of Derivatives with Phenylamine Analogues. *Org. Lett.* **2019**, *21*, 2813-2817.
- (7) Wang, H. L.; Li, Z.; Jia, R. N.; Hou, Y.; Yin, J.; Bian, X. Y.; Li, A.; Müller, R.; Stewart, A. F.; Fu, J.; Zhang, Y. M. RecET direct cloning and Red α recombineering of biosynthetic gene clusters, large operons or single genes for heterologous expression. *Nat. Protoc.* **2016**, *11*, 1175-1190.
- (8) Markley J. L.; Bax A.; Arata Y.; Hilbers C. W.; Kaptein R.; Sykes B. D.; Wright P. E.; Wüthrich K. Recommendations for the presentation of NMR structures of proteins and nucleic acids--IUPAC-IUBMB-IUPAB Inter-Union Task Group on the standardization of data bases of protein and nucleic acid structures determined by NMR spectroscopy. *Eur. J. Biochem.* **1998**, *256*, 1-15.
- (9) Delaglio F.; Grzesiek S.; Vuister G. W.; Zhu G.; Pfeifer J.; Bax, A. NMRPipe: A multidimensional spectral processing system based on UNIX pipes. *J. Biomol. NMR.* **1995**, *6*, 277-293.
- (10) Vranken, W. F.; Boucher, W.; Stevens, T. J.; Fogh, R. H.; Pajon, A.; Llinas, M.; Ulrich, E. L.; Markley, J. L.; Ionides, J.; Laue, E. D. The CCPN data model for NMR spectroscopy: development of a software pipeline. *Proteins.* **2005**, *59*, 687-696.
- (11) Wüthrich, K. *NMR of proteins and nucleic acids*. Wiley-interscience, New York, **1986**.
- (12) Brunge, A. T. Version 1.2 of the Crystallography and NMR system. *Nat. Protoc.* **2007**, *2*, 2728-2733.
- (13) Rieping, W.; Habeck, M.; Bardiaux, B.; Bernard, A.; Malliavin, T. E.; Nilges, M. ARIA2: automated NOE assignment and data integration in NMR structure calculation. *Bioinformatics.* **2007**, *23*, 381-382.
- (14) Schwieters, C.D.; Kuszewski, J.J.; Tjandra, N.; Clore, G.M. The Xplor-NIH NMR Molecular Structure Determination Package. *J. Magn. Res.*, **2003**, *160*, 66-74.
- (15) Hegemann, J. D.; Zimmermann M.; Xie X. L.; Marahiel M. A. Caulosegnins I-III: a highly diverse group of lasso peptides derived from a single biosynthetic gene cluster. *J. Am. Chem. Soc.* **2013**, *135*, 210-222.
- (16) Zong C. H.; Wu M. J.; Qin J. Z.; Link A. J. lasso peptide benenodin-1 is a thermally actuated [1]rotaxane switch. *J. Am. Chem. Soc.* **2017**, *139*, 10403-10409.
- (17) Cheung-Lee W. L.; Parry M. E.; Cartagena A. J.; Darst S. A.; Link A. J. Discovery and structure of the antimicrobial lasso peptide citrocin. *J. Biol. Chem.* **2019**, *294*, 6822-6830.

- (18) Wadzinski, T. J.; Steinauer, A.; Hie, L.; Pelletier, G.; Schepartz, A.; Miller, S. J. Rapid phenolic O-glycosylation of small molecules and complex unprotected peptides in aqueous solvent. *Nat. Chem.* **2018**, *10*, 644-652.
- (19) Hanaya, K.; Ohata, J.; Miller, M. K.; Mangubat-Medina, A. E.; Swierczynski, M. J.; Yang, D. C.; Rosenthal, R. M.; Popp, B. V.; Ball, Z. T. Rapid nickel(II)-promoted cysteine S-arylation with arylboronic acids. *Chem. Commun.* **2019**, *55*, 2841-2844.
- (20) Chalker, J. M.; Gunnoo, S. B.; Boutureira, O.; Gerstberger, S. C.; Fernández-González, M.; Bernardes, G. J. L.; Griffin, L.; Hailu, H.; Schofield, C. J.; Davis, B. G. Methods for converting cysteine to dehydroalanine on peptides and proteins. *Chem. Sci.* **2011**, *2*, 1666-1676.
- (21) Diakowska, D.; Nienartowicz, M.; Grabowski, K.; Rosińczuk, J., Krzystek-Korpacka, M. Toll-like receptors TLR-2, TLR-4, TLR-7, and TLR-9 in tumor tissue and serum of the patients with esophageal squamous cell carcinoma and gastro-esophageal junction cancer. *Adv. Clin. Exp. Med.* **2019**, *28*, 515-522.
- (22) Fu, J.; Bian, X. Y.; Hu, S. B.; Wang, H. L.; Huang, F.; Seibert, P. M.; Plaza, A.; Xia, L. Q.; Müller, R.; Stewart, A. F.; Zhang, Y. M. Full-length RecE enhances linear-linear homologous recombination and facilitates direct cloning for bioprospecting. *Nat. Biotechnol.* **2012**, *30*, 440-448.
- (23) MacNeil, D. J.; Gewain, K. M.; Ruby, C. L.; Dezeny, G.; Gibbons, P. H.; MacNeil, T. Complex organization of the *Streptomyces avermitilis* genes encoding the avermectin polyketide synthase. *Gene* **1992**, *111*, 61-68.
- (24) Bentley, S. D.; Chater, K. F.; Cerdeño-Tárrega, A. M.; Challis, G. L.; Thomson, N. R.; James, K. D.; Harris, D. E.; Quail, M. A.; Kieser, H.; Harper, D.; Bateman, A.; Brown, S.; Chandra, G.; Chen, C. W.; Collins, M.; Cronin, A.; Fraser, A.; Goble, A.; Hidalgo, J.; Hornsby, T.; Howarth, S.; Huang, C. H.; Kieser, T.; Larke, L.; Murphy, L.; Oliver, K.; O'Neil, S.; Rabinowitsch, E.; Rajandream, M. A.; Rutherford, K.; Rutter, S.; Seeger, K.; Saunders, D.; Sharp, S.; Squares, R.; Squares, S.; Taylor, K.; Warren, T.; Wietzorrek, A.; Woodward, J.; Barrell, B. G.; Parkhill, J.; Hopwood, D. A. Complete genome sequence of the model actinomycete *Streptomyces coelicolor* A3(2). *Nature* **2002**, *417*, 141-147.
- (25) Ziermann, R.; Betlach, M. C. Recombinant polyketide synthesis in *Streptomyces*: engineering of improved host strains. *Biotechniques* **1999**, *26*, 106-110.